

SCF 11

Uppsala Dissertations from
Faculty of Science and Technology

21

ELÓNIO MUIUANE

Hydrogeophysics of Tropical Africa

Recent Advances and Perspectives



ACTA UNIVERSITATIS UPSALIENSIS
UPPSALA 1999

Acta Universitatis Upsaliensis

Uppsala Dissertations from the Faculty of Science and Technology

Editor: The Dean of the Faculty of Science and Technology.

Prior to January 1994, the series was called *Uppsala Dissertations from the Faculty of Science*, and a list of earlier issues is presented on the inside cover of this volume.

1. *Dan Windmar*: Water Drop Initiated Discharges in Air. 1994.
2. *Kurt Woschnagg*: Asymmetry in Production of Beauty and Charm Quark Pairs in Electron-Positron Annihilation. 1994.
3. *Anders Bergman*: *In situ* Calibration of Voltage Transformers on the Swedish National Grid. 1994.
4. *Hugo Pérez Rebolledo*: Transient Response of Low Voltage Power Installations to Natural and Simulated Lightning Electromagnetic Fields. 1994.
5. *Ulf Schuberth*: The Reaction $pp \rightarrow p\eta$ Close to Threshold. 1995.
6. *Anders Mörtzell*: Neutral Pion Production in Proton - Proton Collisions Close to the Kinematical Threshold. 1995.
7. *Peter B. R. Björkholm*: Measurement of the Nucleon Structure Functions F_2 and R in Deep Inelastic Muon Scattering. 1995.
8. *Erik Lidström*: Static and Dynamic Properties of Rare Earth Compounds. 1995.
9. *Anna Dyring*: The Structure of the Nucleon: Precision Measurements of Parton Distributions at Small x . 1995.
10. *Sofia Feltzing*: Two Studies of the Galactic Chemical Evolution. 1995.
11. *Michael R. Semple*: Local Fields at Impurity Atoms in Single Crystals and Epitaxial Layers. 1996.
12. *Anders Larsson*: Inhibited Electrical Discharges in Air. 1997.
13. *Stina Haggström*: Production of η -mesons in Proton-Neutron Collisions. 1997.
14. *Johannes M. Dyring*: Detailed Studies of the Reaction $pp \rightarrow p\eta$ using a Straw Chamber Tracking Device. 1997.
15. *Maria Gunther Axelsson*: Production Asymmetry of Strange Quarks in Electron-Positron Annihilation at LEP. 1998.
16. *Karl Hörnell*: Runge-Kutta Time Step Selection for Flow Problems. 1999.
17. *Catherine Östlund*: Analysis of Imaging Spectrometer Data with Lake Environment Applications. 1999.
18. *Stephan Pomp*: Hyperon Polarisation in the Reaction $\bar{p}^{12}\text{C} \rightarrow \bar{\Lambda}\Lambda X$. 1999.
19. *Roger J. M. Y. Ruber*: An Ultra-thin-walled Superconducting Solenoid for Meson-decay Physics. 1999.
20. *Manhal Sirat*: Structural and Neural Network Analyses of Fracture Systems at the Äspö Hard Rock Laboratory, SE Sweden. 1999.
21. *Elónio Muiwane*: Hydrogeophysics of Tropical Africa. Recent Advances and Perspectives. 1999.

Distributor:
Uppsala University Library
Uppsala, Sweden

ISSN 1104-2516
ISBN 91-554-4574-8

Acta Universitatis Upsaliensis

Uppsala Dissertations from the Faculty of Science

Editor: The Dean of the Faculty of Science

1-11: 1970-1975

12. *Lars Thofelt*: Studies on leaf temperature recorded by direct measurement and by thermography. 1975.
13. *Monica Henricsson*: Nutritional studies on *Chara globularis* Thuill., *Chara zeylanica* Willd., and *Chara haitensis* Turpin. 1976.
14. *Göran Kloow*: Studies on Regenerated Cellulose by the Fluorescence Depolarization Technique. 1976.
15. *Carl-Magnus Backman*: A High Pressure Study of the Photolytic Decomposition of Azothane and Propionyl Peroxide. 1976.
16. *Lennart Källströmer*: The significance of biotin and certain monosaccharides for the growth of *Aspergillus niger* on rhamnose medium at elevated temperature. 1977.
17. *Staffan Renlund*: Identification of Oxytocin and Vasopressin in the Bovine Adenohypophysis. 1978.
18. *Bengt Finnström*: Effects of pH, Ionic Strength and Light Intensity on the Flash Photolysis of L-tryptophan. 1978.
19. *Thomas C. Amu*: Diffusion in Dilute Solutions: An Experimental Study with Special Reference to the Effect of Size and Shape of Solute and Solvent Molecules. 1978.
20. *Lars Tegnér*: A Flash Photolysis Study of the Thermal Cis-Trans Isomerization of Some Aromatic Schiff Bases in Solution. 1979.
21. *Stig Tormod*: A High-Speed Stopped Flow Laser Light Scattering Apparatus and its Application in a Study of Conformational Changes in Bovine Serum Albumin. 1985.
22. *Björn Varnestig*: Coulomb Excitation of Rotational Nuclei. 1987.
23. *Frans Lettenström*: A study of nuclear effects in deep inelastic muon scattering. 1988.
24. *Göran Ericsson*: Production of Heavy Hypernuclei in Antiproton Annihilation. Study of their decay in the fission channel. 1988.
25. *Fang Peng*: The Geopotential: Modelling Techniques and Physical Implications with Case Studies in the South and East China Sea and Fennoscandia. 1989.
26. *Md. Anwar Hossain*: Seismic Refraction Studies in the Baltic Shield along the Fennolora Profile. 1989.
27. *Lars Erik Svensson*: Coulomb Excitation of Vibrational Nuclei. 1989.
28. *Bengt Carlsson*: Digital differentiating filters and model based fault detection. 1989.
29. *Alexander Edgar Kavka*: Coulomb Excitation. Analytical Methods and Experimental Results on even Selenium Nuclei. 1989.
30. *Christopher Juhlin*: Seismic Attenuation, Shear Wave Anisotropy and Some Aspects of Fracturing in the Crystalline Rock of the Siljan Ring Area, Central Sweden. 1990.
31. *Torbjörn Wigren*: Recursive Identification Based on the Nonlinear Wiener Model. 1990.
32. *Kjell Janson*: Experimental investigations of the proton and deuteron structure functions. 1991.
33. *Suzanne W. Harris*: Positive Muons in Crystalline and Amorphous Solids. 1991.
34. *Jan Blomgren*: Experimental Studies of Giant Resonances in Medium-Weight Spherical Nuclei. 1991.
35. *Jonas Lindgren*: Waveform Inversion of Seismic Reflection Data through Local Optimisation Methods. 1992.
36. *Liqi Fang*: Dynamic Light Scattering from Polymer Gels and Semidilute Solutions. 1992.
37. *Raymond Munier*: Segmentation, Fragmentation and Jostling of the Baltic Shield with Time. 1993.

Distributor: Uppsala University Library, Box 510, S-751 20 Uppsala, Sweden

Elónio Muiuane

Hydrogeophysics of Tropical Africa. Recent Advances and Perspectives

Dissertation in Geophysics, to be publicly examined in Axel Hamberg-salen, Geocentrum, Villavägen 16, on December 10, 1999 at 10:00 a.m., for the degree of Doctor of Philosophy. The examination will be conducted in English.

Abstract

Muiuane, E., 1999. Hydrogeophysics of Tropical Africa. Recent Advances and Perspectives. Acta Universitatis Upsaliensis, *Uppsala Dissertations from the Faculty of Science and Technology* 21. 140 pp. Uppsala. ISBN 91-554-4594-8.

In the present work an attempt is made to put into perspective the hydrogeophysical investigations for rural water supply carried out over the last two decades in tropical Africa, paying special attention to groundwater targets in the weathered rocks in and above the crystalline basement. The applicability of geophysical techniques in groundwater investigations in tropical Africa, particularly the DC resistivity and electromagnetic techniques is discussed in the light of recent developments in instrumentation, data collection and interpretation procedures.

Although there has been an increase in the use of 2D resistivity surveying systems, standard VES is still the main tool of geophysical surveys for groundwater in Africa, where it is often used to characterise the lithology of the weathered layer. In the present work, two automatic 1D inversion schemes based on iterative least squares procedures with singular value decomposition are presented. In order to reinforce the convergence of the inversion schemes towards a global minimum, the standard least squares procedure is combined with other measures of robustness and search strategies in the parameter space. Tests with synthetic and field data prove their usefulness for fast interpretation of DC resistivity data. Compared with plane wave RMT data DC resistivity data generally seem to have less resolving power for the models tested.

Elónio Muiuane, Department of Earth Sciences, Uppsala University, Villavägen 16, S-752 36 Uppsala, Sweden

ACTA UNIVERSITATIS UPSALIENSIS
*Uppsala Dissertations from
the Faculty of Science and Technology*
21

ELÓNIO MUIUANE

Hydrogeophysics of Tropical Africa

Recent Advances and Perspectives



UPPSALA 1999

Dissertations for the Degree of Doctor of Philosophy in Geophysics,
presented at Uppsala University in 1999

Abstract

Muiuane, E., 1999. Hydrogeophysics of Tropical Africa. Recent Advances and Perspectives. Acta Universitatis Upsaliensis, *Uppsala Dissertations from the Faculty of Science and Technology* 21. 140 pp. Uppsala. ISBN 91-554-4594-8.

In the present work an attempt is made to put into perspective the hydrogeophysical investigations for rural water supply carried out over the last two decades in tropical Africa, paying special attention to groundwater targets in the weathered rocks in and above the crystalline basement. The applicability of geophysical techniques in groundwater investigations in tropical Africa, particularly the DC resistivity and electromagnetic techniques is discussed in the light of recent developments in instrumentation, data collection and interpretation procedures.

Although there has been an increase in the use of 2D resistivity surveying systems, standard VES is still the main tool of geophysical surveys for groundwater in Africa, where it is often used to characterise the lithology of the weathered layer. In the present work, two automatic 1D inversion schemes based on iterative least squares procedures with singular value decomposition are presented. In order to reinforce the convergence of the inversion schemes towards a global minimum, the standard least squares procedure is combined with other measures of robustness and search strategies in the parameter space. Tests with synthetic and field data prove their usefulness for fast interpretation of DC resistivity data. Compared with plane wave RMT data DC resistivity data generally seem to have less resolving power for the models tested.

Elónio Muiuane, Department of Earth Sciences, Uppsala University, Villavägen 16, S-752 36 Uppsala, Sweden

© Elónio Muiuane 1999

ISSN 1104-2516

ISBN 91-554-4594-8

Printed in Sweden by Elanders Gotab, Stockholm 1999

CONTENTS

Acknowledgements	9
1. General Introduction	11
1.1. Background	12
1.2. Future Perspectives	15
1.3. Scope of the Work	16
2. Tropical Africa	19
2.1. Climate	19
2.2. Geological Background	21
2.2.1. Introduction	21
2.2.2. Crystalline Basement	21
2.2.3. Sedimentary Basins	23
2.3. Geomorphology	23
2.4. Hydrogeology of Tropical Africa	23
2.4.1. Hydrogeological Parameters	25
2.4.2. Climatic Controls	27
2.4.3. Geological Controls	27
2.4.3.1. Lithology	27
2.4.3.2. Weathering	27
2.4.3.3. Fractures and Dykes	30
2.4.4. Geomorphological Controls	30
2.4.5. Groundwater Targets in the Crystalline Basement in Africa	32
2.4.5.1. Introduction	32
2.4.5.2. Weathered Bedrock Aquifers	33
2.4.5.3. Fractured Bedrock Aquifers	34
2.4.5.4. Composite Aquifers	35
2.4.5.5. Perched Water Aquifers and Sand Rivers	35
2.5. Hydrogeology of Sedimentary Basins in Africa	35
2.5.1. Introduction	35
2.5.2. Groundwater Targets in the Sedimentary Basins	36
2.5.2.1. Unconsolidated Sedimentary rock Aquifers	36
2.5.2.2. Sandstone Aquifers	36
2.5.2.3. Carbonate Aquifers	37
2.5.2.4. Aquifers in the Interface Sediment Cover / Basement	37
2.6. Summary	37
3. Hydrogeophysics of Tropical Africa	39
3.1. Introduction	39
3.2. Physical Characteristics of Groundwater Targets	40

3.2.1. Electrical Properties	40
3.2.1.1. Electrical Conductivity	40
3.2.1.2. Dielectric Properties	44
3.2.1.3. Induced Polarisation Effects	45
3.2.2. Density	46
3.2.3. Seismic Velocity	46
3.2.4. Magnetic Susceptibility	46
3.3. Geophysical Methods in Groundwater Prospecting in Africa	47
3.3.1. Overview of Principles, Field and Interpretation Techniques	47
3.3.1.1. DC Resistivity Methods	47
3.3.1.2. Electromagnetic (EM) Methods	48
3.3.1.2.1. Horizontal Loop EM (HLEM) Method	49
3.3.1.2.2. Magnetotelluric (MT) and Audiomagnetotelluric (AMT) Methods	50
3.3.1.2.3. Controlled Source audiomagnetotelluric (CSAMT) Method	51
3.3.1.2.4. Conventional VLF and VLF Resistivity Methods	51
3.3.1.2.5. Time Domain Electromagnetic (TEM) Method	52
3.3.1.3. Seismic Methods	53
3.3.1.4. Potential Field Methods	54
3.4. An Overview of Case Histories	54
3.4.1. Crystalline Basement	54
3.4.2. Sedimentary Basins	57
3.5. Summary	61
4. Recent Developments in Geoelectric Methods for Shallow Studies	63
4.1. Introduction	63
4.2. Resistivity Methods	63
4.2.1. General	63
4.2.2. Basic Principles of Electrical Resistivity Tomography (ERT)	64
4.2.3. Induced Polarisation (IP) Method	65
4.3. Electromagnetic (EM) Methods	67
4.3.1. Frequency Sounding EM Methods	67
4.3.2. Controlled Source Radio MT (RMT) Method	68
4.3.3. Time Domain EM Methods	69
4.3.4. Ground Penetrating Radar (GPR)	69

4.3.4.1. Basic Principles	69
4.3.4.2. Examples of Application in Hydrogeology	71
4.4. Hybrid Methods	72
4.5. Nuclear Magnetic Resonance (NMR) Method	72
4.5.1. Basic Principles	72
4.6. Summary	73
5. Developments in the Interpretation of Geophysical Data	76
5.1. Introduction	76
5.2. Automatic 1D Interpretation of DC Resistivity Sounding Data	78
5.2.1. Outline of the Method	78
5.2.1.1. Stripping the Earth from Top to Bottom	78
5.2.1.2. Reparameterisation of Model Parameters	79
5.2.1.3. Strategy for Finding Initial Models	80
5.2.1.4. The final Model	81
5.2.2. Illustration of the Inversion Scheme	82
5.2.2.1. General	82
5.2.2.2. Modelling Results	83
5.2.3. Discussion and Conclusions	91
5.3. Automatic 1D Inversion of DC Resistivity Data Using a Quality Based Truncated SVD	92
5.3.1. Definition of the Initial Model	92
5.3.1.1. Vertical Resolution	92
5.3.1.2. Resistivity of the Initial Model	93
5.3.1.3. Reparametrisation of Model Parameters	93
5.3.1.4. The Final Model	94
5.3.2. Some Considerations on Theoretical and Practical Aspects of Truncated SVD	94
5.3.2.1. Principles of Truncated SVD Inversion	94
5.3.2.2. Implementation of the Minimum Mean Squared Error (MSE) in a Non-Linear Problem	97
5.3.3. Results of Numerical Studies	98
5.3.3.1. Illustration of the Inversion Scheme with Synthetic Data	98
5.3.3.2. Illustration of the Inversion Scheme with Field Data	108
5.3.4. Discussion and Conclusions	115
6. General Discussion and Conclusions	117
6.1. General Discussion	117
6.1.1. Hydrogeology of Tropical Africa	117
6.1.2. Hydrogeophysics of Tropical Africa	118

6.1.3. Resistivity Data Interpretation	120
6.2. Conclusions	122
6.2.1. Geophysical Data Collection	122
6.2.2. Resistivity Data Interpretation	123
6.3. The Way Ahead	124
References	126

Acknowledgements

To come up to the point of writing these final lines, it has been a very long way since my first study visit to Uppsala in the early 1992. Thus, I could not resist the temptation to express a few words of gratitude to those who directly or indirectly supported me during all these years.

First of all I would like to express my sincere gratitude to my supervisor, Professor Laust Börsting Pedersen, for his patience and encouragement particularly in the initial and final stages of my work.

I am further indebted to the staff at the Solid Earth Physics especially to Drs. Roland Roberts and Christopher Juhlin for their valuable comments and suggestions on some of the work presented in this thesis. Many thanks are also due to Dr. Dan Dyrelius for his advices on rock properties and for providing me with the literature on the subject. A special thank for the members of the Potential Field group, Mehran Gharibi, Dr. Martin Engels, Merhdad Bastani and Behrooz Oskooi for the support and encouragement given during my studies. I am also indebted to Johannes Schmidt for the support given in solving some of the computer problems.

I must also thank Dr. Torleif Dahlin for providing me with the DC resistivity data set from Zimbabwe which was used to test one of the inversion schemes presented here. Thanks are also due to Professor Niels B. Christensen for providing me with the SELMA programme which was used for forward calculations in the two inversion schemes.

SIDA/SAREC, the sponsor of the Hydrogeology and Geophysics Research Programme under which umbrella this work was carried out as well as the Eduardo Mondlane University, Faculty of Science are greatly acknowledged for creating the conditions that made the conclusion of this work possible.

My final acknowledgement are to my wife, Adozinda and daughter Lotta Linnea for their support, encouragement and long suffering patience during my long stays in Uppsala.

1. General Introduction

Despite advances in global water supply coverage during and after the International Drinking Water and Sanitation Decade, 1981-1990, around one billion persons (20 per cent of the global population) lack access to safe drinking water (World Health Organisation, WHO, 1997b). Coverage with adequate sanitation is even lower (estimated at 50 per cent). Lack of access to basic water and sanitation is often associated with poverty and the poor often pay more for an inaccessible supply of small volumes of water of doubtful quality.

The situation is particularly severe in the African continent, where over half of a population of ca. 800 millions is without safe drinking water. During the "Water Decade", 1981-1990, sub-Saharan Africa experienced an increase in water supply coverage from 32% to 46%, while sanitation coverage increased from 28% to 36% (WHO, 1997b). Since then, however, progress has stagnated, and more people are without adequate services in Africa today than in 1990 (figure 1.1-1).

The water supply in the African continent is highly constrained by a wide range of climatic, geologic, socio-economic and technological factors just to mention a few. The main purpose of the present work is to shed some light on some of these aspects. A particular emphasis is given to the applicability of geophysical techniques for groundwater exploration in the context of fresh water supply for domestic and industrial uses in the urban and rural areas of Africa with special emphasis to sub-Saharan Africa.

The present work, basically, consists of two parts. In the first part which consists of chapters two to four, a review of relevant scientific work in hydrogeology and hydrogeophysics of tropical Africa as well as a discussion of recent developments in geoelectric methods in a groundwater perspective are provided. The bulk of the material reported in this review, was mainly drawn from recent publications on groundwater exploration, in connection with drought relief and accelerated development programmes which were commissioned in many parts of the sub-Saharan Africa in the last two decades. The journals that have been scanned most for recent publications are: Geophysics, the Journal of Applied Geophysics, Geophysical Prospecting, Geophysical Journal International, Quarterly Journal of Engineering Geology, Groundwater and some national journals of hydrogeology and hydrology. Relevant information on groundwater exploration in Africa was also drawn from a number of published and unpublished reports of international development and

funding agencies such as the World Health Organisation (WHO), the World Bank (WB), the United Nations Development Programme (UNDP) and numerous Non Governmental Organisations (NGOs). It should be noted however, that the developments in these topics are very fast and thus, much of the literature is widely scattered, diffuse and in most cases not readily accessible. Therefore, the information contained in this review is not intended to be exhaustive. Instead, an attempt has been made to compile and document the most readily accessible and pertinent literature and to put it into a perspective.

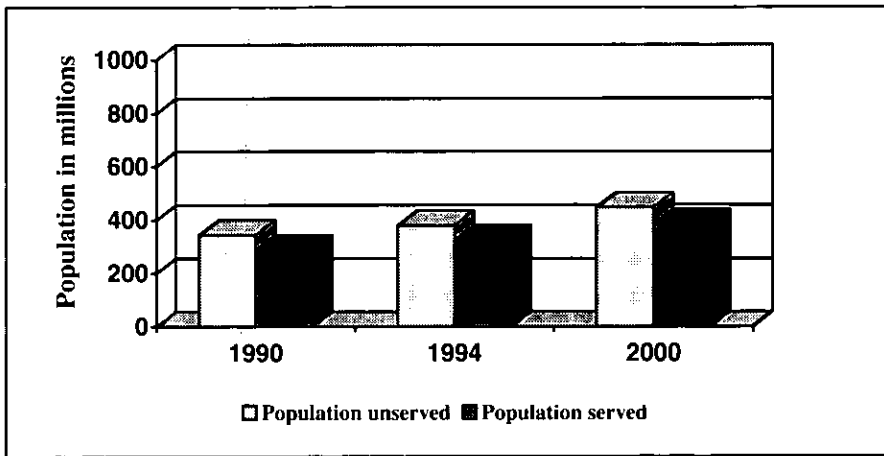


Figure 1.1-1. Water supply services coverage in Africa (Source: WHO, 1997b).

In the second part which consists of chapters five and six, the automatic 1D inversion of DC resistivity data is discussed on the basis of two inversion schemes (Muiuane and Pedersen, 1999a and 1999b). In the last chapter a summary of the work including a few pointers concerning future areas of improvement in the field of groundwater geophysics in tropical Africa are given.

1.1. Background

The African continent as a whole is suffering from a chronic water deficit. A large portion of the continent lies entirely between the tropics and is generally characterised by low average annual precipitation rates. Therefore, its water resources are limited in time and space. According to the World Development Report (WDR, 1994),

a large portion of financial assistance provided to African developing countries by many international funding and development agencies such as WB and UNDP is devoted to the water sector. Despite all this huge investment the situation has not improved very much as is shown by recent estimates (Wright, 1992; WHO, 1997b), which suggest that only ca 30 to 40 % of the population of the sub-Saharan Africa has access to a clean potable water supply of minimum quantity and quality (e.g. 25 litres per head per day; WHO, 1997a). The situation is clearly illustrated in figure 1.1-1.

Due to irregular distribution of precipitation as well as high evaporation rates, the surface water resources tend to be limited and highly marked by seasonal variations in the climate. Therefore, groundwater is becoming increasingly important as a dry season supplementary supply to support stable economic conditions. Even in more humid regions (e.g. along the equatorial belt, with precipitation rates of more than 1000 mm/year), water quality considerations can favour its use. Groundwater is generally free from bacteriological pollution; it has an almost constant quality and temperature and it is available in large quantities. It has been estimated e.g. van Der Leeden et al. (1990), that more than 60 % of the fresh water found on Earth is in the form of groundwater.

It is no coincidence, therefore, that over the past decades groundwater has progressively become a subject of scientific discussion and investigation in the international geophysical community. The amount and standard of technical publications on groundwater subjects testify to the essential soundness of the field (e.g. Stoner and Bakiewicz, 1987; Chapellier et al., 1991 and 1994; McNeill, 1990 and 1991; Ward, 1990; Nabighian, 1991; Sandberg, 1993; Christensen and Sorensen, 1994; Meju et al., 1999 and many others). As a result, the knowledge and understanding of groundwater conditions and their controlling factors have improved radically and the properties of many of the major aquifers are well defined but others remain comparatively unknown and much more work is still needed.

The scientific progress in the field of groundwater geophysics has arisen basically in two ways; (1) in the industrial countries there has been an increasing realisation of the need to conserve and protect water resources and to ensure economic supplies as well as the need of safer conditions in association with radioactive waste disposal (e.g. Ward, 1990; McNeill, 1990; Nobes, 1996; Reynolds, 1997; etc) whereas, (2) in the non-industrialised nations much of the increased emphasis on groundwater resources and the improvements in the investigation techniques are related to the growth in population needs in the form of potable water supplies, live stock watering and small scale irrigation (e.g., Palacky et al., 1981; Dobeck and Romig, 1985; Romig,

1986; Chapellier et al., 1991 and 1994; Wright and Burgess, 1992; Dahlin, 1993; Bourgeois et al., 1994; Giroux et al., 1997; Ritz et al., 1999a and 1999b; etc). On the other hand, in many parts of the non-industrialised countries, there is little potential for further development of surface water schemes without the construction of costly dams. Thus, provision of improved supplies to the remainder of dispersed rural population must come inevitably from groundwater.

In the African continent, groundwater is generally exploited from the Crystalline Basement (CB) aquifers, i.e. within the weathered and/or fractured bedrock of intrusive, metamorphic and/or volcanic origin (e.g. Palacky et al., 1981; Clark, 1985; Acworth, 1987; White et al., 1988; Hazell et al., 1988; Wright and Burgess, 1992; etc). Crystalline Basement (CB) aquifers and other shallow aquifers such as perched (or suspended water aquifers), sand rivers, etc, are usually recharged directly or indirectly by rainfall.

In some areas, economically exploitable aquifers may occur, e.g. in the interface between the thick sediment cover and the bedrock in major sedimentary basins, or in considerably greater depths (up to 1000 m) as is the case in many parts of Sahara and Kalahari deserts, e.g. sandstone aquifers (e.g. Bourgeois et al., 1994; Giroux et al., 1997). In contrast to the previous group, these aquifers are usually not recharged by the rainfall and therefore, they are not sensitive to the present climatic changes and are often referred to as fossil aquifers. On a continental scale, they are more or less of regional character due to their lateral extent and depths involved. However, over the last years they have been increasingly exploited in many parts of Africa.

CB aquifers are of particular importance in the tropical and sub-tropical Africa, both because of their widespread distribution, accessibility and the continent's very dispersed rural populations which, in combination with the poor economic base, are responsible for the small scale of existing groundwater development schemes (e.g. Wright, 1992). However, due to the typically low productivity and discontinuity of basement aquifers, there are a number of important constraints to their current development which may include:

- (1) The frequent high failure rates of boreholes, commonly in the range of 10-40% (Wright, 1992), with the higher rates in the drier regions (e.g. annual precipitation rates less than 650 mm) or where the weathered layer is less developed.
- (2) Limited sensitivity of current exploration techniques and an incomplete understanding of the controls on basement aquifer occurrence.

(3) The low storage capacity of basement aquifers which may result in a periodic depletion during sustained drought periods.

(4) Shallow occurrence, fracture and/or fissure permeability which make the aquifer susceptible to surface pollutants, since the most common means of groundwater withdrawal in many urban, and rural areas are shallow boreholes and/or traditional dug wells.

1.2. Future Perspectives

Due to the rapidly growing population in sub-Saharan Africa, it is foreseen that the demand of water in the coming decades will increase significantly (WDR, 1994). Therefore, there is a need to increase the efficiency of groundwater exploration programmes, which implies an improvement of the current borehole success rates. According to van Dongen and Woodhouse (1994), one aspect of low-cost community water supply that has received less attention is groundwater exploration, particularly the borehole siting strategy. The proper location or siting of a borehole can significantly increase the success rate and reduce the cost of the programme. One of the ways to achieve this objective is to design and implement cost effective, fast and precise groundwater prospecting field procedures. Although many of the investigation techniques applicable in groundwater prospecting in other climatic regions can be used in the arid and semi-arid zones, the scarcity of water in these areas as well as the geological complexity of groundwater structures does invoke different dimensions of hydrogeological study and different standards of economic viability.

The geophysical techniques, especially the electromagnetic (EM) and the direct current (DC) resistivity techniques, have played a very important role in such investigations for many years and improvements in instrumentation and techniques of data acquisition and interpretation are resulting in a widening of their applications. In some cases, they are still being used merely to single out potential areas of groundwater occurrence but there is considerable interest in the possibility of using geophysics to estimate the structural, hydraulic and hydro-chemical parameters of aquifers, i.e. their exact vertical and horizontal extent, their permeability and porosity as well as the chemical characteristics of the pore fluids (e.g. Mbonu et al., 1990; Weller and Börner, 1996; Vanhala et al., 1992; Efferso and Sorensen, 1996).

According to many authors such as Palacky et al. (1981); Senti (1988) and van Dongen and Woodhouse (1994), a large portion of world-wide geophysical expenditure for groundwater exploration is spent in Africa, where geophysical prospecting for groundwater has become as important as mineral prospecting.

Recent results of several field campaigns and exploratory drillings carried out in selected areas with higher than normal failure rates (often >50%) and in many cases at the general locations of failed boreholes suggest that significant success and often higher than normal borehole yields can be obtained by more careful field surveys (Wright, 1992; Barker et al., 1992; Reynolds, 1997). For this end, more focussed studies are needed in order to improve the understanding of the controlling factors of groundwater occurrence. A better combination of techniques and characterisation of the physical and structural properties of groundwater targets in the CB is crucial for an efficient application of geophysical exploration techniques (e.g. Robain et al., 1996; Ritz et al. 1999a).

It is also important to emphasise that groundwater targets and their associated variations in physical properties (e.g. electrical conductivity) and target sizes, are generally smaller compared to anomaly ranges in mineral exploration (McNeill, 1991). Therefore, in such surveys, high resolution techniques are of prime importance in the resolution of pertinent groundwater structures.

1.3. Scope of the Work

Although many geophysical studies for groundwater prospecting in the CB and other geological environments of the tropical Africa have been carried out over the years (e.g. Palacky et al., 1981; White et al., 1988; Chapellier et al., 1991; Barker et al., 1992; Botha et al., 1992; Bourgeois et al., 1994), the virtues and limitations of the techniques are not yet fully established and/or documented, partly due to the incomplete understanding, complexity and widespread variability of the physical and structural characteristics of groundwater aquifers in such environments. Therefore, it is hoped that the present work will highlight some of the problem areas as well as some of the recent developments and their applicability in the practice of groundwater prospecting in such environments.

The purpose of the second chapter is neither to cover the whole subject of hydrogeology in general nor the whole hydrogeology of Africa in particular, but instead to summarise some of the aspects of the latter on the basis of recent field studies (e.g. Clark, 1985; Jones, 1985; Acworth, 1987; Houston, 1988; Wright and Burgess, 1992; etc).

Readers interested in a more elaborate description of some of the hydrogeological concepts referred to here, are therefore, recommended to consult standard text books such as Freeze and Cherry (1979) or Fetter (1988). However, for the sake of clarity, some few basic concepts necessary for a quick understanding of the text, will be introduced in section 2.4.1.

The third chapter gives an overview of the geophysical exploration for groundwater in Africa. It starts with a description of some physical properties of groundwater targets, with a special emphasis to the physical properties of weathered layers. This is followed by an overview and brief description of those techniques currently in use for groundwater studies including a discussion of their advantages and disadvantages. It is to be noted that on the international arena, much of the recent geophysical literature related to groundwater exploration report on new developments in geophysical techniques for groundwater exploration, e.g. the application of Very Low Frequency (VLF) technique for fracture detection, Horizontal Loop EM (HLEM) for quick mapping of vast and remote areas, audio magnetotelluric (AMT) for structural surveys of sedimentary basins, etc. However, most of these methods were developed in the northern hemisphere in countries with temperate or cold climate and, when used in a tropical environment, their effectiveness decreased considerably (e.g. Palacky and Kadokaru, 1979). The geoelectrical methods (i.e. DC resistivity and EM methods) are particularly affected by deep weathering common in the tropical areas. Prospects for future groundwater development in Africa suggest that in the next decades there will be a rapid increase in water demand for both domestic and industrial purposes due to growing urban and rural African population and accelerated development programmes.

Development in many African countries also includes increasing industrialisation and intensive agriculture practice, all increasing the likelihood of groundwater contamination. Therefore, there is a growing awareness on the relationship between the overall availability of water resources and its quality. Therefore, the application of geophysical techniques to study physicochemical processes which might have a significant environmental impact in groundwater resource exploitation and management is also growing rapidly. Such studies are generally characterised by an increasing demand for detailed knowledge of subsurface features and hence, high resolution survey techniques. High resolution implies a dense coverage of the survey area and thus 2D surveying. In chapter four, a review of some recent developments in geoelectric techniques for shallow studies including a brief discussion of their capabilities and limitations in groundwater studies is provided.

The aim of any geophysical survey is to construct a model of the subsurface geology on the basis of the collected data. As pointed out in previous section, the geophysical targets in groundwater prospecting are, generally, characterised by small anomaly contrasts. Moreover, the recent trends and requirements on geophysical techniques are towards fast and detailed description of geological structures especially in connection with hydrogeological and environmental studies. Therefore, robust and fast interpretation procedures are becoming increasingly important. The inversion of geophysical data is discussed in the chapter five. This includes the description of two inversion schemes for 1D automatic interpretation of DC resistivity data, which were developed in the framework of the present study (Muiuane and Pedersen, 1999a and 1999b).

2. Tropical Africa

2.1. Climate

Much of the African continent lies between the tropics, i.e. between the parallels of latitude $23^{\circ} 27'$ north and south of the equator, which are also called the Tropic of Cancer and the Tropic of Capricorn, respectively. The zone of greatest incoming solar radiation moves from the southern hemisphere in January to the Tropic of Cancer in the north during July, followed by a trough of inflow of maritime air masses from the Indian and Atlantic Oceans. Figure 2.1-1 shows the seasonal pressure, the air flow patterns, the trough of low pressure and the zone of converging air from the higher pressure zones on either side, which is referred to as the Inter-Tropical Convergence Zone (ITCZ). The ITCZ is responsible for much of the seasonal variation in rainfall throughout tropical and sub-tropical Africa (Farquharson and Bullock, 1992).

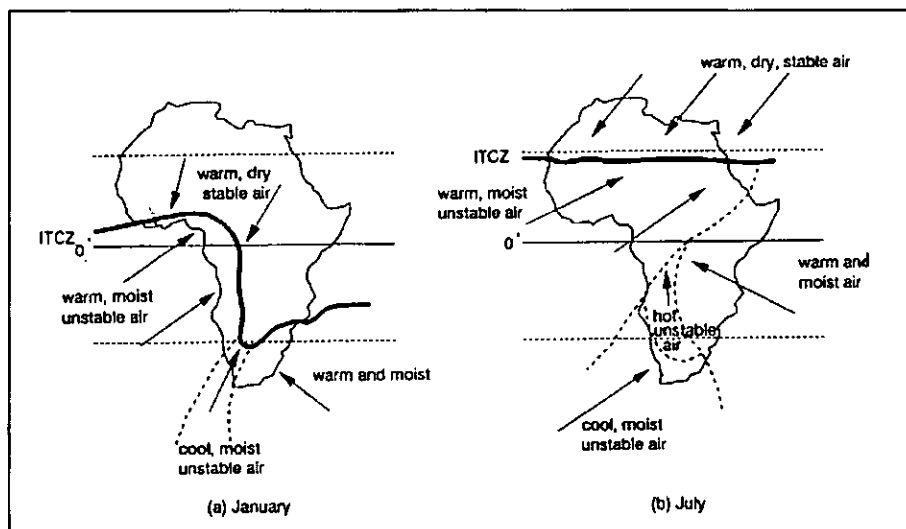


Figure 2.1-1. Mean position of the ITCZ (a) in January and (b) in July (after Balek, 1983).

In general, southern Africa has a summer rainfall whereas the eastern and western parts and the equatorial belt display bimodal seasonal rainfall patterns, i.e. with rain inputs in December/January and July/August, due to the north and south movements of the ITCZ.

Thus, the seasonal system of winds and rainfall depends mainly on the general circulation patterns of the atmosphere, which are driven by the seasonal migration of the sun between the tropics. Figure 2.1-2 displays the distribution of the mean annual rainfall in mm. The highest rainfall is recorded along the equator belt (about 2000 mm/year) and is marked by two distinct peaks, due to the north and south movements of the sun. The lowest rainfall (less than 100 mm/year) are recorded along the Sahara and Kalahari deserts.

Although over much of Africa south of Sahara the mean annual rainfall is high enough for one to expect significant recharge to be available, this rain is usually seasonal and falls within a limited period of the year. Moreover, the incoming solar radiation is very high and thus, the evaporation rates are usually very high, ranging from over 3000 mm/year in arid regions of Sudan to perhaps 1300 to 1400 mm/year in highland regions of Malawi, Rwanda and Burundi (Balek, 1983). Therefore, less water is available for aquifer recharge. Under such a marked and limited seasonal recharge regime, any groundwater development scheme in the CB must be able to last through a prolonged period between recharge events.

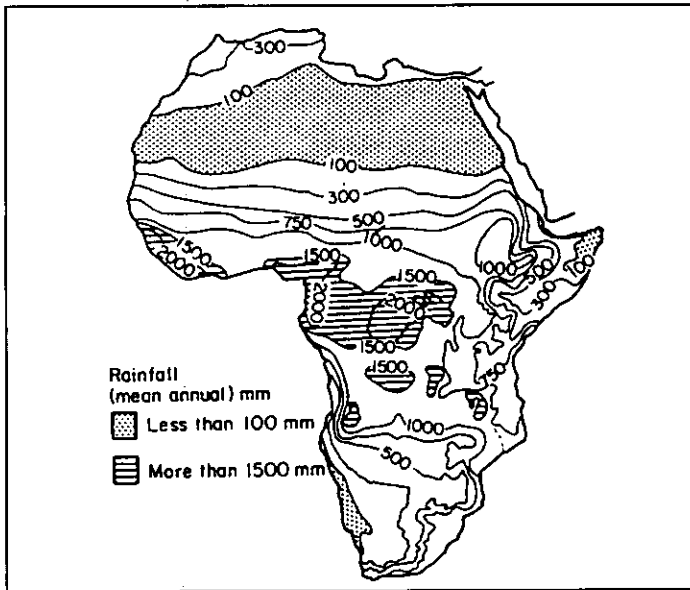


Figure 2.1-2. Distribution of mean annual rainfall in mm (after Clark, 1985). Although some parts of the continent have a mean annual rainfall above the average (e.g. the narrow equatorial strip), in other

parts there have been large scale fluctuations during recent decades (i.e. cycles of abnormally wet and dry conditions).

2.2. Geological Background

2.2.1. Introduction

The present geological outline is intended to give a general overview of geological aspects which may have significant hydrogeological implications, and therefore it will be kept rather brief. Readers interested in penetrating deeper in the subject are referred to more extensive works such as Tankard et al. (1982); Gwavava et al. (1996); Qui et al. (1996) and many others.

In brief, the African continent can be considered as being made up of two distinct subareas based on differences in geologic and hydrogeologic characteristics. One subarea consists of igneous, metamorphic volcanic rocks of different composition, genesis and age and the other subarea consists of a number of unconsolidated and partly consolidated sedimentary rocks infilling shallow and deep basins. Because the rocks that form the first subarea have similar hydrogeologic characteristics, they are grouped as one geologic unit for the purpose of this study and are referred to as Crystalline Basement (CB). Parts covered by sedimentary rocks will be referred to as sedimentary basins. Figure 2.2-1 summarizes the distribution of CB and sedimentary basins in Africa.

2.2.2. Crystalline Basement (CB)

The CB of Africa is made up of three major suites of rocks; (1) granite-gneiss-greenstone association of Archaean cratonic nuclei (older than 2.500 million years); (2) strongly deformed metamorphic suites in mobile belts, mainly of Proterozoic age (older than 590 million years) and (3) anorogenic intrusions which include Phanerozoic (younger than 590 million years) intrusive magmatic rocks related to rifting (Key, 1992; Gwavava et al. 1996). In the CB, granite-gneiss-greenstone belts of the Archaean cratonic nuclei are surrounded by essentially Proterozoic orogenic provinces (mobile belts). Parts of the CB are igneous intrusions associated with anorogenic magmatism which include large Proterozoic intrusives such as the Bushveld Igneous Complex (South Africa) and many other intrusions emplaced later, i.e. from middle Palaeozoic times onwards (Key, 1992;).

The Phanerozoic anorogenic magmatism is mainly related to major faulting, rifting during the Mesozoic and Cenozoic continental

fragmentation (Gondwana Breakup) and subsequent (since Mesozoic) development of the East African Rift System. A number of small and large scale dykes and sills are known to have originated during this period, although some display an older age, e.g. the Great Dyke in Zimbabwe is estimated to have been emplaced at about 2.460 Million years (Gwavava et al., 1996). On a continental scale however, the Phanerozoic intrusions are considered to be of limited areal extent (e.g. southernmost tip and northwestern coastal zone of Africa) and therefore, they are not much relevant for the purposes of present study. In the African continent, CB, generally refers to intrusive rocks and to recrystallized sedimentary and volcanic rocks.

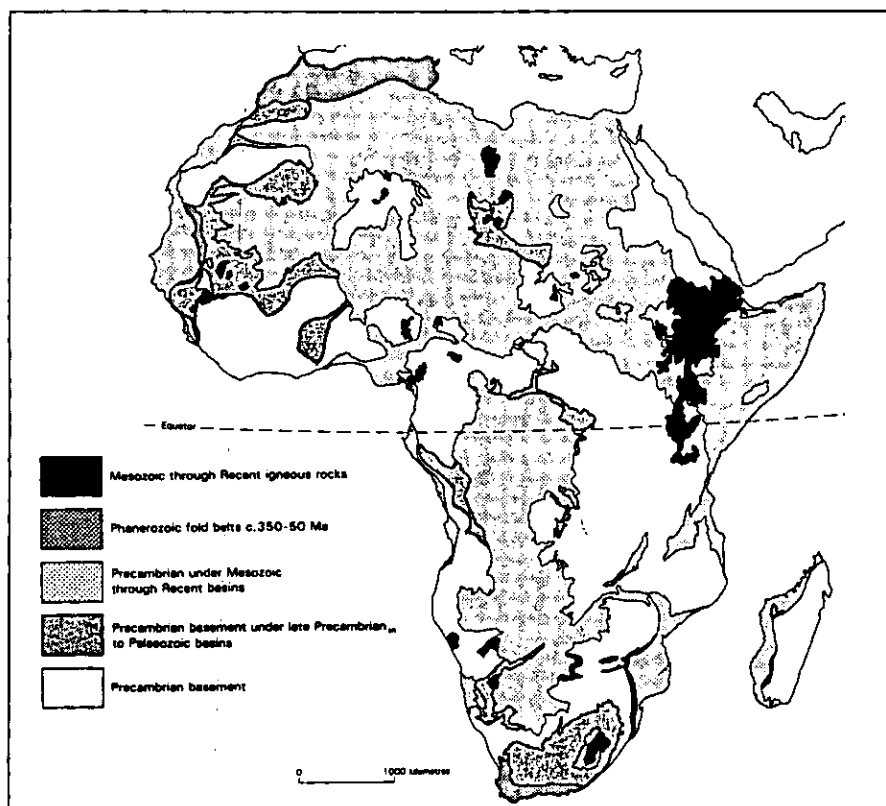


Figure 2.2-1. A simplified geological outline showing the distribution of the CB (i.e. Mesozoic through recent igneous rocks, the Phanerozoic folds belts and the archaen blocks) and major sedimentary (Mesozoic through recent basins and Precambrian to Palaeozoic) basins in Africa (modified from Key, 1992).

As will be described with more detail later, the hydrogeological conditions as well as the associated groundwater mechanisms in these two units are quite distinct.

2.2.3. Sedimentary Basins

Elsewhere in Africa essentially unmetamorphosed major sedimentary basins form important components of cover. The oldest known cover rocks are of Archaean age (older 2500 million years) and Lower Proterozoic sedimentary and volcanic sequences overlying the Kaapvaal Craton, e.g. the Pongola and Witwatersrand (South Africa). In terms of crustal development, the most important geologic event in the Phanerozoic is the breakup of the supercontinent Gondwana. In an early stage (i.e. Permian to Jurassic) the continent was subjected to intense tectonic activity during which large rift basins were filled with continental sedimentary deposits (Tankard et al., 1982 and Key, 1992). The sedimentary deposits include Karoo sedimentary sequences (southern Africa) which are made up of consolidated and partly consolidated sediments such as tillites, shales, sandstones, mudstones, carbonates (e.g. the Kalahari beds and margins of the CB), the extensive sedimentary basins (e.g. Chad and southern Sudanese Basins), and the volcano-sedimentary rocks related to rifting, e.g. the East African Rift System and the sedimentary basins along the coastal regions of Kenya, Tanzania, Mozambique and some parts of west Africa (figure 2.2-1).

2.3. Geomorphology

Across much of tropical Africa, the topography is dominated by high, old plateau landsurfaces whose altitude increases eastwards towards the shoulders of the Rift Valley. In places, the CB complex is overlain by a thick cover of in situ, chemically-weathered overburden (e.g. Jones, 1985; Acworth, 1987). As will be detailed in section 2.4., the geomorphology plays an important role (in both local and regional scales) in the weathering processes and hence, in the hydrogeology of an area.

2.4. Hydrogeology of Tropical Africa

Tropical Africa, as far as water resources is concerned has few permanent surface water resources, away from the major rivers and lakes. The population in this vast area is, therefore, wholly or partly

dependent on groundwater for its water supply. Major aquifers do occur in large sedimentary basins such as the Chad Basin, the Kalahari beds, but a large portion of tropical Africa is underlain by the relatively impermeable rocks of the CB. It has been estimated that the basement complex underlies an area inhabited by more than 50 million people (Clark, 1985), and providing adequate water supplies for these people is a major problem for many African countries.

Crystalline rocks are usually characterized by having very low primary porosity (less than 1%) and permeability. However, under certain geological, climatic and geomorphological conditions, these rocks may develop into formations which are capable of storing and transmitting water at rates fast enough to supply reasonable amounts to wells, generally not less than $1 \text{ m}^3/\text{h}$ (Wright, 1992). In a groundwater perspective of the CB, the most important processes are the weathering, i.e. the breakdown and alteration of rock material near the Earth's surface as a response to the change of local physical conditions (Carroll, 1970) and the tectonic events which lead to formation of fractures, fissures and dykes. Weathering sequences, both ancient and modern, provide some of the most important shallow aquifers (e.g. Wright, 1992; Acworth, 1987; Houston and Lewis, 1988; White et al. 1988).

The African CB has been affected in different periods of its development by a wide range of brittle fracturing and tectonic events, which led to generation of open folds and crenulations which have a critical influence in groundwater storage (Clark, 1985). The fracturing varies in age from Archaean, within the greenstone belts, to Phanerozoic, for faults related to movement of the African Plate (Gondwana Breakup), with ongoing Quaternary faulting in the major tensional rifts such as the East African Rift System. Thus, there are two major modes of groundwater occurrence in the CB: (1) the weathered bedrock, often referred to as regolith aquifers and (2) the fractured bedrock aquifers. The fact that the weathering and fracturing have a strong influence in hydrogeology of crystalline rocks suggests that the groundwater occurrence in these geological environments is structurally controlled (e.g. Clark, 1985; Key, 1992). Moreover, the relatively low permeability and discontinuity of such features excludes the possibility of occurrence of regional aquifers and thus, the aquifers are mainly of local character and each site has to be treated as unique. In the following sections the factors controlling the occurrence of groundwater will be summarised.

2.4.1. Hydrogeological Parameters

In hydrogeology, the concept of intrinsic permeability, k , which is defined as the property or capacity of a porous rock, sediment, or soil for transmitting a fluid, i.e. the measure of the relative ease of fluid flow under equal pressure (Bates and Jackson, 1987), is central. The intrinsic permeability which is often given in units of Darcy [$\approx 10^{-11} \text{ m}^2$] is defined as follows:

$$k = \frac{K\mu}{\rho g} \quad (2.1)$$

Where K is the hydraulic conductivity (in units of velocity), μ is the dynamic viscosity, ρ is the fluid density. However, in practical work on groundwater, the term hydraulic permeability (K) is utilised. Representative values of hydraulic conductivity and porosity for some common Earth materials are given in table 2.4.1.

Table 2.4.1: representative values of hydraulic conductivity and porosity (source: Bowen, 1986).

Rock Material	Hydraulic conductivity (m/day)	Porosity (%)
Coarse gravel	150	28
Coarse sand	45	39
Silt	0.08	46
Clay	0.0002	42
Fine sandstone	0.2	33
Limestone	0.94	30
Dune sand	20	45
Loess	0.08	49
Tuff	0.2	41
Basalt	0.01	17
Weathered granite	1.4	45

A hydrogeological system can, in general, be divided in two main zones, an unsaturated or partially saturated and often seasonally fluctuating zone which is referred to as vadose zone and a zone lying below the water table and thus in principle 100% saturated with water (figure 2.4-1). The grain size and characteristics of the material in both zones play a very important role in terms of hydrogeological behaviour of the system. Very fine material such as clay and silts

have a very large total porosity, i.e. they can store a large amount of water. However, due to their fine grain structure, layers composed of such type of material tend to retard the flow of fluids, i.e. they have a relatively low permeability. In hydrogeological terminology clayey and silty layers are referred to as aquitards or aquicludes depending on the value of permeability (see figure 2.4-1). On the other hand, coarse grained material such as sands and gravels are both porous and permeable, i.e. they can store and transmit water and thus, they are referred to as aquifers. Conversely, a formation that can neither store nor transmit water such as the fresh bedrock is said to be an aquifuge. In the practice, these units play different roles in different contexts, e.g. while an aquitard is generally undesirable in a purely hydrogeological context, it may be the main target in for example an environmental and/or resource protection perspective. An aquifer is said to be unconfined, phreatic or water table aquifer if it is overlain by a permeable layer and confined or artesian if it is overlain by an impermeable layer e.g. and aquitard. In some cases, after a period of rainfall, a water layer may become trapped above a shallow aquitard overlying an aquifer in which case is said to be a perched water table aquifer.

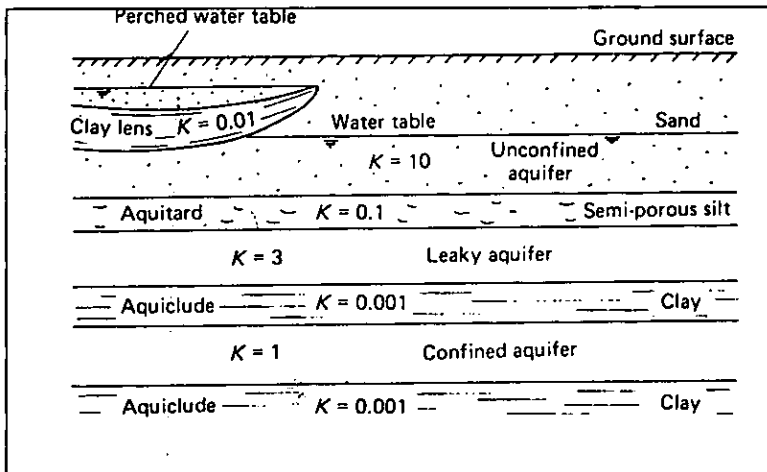


Figure 2.4-1. A conceptual model of a hydrogeological system illustrating the main units (from Shaw, 1994).

Although the quality and productivity of aquifers can be characterised by many other hydraulic parameters, throughout this work the concepts of permeability and discharge (total amount of water drained

per unit time; e.g. quantity in m^3/h) will be used for this purpose. Readers interested in more details concerning other parameters are thus, referred to standard text books such as Freeze and Cherry (1979) and Fetter (1988).

2.4.2. Climatic Controls

Rainfall and groundwater flow processes play a very important role in the formation of a weathered layer because they control the chemical reactions, leaching processes and aquifer recharge. Jones (1985) points out that one of the basic requirements for deep weathering to take place is the availability of an annual rainfall surplus for recharge. Therefore, thick weathered layers are to be expected in humid and sub-humid areas with high temperatures. The influence of the climatic conditions on the weathering intensity and hence on the groundwater occurrence will be described in section 2.4.3.2.

2.4.3. Geological Controls

2.4.3.1. Lithology

Although lithology is not in itself greatly important in basement hydrogeology, since all crystalline rocks are virtually impermeable in their unfractured and/or unweathered state, mineralogy, texture and granularity do affect the ways in which rocks fracture and decompose. According to Greenbaum (1992), differences in lineament pattern and density are evident from one basement formation to another. He highlighted this fact by pointing out that fractures that can be traced for several kilometres through the younger granites appear to terminate abruptly in the older gneiss formation. This in turn has an important effect upon weathering. In arid and semi-arid climates deep weathering tends to be concentrated along fissured zones. Acworth (1987) described the complex relationship between the many factors responsible for the processes of weathering on a groundwater perspective of the CB. Therefore, understanding the nature of lineaments and their hydrogeological role is crucial.

2.4.3.2. Weathering

Weathering is defined as the breakdown and alteration of materials near the Earth's surface to products that are more in equilibrium with

the newly imposed physicochemical conditions (Carroll, 1970). This definition is easy to follow for a plutonic rock; the rock is formed under conditions of high temperature and pressure in the absence of air and water, and when exposed at the Earth's surface the rock is subjected to reduced pressure and temperature and the presence of water to which it must adjust. Weathering processes are conventionally classified as chemical or physical. Chemical weathering generally results in a residuum of clayey or sandy materials depending upon the degree of weathering, whereas physical weathering often results a residuum of largely unaltered rock material. The degree of weathering is determined mainly by the climate, lithology, geomorphology and duration of exposure to the weathering agents (Carroll, 1970). The fundamental differences in the mode of weathering of dry and humid regions are due to moisture in the form of rainfall and temperature. The first part of the adjustment is brought about by oxidation; in humid tropical climates, with annual temperature of more than 19°C and annual rainfall of over 1000 mm, this is followed by leaching. When a strongly leaching condition occurs in a tropical climate, lateritization takes place. Lateritic layers, which consist of thin soil layers enriched with alumina, ferric oxide and titanic, are the most common soil features in the tropical climates (Balek, 1983). On the other hand, where there are no strong leaching conditions, or in sub-humid tropical climates, with annual rainfall less than 1000 mm, clayey soil material accumulates. Various authors (e.g. White et al., 1988; Palacky, 1987), have shown that the characteristics of the regolith are at least partly related to mean annual rainfall (figure 2.4-2). Kaolinite is the dominant clay mineral produced by weathering of CB rocks in most areas but especially where the rainfall is greater than 1000 mm. In lower rainfall areas, montmorillonite and to lesser extent illite are produced. Moreover, montmorillonite has a much smaller particle size than kaolinite, thus giving it greater water adsorption properties. Therefore, the regolith in the lower rainfall areas where montmorillonite predominates will tend to have higher concentrations of iron, magnesium, calcium and sodium. In general, high average temperatures in moist areas increase rock weathering by chemical processes, whereas high average temperatures in arid areas decrease chemical weathering and promote physical disintegration. This explains the occurrence of thick weathered layers (up to 80 m) in humid and sub-humid tropical regions (e.g. Jones, 1985; Acworth, 1987). Low average temperatures in moist areas cause soil freezing and decrease of both physical and chemical weathering processes. Not all rock types are equally affected by weathering. Mafic and ultramafic rocks are more susceptible to intense chemical weathering than felsic rocks which have a higher content of resistant minerals (e.g.

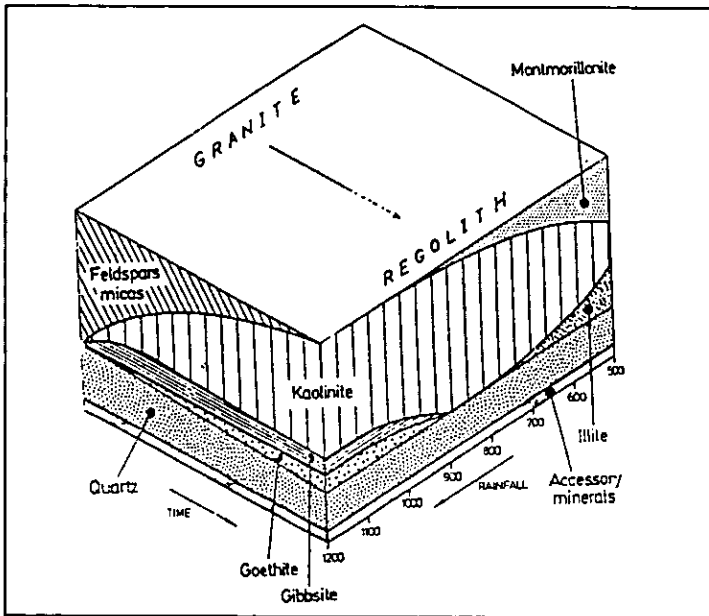


Figure 2.4-2. Relationship between regolith mineralogy, degree of weathering, mean annual rainfall and time of exposure to the weathering factors (after White et al., 1988).

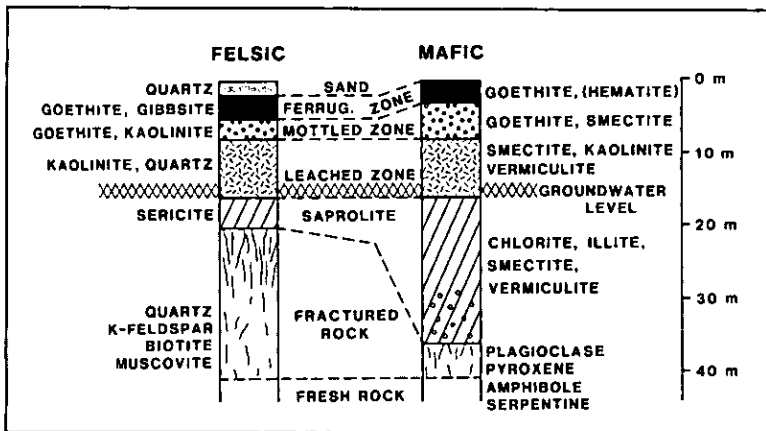


Figure 2.4-3. Relationship between weathering intensity and rock type (after Palacky, 1987). The sandy cover layer in the weathering profile of the mafic rock is missing-and the thicknesses of sapolite and the fractured rock are quite different in both cases.

quartz, muscovite). Therefore, the weathering profile or regolith over a mafic rock tends to be deeper than over a felsic rock (figure 2.4-3). As will be explained in more detail later, these factors have very important geophysical and hydraulic implications (e.g. White et al. 1988).

2.4.3.3. Fractures and Dykes

One of the factors controlling weathering and hence groundwater occurrence in the CB is the degree of fracturing and fissuring. The African continent has been subjected to a series of tectonic cycles since the early Archaean (Tankard, 1982; Key, 1992) and as a result brittle faults and fractures were generated. From the Phanerozoic onwards, the fracturing is mainly related to the movement of the African Plate and to the ongoing Quaternary faulting in the major tensional rifts such as the East African Rift System (Key, 1992). A large number of dolerite dykes and sills have been generated during the Phanerozoic tectonic cycle (Key, 1992). The dykes preferentially weather to control present drainage networks and consequently have important groundwater implications. In general, water boreholes are commonly successfully sited at the margins of the thicker (up to 50 m) dykes (e.g. Greenbaum, 1992; Gwavava et al., 1996). On the other hand, the dolerite sills being planar structures, in some areas of the sedimentary basins (e.g. Bourgeois et al., 1994) form the basement of the aquifers.

The fracture systems are related either to decompression or to compression forces. Fractures, faults and fissure systems have a critical influence on groundwater storage because they stimulate the weathering processes and hence, increase the secondary porosity and permeability of the rocks. Therefore, thick weathered layers are to be expected in areas which have experienced an active tectonic history (Greenbaum, 1992).

2.4.4. Geomorphological Controls

Geomorphology plays a dominant role in the occurrence of groundwater in basement areas because it controls the leaching history and hence, the nature and depth of the weathering mantle (regolith), which provides essential groundwater storage. Most of the tropical Africa has been exposed as continental land above sea level for over 200 million years (Jones, 1985). The modern landform in the basement

complex is generally dominated by the African erosion surface characteristically expressed as extensive plains of very low relief, whose altitude decreases westwards, away from the shoulder of the Rift Valley. In places, the plains form seasonally waterlogged bottomlands often referred to as dambos or bas-fonds, which are occasionally interrupted by inselbergs (figure 2.4-4). In the vicinity of an inselberg there is a hydrogeological differentiation due to relief and the thickness of the weathering profile can vary with the distance. The process of dambo formation is still a matter of debate but two hypotheses are currently widely accepted (e.g. McFarlane, 1992). Raunet (1985) points out that in the savanna plainlands of Africa with mean annual rainfall between 400-1400 mm, the dambos constitute important recharge units to the basement aquifers. However, where the mean annual rainfall is less than 400 mm direct recharge is negligible and thus groundwater resources are associated with runoff either in the river alluvium, valley bottoms or in the underlying regolith sequences.

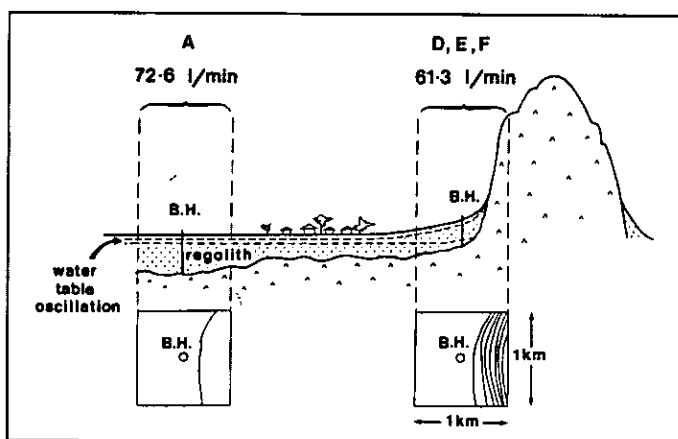


Figure 2.4-4. Schematic representation of borehole site options in the vicinity of an inselberg (after McFarlane et al., 1992). Boreholes (B.H.) located at sites of high relief zones (D,E,F), have relatively high yields despite thin regolith. However, the yields are lower compared to sites located at lower relief sites (A).

As to the dependance of the thickness of the weathering profile to the time of exposure, King (1962) points that the African erosion surface has undergone cyclic erosion processes since the late Jurassic (144 million years ago). Therefore, the thickest weathering profiles are located over old erosion surfaces (e.g. the Congo erosion surface). If

carefully followed, these indications allow the prospector to single out areas of potential groundwater occurrence. In some cases, a preliminary geomorphological survey might give indications as to whether or not a more cost intensive survey technique, such as geophysics, might be of value.

2.4.5. Groundwater Targets in the CB in Africa

2.4.5.1. Introduction

The porosity and permeability of unweathered CB rocks are very low and thus, their groundwater storage capacity is very small. Despite this, large numbers of boreholes have been successfully developed throughout Africa in areas underlain by basement rocks (Clark, 1985; White et al., 1987; Houston and Lewis, 1988). Groundwater aquifers occur within the weathered residual overburden, often referred to as regolith and the fractured bedrock. Regolith aquifers are generally planar, continuous over relatively large areas, and are characterised by having relatively high to moderate storage coefficients, S , (i.e. the volume of water which an aquifer releases from or takes into storage per unit surface area per unit change in the component of head normal to the surface; Bowen, 1986) in the range of 0.1 to 0.00005. In general, unconfined aquifers have higher values of S compared to confined aquifers. Fractured bedrock aquifers, on the other hand, are highly discontinuous within small areas and are characterised by having low storage capacities $< 1\%$, (Clark 1985) but relatively high permeabilities (figure 2.4-6). As will be explained in more detail in the next sections, the relative importance of these two systems as aquifers depends upon a combination of climatic, geomorphological, and geological conditions.

However, experience from groundwater exploration in the CB has shown that viable aquifers wholly within the fractured or weathered bedrock are of rare occurrence. In order to be effective, development of CB aquifers requires interaction of both the fractured bedrock with the overlying or adjacent saturated regolith. This conceptual hydrogeological model is considered to be representative of groundwater conditions beneath large areas of the CB in Africa. In the following sections, the most common groundwater targets in the African CB complex are described.

2.4.5.2. Weathered Bedrock Aquifers

The regolith consists of an unconsolidated or semiconsolidated mixture of clay and fragmental material ranging in grain size from silt to boulders (figure 2.4-6). It can be subdivided in (1) the soil surface which is generally restricted to a thin mantle, (2) unconsolidated deposits resulting from the action of running waters which is commonly referred to as fluvial or alluvial deposits, and (3) the saprolite. The saprolite is the clay-rich, residual material which is derived from in-place, predominantly chemical weathering of bedrock. Depending upon groundwater flow mechanisms, the saprolite is often highly leached and, being granular material with principal openings between mineral grains and rock fragments, its porosity can be very high. The bulk of the water storage is provided within this layer. However, to contain significant aquifers, this layer must attain a minimal areal extent and thickness.

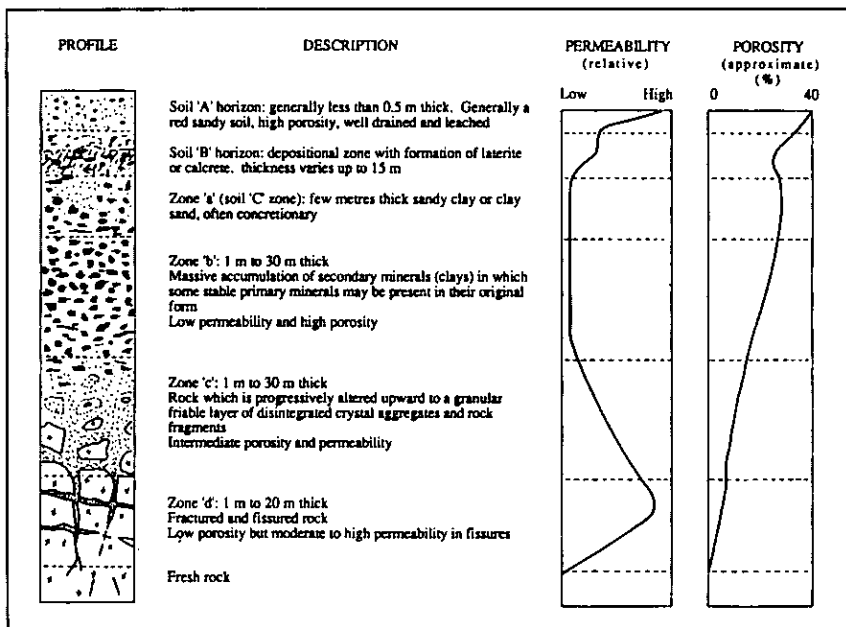


Figure 2.4-6. Porosity and permeability along a typical weathering profile (after Acworth, 1987). The figure shows two distinct zones of hydrogeological interest; the saturated low permeability zone with the fractured low porosity zone at the base. The fractured rock acts as a drain for the overlying saturated layer.

Several authors (Jones, 1985; Houston and Lewis, 1988; Wright, 1992) studied the relationship between the yield of a borehole with respect to its depth and the thickness of the regolith. They all pointed out that there are depths of useful drilling below which it is uneconomic. The optimum depths are mainly controlled by the rock type and climate as these factors tend to influence the weathering intensity, porosity and leaching processes. There is evidence to suggest that, significant borehole yields are to be expected in areas where the regolith is thick (>10 m, Houston and Lewis, 1988) and at high altitudes on the older erosion surfaces and where the rainfall is high (> 600 mm; Jones, 1985).

2.4.5.3. Fractured Bedrock Aquifers

The fractured bedrock aquifers refer to water-bearing fissure systems which can be associated with faults, joints, fractures, and dykes. Fissuring tends to be most intense adjacent to the smashzone of the fault line and a few meters from the main structure may be negligible. This evidence suggests that, in a fractured bedrock aquifer, groundwater conditions are typically anisotropic, heterogeneous and limited in space. Therefore, regional aquifers in the CB are of rare occurrence and each site has to be treated as unique (Clark, 1985).

Fracture and fissure occurrence decrease with depth due to rock loading and the lack of weathering. This evidence again places a limit to the depths of boreholes on the bedrock aquifers. The depth limits vary with lithology and geologic history of an area. Data from boreholes of a granit-gneis area in southern Zimbabwe (Houston and Lewis, 1988) show a greater frequency of fractures in the upper 20 m of bedrock below the regolith interface, whereas data from an area consisting of fissured metasediments in Uganda, suggest an optimum depth range of 30 m to 90 m (Faillace, 1973). However, despite their discontinuous character and low storage capacities, cases of occurrence of highly productive fractured bedrock aquifers have been reported in Moroto, Uganda and in Mopa, Nigeria with borehole yields of up to 40 and 27 m³ per hour respectively (Clark, 1985).

Moreover, fault lines and associated fissure systems in crystalline rocks present lines of weakness for erosion and weathering. The river and the drainage systems, therefore, tend to follow these lines. Thus, the water-bearing fissure systems, in general, lie along valley bottoms rather than on its flanks (Acworth, 1987).

2.4.5.4. Composite Aquifers

Aquifers composed of relatively high storage, low permeability regolith overlying low storage, high permeability fissured bedrock are referred to as composite aquifers. Results to date suggest that boreholes sunk in a composite aquifer are generally more productive than any other one draining either of the aquifers types mentioned above (e.g. White et al., 1988). Therefore, the strategy for successful groundwater prospecting campaign in the CB is to locate areas with both a thick weathered and fractured bedrock. In such cases, the high permeability fractured bedrock acts as a drain and is replenished by the overlying saturated regolith and thus providing an increased borehole yield.

2.4.5.5. Perched Water Aquifers and Sand Rivers

The term perched aquifer refers to the uppermost water-bearing layer above a main aquifer, whereas sand rivers generally consist of alluvial sands present in the active stream channel beneath flood plains. Both aquifer types generally have a seasonal and local character. In both cases, the water bearing layer is commonly made up of alluvial and in some cases of aeolian sands overlying an impermeable substratum which might be the fresh bedrock or a clayey layer. These shallow deposits may have high specific yield and permeability. However, the shallow occurrence makes the aquifers susceptible to pollution. Despite this fact, due to their easy accessibility and to the degree of scarcity of water as well as to a wide range of socio-economic constraints, which are beyond the scope of the present work, in many regions of tropical Africa such aquifers are the most important source of water for both domestic consumption and small scale farming (Palacky et al., 1981).

2.5. Hydrogeology of Sedimentary Basins in Africa

2.5.1. Introduction

Sedimentary rocks, consolidated and unconsolidated, in general are characterized by moderate to high primary porosities and permeability depending upon geological history and composition. As can be seen from figure 2.2-1, large parts of the African continent, especially north of Sahara, the western and eastern parts are covered by

sedimentary basins. Two hydrogeological environments can be distinguished namely 1) the coastal sedimentary basins and 2) the major inland sedimentary basins such as Kalahari, Sahara and Congo basins. According to Balek (1983) and Bowen (1986) there are three significant aquifers types in the sedimentary basins, namely 1) a phreatic aquifer in the sandy beds (sand dunes), 2) a heterogeneous aquifer in the underlying and highly-jointed basalt and 3) a confined aquifer in the deeper lying sandstone. In the following sections some of the most common aquifers in the sedimentary basins are outlined.

2.5.2. Groundwater Targets in the Sedimentary Basins

2.5.2.1. Unconsolidated Sedimentary Rock Aquifers

Unconsolidated sedimentary rock aquifers of significant size and extent generally occur along the coastal areas (e.g. in sand dunes), in alluvial deposits along major rivers and lakes, and in the uppermost horizon of a sedimentary basin. The unconsolidated sedimentary rock aquifers are generally phreatic but in some cases deeper confined aquifers may occur.

2.5.2.2. Sandstone Aquifers

In many regions of the inland sedimentary basins, sandstone strata form regional aquifers that have vast quantities of potable water (see examples of section 3.4.2). The enormous area of desert in North Africa (Sahara) and Southern Africa (Kalahari) are underlain by some of the largest artesian aquifers in the world. The water-bearing beds are mostly sandstones which range in age from Paleozoic (590 million years) to Mesozoic (56 million years) and in places they may attain thicknesses of several hundreds of meters (e.g. Balek, 1983; Bowen, 1986). Over the recent years there has been an increased exploration for such aquifers (e.g. Bourgeois et al., 1994 and Giroux et al., 1997). In contrast to the CB (with moderate to high precipitation rates), the sedimentary basins are mainly located in arid zones and therefore, there is no significant direct recharge from the rainfall. Isotopic research results to date suggest that the groundwater in these deep regional aquifers accumulated slowly in Peistocene times under more favorable climatic conditions than during the present time and may therefore be considered nonrenewable water resources and thus, requiring careful assessment and monitoring.

2.5.2.3. Carbonate Aquifers

Carbonate rocks such as dolomite and limestone result from geochemical alteration of dolomite and calcite, respectively which are of sedimentary origin. Old and intensively metamorphosed and indurated carbonate rocks have generally negligible porosity and permeability and thus, their hydrogeological characteristics are similar to those of unweathered and unfractured igneous and metamorphic rocks. However, carbonate rocks apart from developing appreciable secondary permeability and porosity as a result of weathering, fracturing and fissuring, they may develop secondary vertical and horizontal openings due to dissolution processes often referred to as karstification along bedding planes by circulating water. Zones of increased porosity and permeability are to be expected where fracture intersections and lineaments are concentrated.

Geologically young carbonate rocks commonly have porosities that range from 20% for coarse, blocky limestone to more than 50% for poorly indurated chalk (Freeze and Cherry, 1979) and therefore, they form excellent groundwater aquifers. In the African continent, important carbonate aquifers have been reported in several areas of Southern Africa on the margins of the Kalahari sedimentary basin, e.g. in Kabwe, Zambia (Houston and Morrey, 1982), Kanye, Botswana (Gieske, 1993) and Wondergat-Dinokana, South Africa (Yongxin et al., 1993).

2.5.2.4. Aquifers in the Interface Sediment Cover/ Basement

If overlain by porous and permeable sediments, the bedrock itself constitutes an important groundwater target (exploited up to depths of 150 m; Wright, 1992). The bedrock acts as an aquiclude with groundwater trapped in the immediate overlying cover rock. In these situations the survey objectives would be the determination of the depth to the bedrock and the nature of the cover material.

2.6. Summary

The CB aquifers are of particular importance in tropical Africa because of their widespread distribution, accessibility and highly dispersed rural population. Their occurrence depends on the weathering and fracturing processes which in turn are controlled by a wide range of factors whose patterns are highly variable in space and time. On the other hand, the fact that many such aquifers are structurally

controlled precludes the occurrence of regional aquifers and therefore, each site must be taken as unique. Therefore, the exploration of the CB aquifers involves small scale surveys and in general not exceeding some few hundred meters in length. The main focus of the surveys in such areas is not only to detect a deep, weathered zone but most importantly to define its lithological characterisation in terms of clay content because this has important hydrogeological implications.

Apart from the lithology and fracturing, the development of a deep weathered layer depends mainly upon the rate at which the chemical reactions and transport of reaction products take place and hence, on the availability and rate of flow of groundwater. On the other hand, the rate at which groundwater flows is influenced by three factors, namely 1) the rate of recharge, 2) the hydraulic gradient between the recharge and discharge points and 3) the hydraulic conductivity of the regolith. In general, borehole yields show a tendency to decrease towards the deserts, partly as a result of lower rainfall but also as a result of more clayey regolith and thus reduced transmissivity (Acworth, 1987).

Over large areas of the African continent, the surface is dominated by extensive erosion surfaces, with very low groundwater gradient and therefore slow groundwater flow and little weathering. Where recent tectonic influences have caused tilting and uplift of the previously stable planation surfaces (e.g. towards the the shoulders of the Rift Valley), the hydraulic gradient is higher and thus, the weathering processes are more intense. This, in many cases, results in an increase of the thickness and transmissivity of the regolith.

The research results to date show that the groundwater occurrence in the CB is influenced by a wide range of factors. More studies are still needed in order to establish more accurately the correlations of measurable physical and structural parameters, such as regolith resistivity and thickness with aquifer occurrence and its hydraulic characteristics (e.g. Houston and Lewis, 1988; White et al., 1988; Herbert et al., 1992; Carruthers and Smith, 1992).

Recent developments in drilling and geophysical prospecting techniques are making the use of deep sandstone aquifers occurring in many sedimentary basins viable. However, because many such aquifers are of fossil nature (i.e. not renewable) their exploitation requires a careful assessment in order to prevent a premature resource depletion or pollution.

3. Hydrogeophysics of Tropical Africa

3.1. Introduction

The principles of geophysical techniques are extensively described in the literature (e.g. Telford et al., 1990; Parasnis, 1997; Reynolds, 1997). Elsewhere in the world, a variety of geophysical methods have been successfully used for groundwater prospecting for many years, including electrical methods, seismic refraction, gravity and magnetic and borehole geophysics (e.g. Zohdy et al., 1974; Dobecki and Romig, 1985; Romig, 1986). The main purpose of this chapter is not to cover these topics but instead, to document and discuss recent cases of application of geophysical techniques in groundwater exploration in some of the African geological environments described in the previous chapter, including a condensed description of some physical characteristics relevant to groundwater targets in such areas.

According to Fitterman and Stewart (1986), the most fundamental questions on groundwater which geophysical techniques can help answer can be formulated as follows:

- Where is it?
- How much of it is there?
- What is its quality?
- At what rate can the resource be used without adverse affects?

Due to the very close connection between electrical conductivity measured by geoelectrical methods and groundwater salinity which determines its quality, the last two questions can be suitably answered by these methods (Goldman et al., 1994). However, as regards the first two questions the feasibility of geoelectrical techniques is more questionable. This is due to the fact that the electrical conductivity of fresh groundwater-bearing formations does not differ significantly from that of many dry lithological units (Palacky, 1987). More often than not, groundwater exploration problems include marginal detectability of relevant hydrogeological units and the well-known thin-layer-equivalence problem of geoelectrical sounding interpretation (e.g. Sandberg, 1993; Sharma and Kaikonen, 1999 and many others). The answer to the question of how the efficiency of fresh groundwater exploration may be drastically improved is therefore quite clear, i.e. the appropriate geophysical technique must be sensitive to that physical parameter which distinguishes fresh water from any other material in the subsurface and the parameter resolution must be improved. Thus, to make an intelligent decision on the use of a

technique, at least a rudimentary knowledge of the physical properties of the groundwater targets and the surrounding media is crucial.

As was mentioned in the first chapter geoelectric methods are affected by deep in situ weathering common in the tropical Africa (e.g. Palacky and Kadokaru, 1979; Palacky et al. 1981; McNeill and Labson, 1991; Parasnis, 1997). Therefore, there is still a lot of work to be done, both on local and regional scale in order to establish the applicability of these techniques for groundwater exploration in many such environments.

3.2. Physical Characteristics of Groundwater Targets

The physical characteristics of most igneous, metamorphic and sedimentary rocks have been extensively described in the literature (e.g. Schön, 1996). The purpose of this section is basically to summarise some of the aspects which may play a significant role from a groundwater perspective, particularly the influence of the physical characteristics of the weathered layers in the effectiveness of geophysical surveys as well as the hydrogeological implications.

Despite the importance and widespread occurrence in the tropics of weathered layers, their physical characteristics remain poorly understood. Although some of the aspects of the weathered layers have been extensively investigated and documented over the last years, the knowledge still remains diffuse and in many cases only of local character. This is partly, due to the influence of many factors including climate, lithology, morphology and water regime in the weathering processes and hence on the physical characteristics of the weathering products. The excellent works of Palacky (1979 and 1987) describe the electrical characteristics of weathered layers on a mineral prospecting perspective, but nonetheless, they provide a background for understanding the factors affecting the weathering processes and the resistivity characteristics of the weathering products. Therefore, the following sections are not intended to replace the works cited above but instead, to complement them where possible with special emphasis on their geohydrological implications.

3.2.1. Electrical Properties

3.2.1.1. Electrical Conductivity

There are many places in the literature where to find extensive description of the electrical properties of rocks (e.g. Keller, 1987; Ward,

1990; McNeill, 1990; Ruffet et al., 1995; Nobes, 1996; Schön, 1996). Therefore, the present section will be kept rather brief. From a groundwater perspective, of all physical properties of the rocks, the electrical conductivity [S/m], or its inverse the electrical resistivity [Ωm] are the most relevant, not only because of its wide range of variation but mainly because of the electrolytic character of the conductivity (σ_w) of most unconsolidated geological formations (clay-free).

For clayey unconsolidated formations and particularly at low electrolyte conductivities, there is an additional conductivity term which is often referred to as interface conductivity (σ_c) due to the electrochemical processes (Cation Exchange Capacity, CEC, effects) in the interface clay and electrolyte. Therefore, the bulk conductivity (σ) is made up of these two conductivity terms and can be expressed as follows (McNeill, 1990):

$$\sigma = \sigma_w \phi^n + \sigma_c \quad (3.1),$$

where ϕ is the porosity, n is the shape factor, a parameter that incorporates the effects of different grain sizes on the pore dimensions and hence on the flow paths. Since the electrolytic and the interface conductivity terms are associated with different electrochemical processes and hence, with different geological and structural characteristics, it is understood that its separation can yield important information for a better characterisation of hydrogeological systems, i.e. in terms of aquifers and aquitards (see e.g. section on IP).

For the purposes of many studies in exploration geophysics, a quasi-static approach is assumed (i.e. the displacement currents in Maxwell's equations are neglected) and the bulk conductivity is assumed to be a real parameter (e.g. Ward and Hohman, 1987; Keller, 1987). However, in the general form the electrical conductivity can be expressed as a complex quantity as follows (e.g. Ward, 1987; Weller et al., 1996):

$$\sigma(\omega) = \sigma'(\omega) + i\sigma''(\omega) \quad (3.2),$$

where σ' and σ'' are the real and the imaginary parts of the complex conductivity. Recent studies (e.g. Ruffet et al., 1995) show that the frequency dependence of the imaginary part of the complex conductivity can be used to infer on the geology and/or hydrogeology

of the subsurface. This is due to the fact that different mechanisms of a physical or chemical nature are involved depending on the frequency range and therefore, can be separated. However, these studies have not yet resulted in significant new methods. The dependence of the complex electrical conductivity on the frequency and its implications to some geophysical applications (e.g. IP and GPR) have been also reported by many authors (e.g. Schön, 1996; Weller et al., 1996; Nobes, 1996).

Conductivity Characteristics of Weathered Layers

The conductivity characteristics of weathered layers have been under scrutiny for some time (e.g. Palacky and Kadokaru, 1979; Palacky, 1987; Robain et al., 1996; Ritz et al., 1999a).

In general, the weathering zones represent a progressive chemical degradation from fresh rock (i.e. very low clay content to clay-free) to soil (very high clay content). The occurrence of a high resistivity lateritic overburden, which is thought to be associated with leaching processes is a common characteristic in many weathered zones. The succession of these zones does not change, but thicknesses of individual zones may vary or even become insignificant. The upper interfaces between zones are mostly planar as they are related to the presence of the water table, but the shapes of the lower interfaces are more influenced by the presence of fractures, fissures and cracks and thus, tend to be more irregular. Figure 3.2-1 depicts a cross section over a crystalline rock environment in which weathering leads to a consistent change in resistivity with depth over wide areas.

The resistivity of weathered layers varies over a wide range and is affected by many factors such as porosity, conductivity of included soil moisture, degree of saturation and clay content. These factors, in turn, are influenced by climate, lithology, time of exposure to the weathering agents, and terrain morphology. Various authors (White et al., 1988; Palacky and Kadokaru, 1979; Palacky, 1987) show that the resistivity of the regolith is at least partly related to mean annual rainfall and clay mineralogy. Regolith formed over areas with low mean annual rainfall (less than 700 mm) tends to be clayey (e.g. Montmorillonite) and hence more conductive than regolith formed over areas with high mean annual rainfall (e.g. kaolinite), (see figure 2.4-1). This has important implications for borehole siting since it tends to mask any regional relationship between resistivity and specific capacity. On the other hand, clay particles in the regolith tend to clog the pores and thus reduce the permeability. This evidence suggests that in addition to the determination of a zone of deep

weathering, it should be possible to use geophysics to locate areas of suitable lithology; therefore the relationship between formation resistivity and specific capacity of the aquifers in any particular region must be known roughly. Table 3.2-1 shows some typical optimum resistivity values for aquifers in the CB of the Victoria province, Zimbabwe. As to the effect of seasonal changes of the climate to the resistivity, Palacky and Kadekaru (1979) show that only the resistivity of the upper layer (1-10 m thick soil layer) was affected but not the resistivity of the underlying weathered layer.

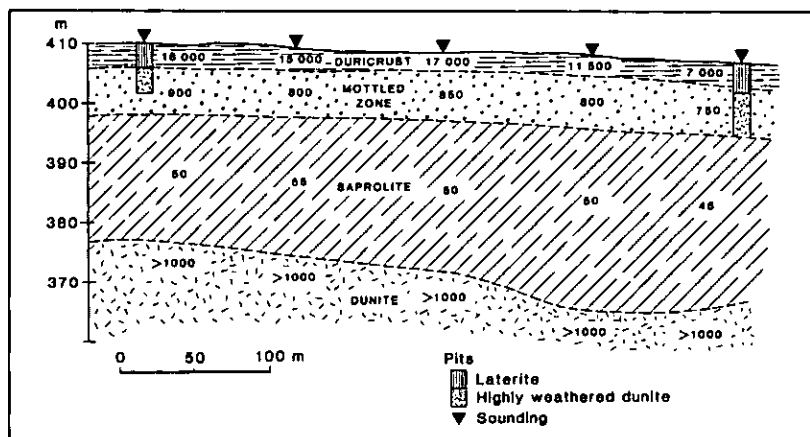


Figure 3.2-1. Typical electrical resistivity (Ωm) values over a crystalline basement environment (after Palacky, 1987). It is to note the occurrence of a high resistivity overburden (lateritic layer or duricrust) and the low resistivity saprolite.

The resistivity dependence on the lithology is related to the content of quartz and other more resistant rock forming minerals. Mafic and ultramafic rocks (basalt) are more susceptible to intense chemical weathering than felsic rocks (granite) which have a higher content of resistant minerals (e.g. quartz, muscovite). Therefore, higher clay contents and hence lower resistivity values are to be expected in areas where mafic rocks predominated. Table 3.2-2 summarizes the resistivity ranges of some common rocks of the CB in Africa. Note that these ranges are typical, values below and above these ranges may occur in other areas of the CB.

Table 3.2-1: Optimum resistivity values for aquifers in the Vitoria province, Zimbabwe (after White et al., 1988). Note that apart from the lithology, the characteristics of the weathered products are highly determined by the rainfall.

Rock type	Resistivity (Ωm)
Granite regolith Rainfall > 700 mm Rainfall < 700 mm	100-500 250-400
Gneiss regolith Rainfall > 700 mm Rainfall < 700 mm	50-400 200-350

Table 3.2-2: Resistivity ranges (Ωm) of weathered layers formed over African igneous rocks (after Palacky, 1987).

Rock type	Granite	Shist	Amphibolite
Weathered layer	250	10-30	5-15
Transition zone	40-200	250-400	10-80
Fresh rock	>1500	>1000	>500

3.2.1.2. Dielectric Properties

Over the last years, there have been a number of studies concerning the application of EM techniques in the uppermost part of the subsurface, i.e. at Ground Penetrating Radar (GPR) frequency range. In such cases, the quasi-static approach in the Maxwell's equations is no longer valid and the displacement currents must be taken into account and therefore, the dielectric permittivity, ϵ , becomes important. On the other hand, there have been some fresh attempts to establish the relationship between the dielectric permittivity and the water content (e.g. Heimovaana et al, 1994; Saarenko 1998; etc). The dielectric permittivity properties of rocks are poorly covered in the literature, but nonetheless, a more extensive description of this property can be found e.g. in Schön (1996). Therefore, the present section will summarize some few new concepts pertinent to groundwater applications. According to Keller and Frischknecht (1966), when an electrical field is applied in a material, a separation of charges takes place and this phenomenon is referred to as polarisation. The dielectric value, a dimensionsless parameter, is a measure of the relative ability of a material to store a charge for a given applied

field strength, while dielectric loss is a measure of the proportion of the charge transferred in conduction and stored in polarisation. The dielectric permittivity, is a complex number and is a function of frequency. Relative dielectric permittivity, ϵ , also referred to as the dielectric value or dielectric constant, is the ratio of the complex dielectric permittivity to the dielectric permittivity of free space, ϵ_0 [8.854×10^{-12} F/m]. The dielectric value can then be expressed as (Nobes, 1996; Saarenko, 1998):

$$\epsilon = \epsilon' + i\epsilon'' \quad (3.3),$$

where ϵ' and ϵ'' denote the real and imaginary (also known as dissipation term or electric loss part) parts respectively. It is customary to split the imaginary part in a frequency dependent and independent terms as follows (Nobes, 1996):

$$\epsilon(\omega) = \epsilon'(\omega) + i[\epsilon'' + \sigma_{dc}/(\epsilon_0\omega)] \quad (3.4),$$

where the second term in the brackets is the usual conduction term, σ_{dc} is the zero frequency conductivity. The real part of the relative dielectric permittivity can take on values from 1 (for air) to 81 (for free polar water at 20°C; Saarenko, 1998). According to Nobes (1996), the imaginary part or the loss term is associate with different electrochemical mechanisms such as: (1) electrical conduction witch generates heat; (2) viscous dielectric relaxation of water; (3) ionic transport on clay mineral surfaces; and (4) scattering processes. Different loss mechanisms dominate at different frequencies and the knowledge of the loss term has been used in a recent study to obtain the electrical conductivity (e.g. Heimovaara, 1994; Heimovaara et al., 1994).

3.2.1.3. Induced Polarisation Effects

The occurrence of IP effects has been described by many authors (e.g. Ward, 1990; Weller and Börner, 1996; Parasnis, 1997 and many others). The basic principles of the occurrence of IP effects are based on the fact that when an electric current flowing in the subsurface is interrupted, the associated voltage does not drop instantaneously but instead it fades away slowly (Parasnis, 1997). One of the foundations of the IP method follows from the frequency dependence of the

complex conductivity. Due to their high cation exchange capacity (CEC), clay particles are known to be associated with some of the IP anomalies observed in many areas. As it will be described in section 4.2.3, the IP effects associated with clay particles, which are commonly referred to as membrane polarisation, are of particular importance in groundwater studies.

3.2.2. Density

The bulk density of rocks depends mainly on mineral composition and the content of the enclosed pore or fracture space. The densities of regolith are comparable to those of unconsolidated sediments, i.e. they lie in the range of 1.0 to $2.4 \times 10^3 \text{ kg/m}^3$ (Hinze, 1990). The density of unweathered bedrock varies with the rock type but commonly is not less than $2.0 \times 10^3 \text{ kg/m}^3$, with mafic and ultramafic rocks displaying higher density values than felsic rocks. As will be illustrated in section 3.4, generally, there is a relevant density contrast between the regolith and the unweathered bedrock and thus, gravimetry and any other geophysical method whose relevant physical property is related to density such as the seismic velocity (Schön, 1996) can be suitably used to determine the thickness of the weathered layer and the depth to the bedrock or its morphology (Reynolds, 1997).

3.2.3. Seismic Velocity

The weathering profile almost invariably consists of a low velocity regolith overlying a high velocity unweathered bedrock. Therefore, in many cases, a velocity contrast exists between these two units which justifies the use of the seismic methods. Until quite recently, only the P-wave velocity was measured in shallow studies. However, in a groundwater perspective, the measurement of both types of velocities is of interest, because apart from structural information which is obtained when using the P-wave velocity alone, more information concerning the subsurface can be obtained such as the depth to the water table (Lankston, 1990).

3.2.4. Magnetic Susceptibility

The magnetic characteristics of most geological formations in general and of weathered layers in particular depend primarily on the content

of ferrimagnetic components in the parent rock. However, in the process of chemical weathering new chemical elements may result, e.g. oxidation and leaching of magnetic Fe^{2+} and accumulation of Fe^{3+} which is less magnetic. Thus, an originally magnetic formation may become nearly unmagnetic (e.g. Greef, 1993). Since weathering is more intense in zones of weakness, such as faults, dykes, etc, this often offers the possibility of using the magnetic method to map such features. Common geological situations in the African continent are the occurrence of dolerite dykes in the CB as zones of weakness and therefore where the likelihood of a deep regolith and increased fracture permeability are high. In the sedimentary basins doleritic sills may occur at the base of the sediment cover, in which case they act hydrogeologically as an aquiclude, trapping the groundwater in the overlying sediments. In both cases, the magnetic methods can be suitably used to map these features since dolerite is a fairly magnetic geologic formation.

3.3. Geophysical Methods in Groundwater Prospecting in Africa

3.3.1. Overview of Principles, Field and Interpretation Techniques

3.3.1.1. DC Resistivity Methods

A survey of the literature suggests that of all the geophysical techniques, DC resistivity is the most commonly employed in groundwater studies in Africa, particularly the conventional (i.e. one sounding at a time) Vertical Electrical Sounding (VES) mode with Schlumberger configuration (Senti, 1988 and van Dongen and Woodhouse, 1994). Some of the merits that make the technique so popular are its ease to use, relatively low cost of equipment and the availability of interpretation aids. However, many authors (e.g. Dahlin, 1993; Robain et al., 1996; Ritz et al., 1999b) have shown that the technique is less favourable in many areas of the crystalline basement due to lateral inhomogeneities and spatial variability of groundwater targets. Thus, over the last years 2D resistivity surveying systems, which are capable of reducing the effects of lateral inhomogeneities are being increasingly used. These systems operate mainly with Wenner configuration electrode arrays (see chapter four).

On the other hand, the VES technique suffers from inherent equivalence and suppression problems, which introduce a large degree

of ambiguity in the interpretation process. Equivalence and suppression in geoelectric sounding are well known problems and have been topical for many years (e.g. Sandberg, 1993; van Overmeeren, 1981; Sharma and Kaikkonen, 1999 and many others). In general practice, attempts to reduce the degree of ambiguity are made either by 1) correlation of several sounding curves, or by 2) knowledge of the local geology or drilling information (van Overmeeren, 1981; Carruthers and Smith, 1992; Sandberg, 1993) or by 3) integrated use and joint inversion of geophysical data sets. However, resistivity surveys in rough terrains in Africa are too cumbersome and time consuming and thus, in most practical cases, fewer measurements are made than would be desirable and due to the remoteness of many sites additional geological information (drill log, say) is scarce. On the other hand, since many small scale groundwater surveys in Africa operate with limited budgets, the application of more than one geophysical technique is in most cases not possible. However, Sharma and Kaikkonen (1999), show that even after joint inversion of DC resistivity and EM data sets the suppression problem cannot be solved and only in the case of a resistive intermediate layer the reduction of equivalence is apparent.

3.3.1.2. Electromagnetic (EM) Methods

Electromagnetic techniques in both frequency and time domain are increasingly becoming valid alternative techniques to DC resistivity methods, for hydrogeological studies in rough terrains with resistive overburden common in arid and semi-arid climates of Africa. EM techniques are most useful for looking for relatively conductive material and least useful for working with resistive targets. Like the DC resistivity sounding, the EM sounding techniques are affected by the problem of equivalence and suppression described in previous section. An extensive discussion of the merits and disadvantages of the different EM techniques that are now commonly used for groundwater studies is given by McNeill (1990). The major disadvantage of the use of EM techniques lies in the relatively high (compared with conventional DC resistivity) cost of the equipment (McNeill, 1991). Moreover, the interpretation techniques are not as fully developed as for conventional DC resistivity.

3.3.1.2.1. Horizontal Loop EM (HLEM) Method

The application of HLEM to conductivity measurements in connection with groundwater studies in Africa is quite recent. It was the result of the introduction of light instruments where frequency f and coil separation L are chosen to satisfy the so-called low induction number approximation (LIN), in which case the depth of penetration is governed by the coil separation, e.g. the ground conductivity meters such as EM31 and EM34 systems (McNeill, 1980) operate under this principle. Such systems are mainly used for profiling purposes but some qualitative information of the layering may be obtained by using multi-spacing systems such as the EM34-3.

The HLEM technique is mainly employed for the detection of steeply dipping and sub-horizontal conductive features such as faults, fractures and dykes (Palacky et al., 1981; Hazell et al., 1988; Frischknecht et al., 1991; Zeil et al., 1991). In some cases it can be used for exploring localized thickening of the weathering layer (e.g. McNeill, 1991). In many cases, the EM profiling methods have proven to be more efficient compared to resistivity techniques (see Table 3.3-1). However, these LIN systems have a disadvantage in that only part of the information is evaluated, e.g. only the out-of-phase component of the secondary magnetic field will be used to convert the data into the apparent conductivity (McNeill, 1980). An operational problem with all HLEM systems is that the intercoil spacing, the coil alignment and the instrumental zero must be closely controlled, which in some cases is difficult to do (e.g. Frischknecht et al., 1991; McNeill, 1996).

Other HLEM technique which has been occasionally used in groundwater prospecting in Africa is the Slingram technique. In this method which in many cases operate in a single frequency, both the inphase and out of phase component are measured whereby the interpretation is mainly done on a qualitative basis. Attempts to convert the Slingram information (i.e. the field components) in a more diagnostic parameter such as the apparent resistivity are still under way. However, there are some few cases of its successful application in groundwater prospecting in Africa, e.g. in Modipane, Botswana (ABEM Manuals). Other variants of HLEM systems are the MaxMin II and III which usually operate with five frequencies.

Over the last decades, there have been attempts to explore the advantages of HLEM over DC resistivity techniques particularly in terms of the layering of the surface. However, there are still some operational problems (e.g. sensitivity of the systems to the coil orientation, misalignment of the coils and the setting and maintenance of the zero of the instruments) with the current systems.

Table 3.3-1: Comparison of relative merits of resistivity and electromagnetic profiling techniques (after Hazell et al., 1988).

DC Resistivity	HLEM
3 Km per day (at station interval of 20 m)	9 Km per day (at station interval of 20 m)
Three- or four-men team	Two-men team
Contact resistance problems in dry or hard ground	No ground contact needed
Depth penetration much shorter than electrode spread	Depth penetration equal to and greater than coil spread

3.3.1.2.2. Magnetotelluric (MT) and Audiomagnetotelluric (AMT) Methods

The basic principles of conventional magnetotelluric (MT) method are described extensively in the literature e.g. Zonge and Hughes (1991) and Vozoff (1991). In principle, both techniques (i.e. MT and AMT) measure the horizontal electric and magnetic field associated with natural electromagnetic fields. From both components the apparent resistivity and phase are calculated. The difference between the conventional MT and the AMT is that for a long time, the former was restricted to deep studies, i.e. in the low frequency range (10^{-3} to 10 Hz) due to the difficulties in measuring MT signals at frequencies above 10 Hz, whereas in the AMT method the measuring frequency range extends towards audio frequencies, i.e. from 10 to 10^4 Hz. Therefore, the AMT method gives access to more near-surface investigations, compatible with hydrogeological exploration. The operational procedures of AMT method as well as the advantages and disadvantages of current measuring systems are described in many places in the literature e.g. McNeill (1990). Examples in the literature of groundwater studies carried out by using MT and AMT are somewhat rare perhaps due to the nonavailability of cost effective systems up to a few years ago. However, over the recent years, there has been an increased use of these techniques for regional groundwater surveys in major sedimentary basins, e.g. Bourgeois et al. (1994), Giroux et al. (1997) in Africa and Meju et al. (1999) in Brasil. The results obtained by these workers, suggest that the techniques work well in some favorable geological conditions (see section 3.4). However, like in the MT technique, the interpretation of AMT data is seriously limited by the problem of static shift, particularly if, as is often the case, the near surface conductivity is variable (Vozoff, 1991). In the practice, there are several procedures for correction of

static shifts each one with its merits. Many authors use an independent, static shift free data set to correct this effect, e.g. Sternberg et al. (1988) and Meju et al., 1999, used a time domain EM (TDEM) data set to correct the static shift effect on MT and AMT data respectively. The most promising approaches are the ones that use processing techniques such as spatial filtering or phase integration (Zonge and Hughes, 1991) and the procedure involving the decomposition of MT impedance tensor (Groom and Bailey, 1989). Bourgeois et al. (1994) show that in simple and uniform geological situations such as the Kalahari sands at the surface, no static shift effects occur and the AMT technique can yield valuable and high quality data.

3.3.1.2.3. Controlled Source Audiomagnetotelluric (CSAMT) Method

The problems of adequate signal strength and variability of source field azimuth in MT and AMT can be circumvented by employing artificial signal sources (see chapter four). The artificial source provides a stable, dependable signal resulting in higher precision and more economical measurements than are usually obtainable with conventional MT and AMT measurements (McNeill, 1990; Zonge and Hughes, 1991). However, in applying some CSAMT systems, due care must be taken in order to avoid additional interpretational problem due to source effect, i.e. the survey data is also affected by geoelectric conditions underneath the transmitter site. This effect which is often referred to as transmitter overprint and the non planewave effects due to the closeness of the source if not properly accounted for can be misleading. Zonge and Hughes (1991) discuss these effects and some of current procedures for their correction. Although its physical basis is well established, the application of CSAMT in groundwater prospecting in Africa is not yet so widespread, partly due to the nonavailability of reliable measuring systems.

3.3.1.2.4. Conventional VLF and VLF Resistivity Methods

The usefulness of the VLF technique as a fast and cost-effective tool for the mapping of linear features such as faults, shear zones and steeply dipping features has been discussed at length in the literature and an excellent recent review is given by McNeill and Labson (1991). The major difference between the conventional VLF and the VLF resistivity is that in the latter the electric as well as the

magnetic field components are measured and from them the apparent resistivity is determined as in MT. Therefore, the VLF resistivity technique is also affected by the static shift effects. However, since the VLF systems are light weight and fast to use, one way of reducing this error is to take many measurements along the survey line and to apply a moving average to the data (McNeill, 1991).

Until quite recently, most of the VLF systems employed in field surveys operated exclusively with remote transmitters. However, VLF technique using a remote transmitter have some disadvantages such as (1) the transmitter can shut down without notice and (2) the limited coverage and thus, poor coupling of conductor strike with the VLF transmitters. The prospects of the applicability of the VLF technique using a remote transmitter are better in the northern part of African (i.e. some transmitters have signal strengths well above 48 dB) than in the southern part (McNeill and Labson, 1991). In fact, the single conclusive example widely known in the literature is given by Palacky et al. (1981), who used the NAA, Cutler, USA and the FOU, Bourdeaux, France VLF transmitters to map groundwater aquifers in Upper Volta (today Burkina Faso). In the southern part of Africa there have been some unsuccessful attempts to test the applicability of VLF technique (Botha et al., 1992). The reason is probably due the low signal strengths, i.e. much lower than 48 dB (McNeill and Labson, 1991 and Carruthers and Smith, 1992). With the recent developments in this field, particularly the development of local portable transmitters, the problem of poor coverage by remote transmitters as well as the poor coupling of conductor strike with available VLF transmitters can be circumvented. In this context, reasonable results have been recently reported by Zeil et al. (1991); Carruthers et al. (1991) and Botha et al. (1992).

3.3.1.2.5. Time Domain Electromagnetic (TEM) Method

The EM techniques discussed so far all operate in the frequency domain. The use of time domain electromagnetic (TDEM) techniques in groundwater studies is becoming popular, particularly for determination of hydrostratigraphy, i.e. the mapping of aquifers, confining layers, and basement, as well as the determination of the quality of the water found in the various aquifers. The principles of the application of TEM techniques in groundwater exploration are given in Fitterman and Stewart (1986). TEM surveys can also be employed for mapping as well as for sounding purposes in the same manner as in the frequency domain techniques (see section 3.3.1.2.1.).

Compared with other EM sounding techniques, TEM has several advantages because it is faster, it is less affected by static shift as is the case with AMT and MT and the resolution of several types of equivalence is better (e.g. Fitterman and Stewart, 1986). The technique has been applied in some groundwater surveys in Africa as is reported in some works (e.g. Botha et al., 1992; Carruthers and Smith, 1992; Shaumann, 1997). There is also some evidence to suggest that its combined use with DC resistivity can generally lead to a significant reduction in the problems of equivalence which occur when either is used on its own (e.g. Carruthers and Smith, 1992). This is particularly useful for the type of groundwater targets common in the CB in Africa. However, the major problem of the TDEM technique particularly the modern systems (VETEM; see section 4.4.2) is that the decaying transient covers an enormous dynamic range (about four decades; McNeill, 1991) and thus, the equipment is complicated and expensive. This is probably one of the reasons that still limits the widespread use of the technique for groundwater exploration in Africa.

3.3.1.3. Seismic Methods

The seismic methods currently applied for groundwater studies include seismic refraction, reflection, cross-hole tomography and vertical seismic profiling. An excellent review of seismic techniques applied in shallow depths is given by Steeples and Miller (1990). The application of seismic methods in groundwater is mainly for the determination of the depth to the bedrock and the thickness of the overlying layer. The combined recording of both P- and S-wave velocities has been suggested as the next major step in refraction seismics since it can provide better resolution of the type of subsurface materials, particularly when groundwater is involved, e.g. for the determination of the depth to the water table (Dobecki and Romig, 1985 and Lankston, 1991). Although in not widespread use in Africa, probably due to the high cost of equipment, the examples available in the literature suggest that in some favourable areas the technique works well and is cost-effective. Van Overmeeren (1981) used the refraction seismic data to constrain the DC resistivity interpretation in a groundwater survey in Sudan.

3.3.1.4. Potential Field Methods

Gravimetry has been widely applied in groundwater exploration for determining thickness of unconsolidated sediments in sedimentary basins and alluvial valleys, particularly in the reconnaissance phase of the survey. Several examples of gravimetric mapping of bedrock topography with the intent of locating buried channels have been reported (van Overmeeren, 1981 and van Dongen and Woodhouse, 1994). On the other hand, magnetic surveying for groundwater applications has been employed mainly for dolerite dyke detection and in search for thick zones of unconsolidated sediments overlying igneous or metamorphic bedrocks (Dobeki and Romig, 1985; Zeil et al., 1991; Bourgeois et al., 1994 and van Dongen and Woodhouse, 1994).

3.4. An Overview of Case Histories

3.4.1. Crystalline Basement

Locating Fractured Bedrock beneath a Conductive Regolith in a CB Environment: Zimbabwe

Large parts of southern Africa were affected by severe droughts during the 1980s and early 1990s. Therefore, accelerated borehole siting programmes aimed at providing water supply for rural communities were carried out. The necessary accelerated character of the programmes implied that all aspects of borehole siting had to be carried out using fast and cost-effective geophysical techniques. Two such programmes were carried out in the Victoria Province (Barker et al., 1992) and southeast Zimbabwe (Carruthers and Smith, 1992).

The geology of the CB in Zimbabwe consists of igneous and metamorphic rocks overlain by a variable thickness of regolith. Kaolinite is the principal clay mineral but in areas with annual rainfall less than 800 mm montmorillonite may develop as well (see section 2.4.3.2.). The weathering profile in the Zimbabwean CB is generally thin (White et al., 1988) and thus, reliable groundwater aquifers are associated with major fracture systems which can be mapped by using geophysical surveys integrated with the results of other techniques such as photogeology, remote sensing and hydrogeology. Commonly, the weathered profile in the CB consists of a subhorizontal layered sequence, with the intermediate layer of lower resistivity (representing the actual target zone), lying between more resistive cover and the (fractured) bedrock (figure 3.2-1). The components of the weathered layer are generally discontinuous and an

understanding of their relative contributions to groundwater occurrence is important in determining the best exploration and development strategies: whether the aquifer should be exploited by shallow wells completed within the saprolite or by deeper boreholes which intersect productive fractured bedrock. In most cases, the nature of the aquifer determines which geophysical methods are most appropriate and therefore, it is necessary to have a clear concept of its type, thickness, depth and permeability. Both works used a combination of DC resistivity sounding and EM profiling methods to locate a zone of thick regolith, (e.g. generally not less than 10 m), overlying fractured bedrock. For DC resistivity sounding the offset Wenner sounding mode was employed as this configuration is less sensitive to the spurious effects of near-surface lateral resistivity variations (Barker, 1981). For the EM profiling a Geonics EM-34 ground conductivity meter, a system which operates under the low induction numbers condition and provides a direct reading of apparent conductivity (McNeill, 1980). Although this system is widely used in many surveys in Africa, in conductive environments it may yield misleading results if the low induction number condition does not hold.

A sample survey result obtained by Barker et al. (1992) is shown in figure 3.4-1. Eight DC resistivity soundings were performed at locations A through H. The conductivity profile was measured with the instrument (EM34) in horizontal dipole mode (i.e. vertical coils) and with a coil spacing of 20 m. The geoelectrical section shows clearly a three layer sequence, whereby the resistivity of the regolith displays a minimum approximately in the centre of the valley which coincides with the maximum in the apparent conductivity profile. This was interpreted by the authors as a clay-rich valley centre with sand-rich valley sides. However, the authors point out that such an anomaly could also be associated with either a water bearing regolith and/or fractured bedrock or clayey regolith. If the judgement is based solely on these two techniques there is nothing to choose between a bore located in point A, B and F for example. Therefore, a potential borehole site in this valley would have to be a compromise between the thickness of the regolith and a lateral move in order to avoid the impermeable clay-rich zone towards the centre of the valley.

In the second example also from the CB basement in Zimbabwe (figure 3.4-2), the effect of equivalence and suppression are illustrated. As mentioned before, the intermediate layer of lower resistivity in the typical sounding curve represents the target zone, lying between a more resistive cover and the bedrock.

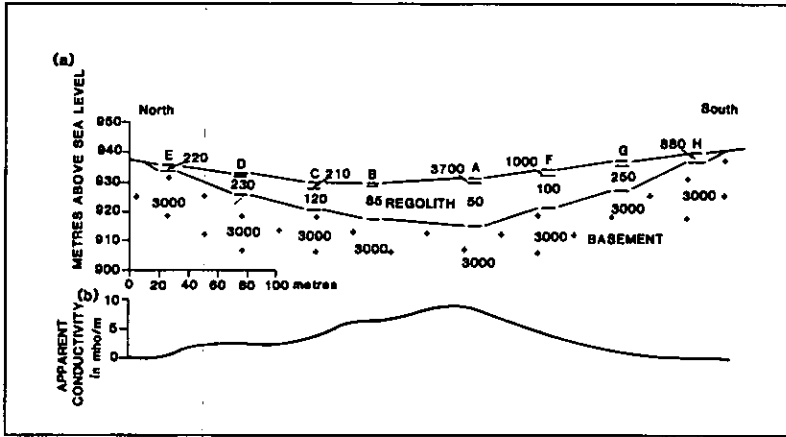


Figure 3.4-1. Geoelectrical section along a valley in Zimbabwe (after Barker et al., 1992).

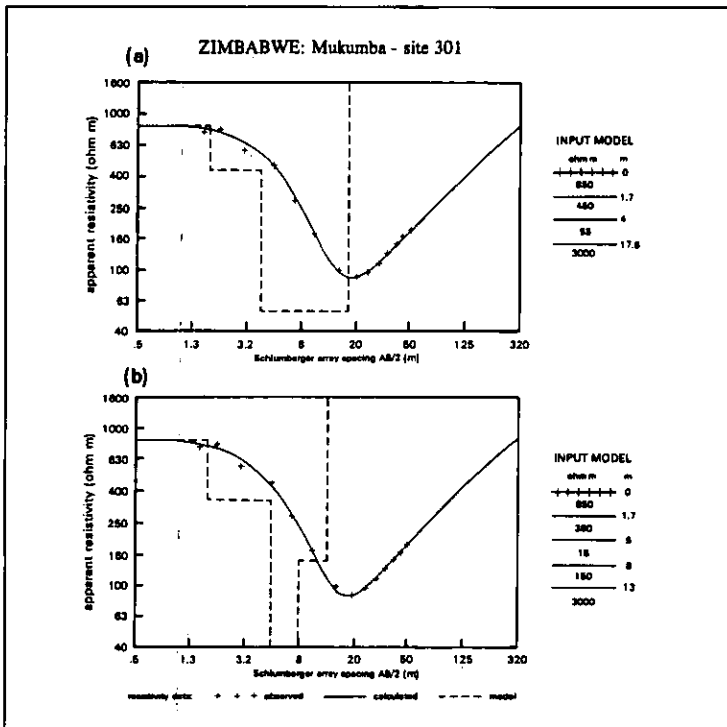


Figure 3.4-2. Alternative interpretations of DC resistivity soundings in a CB environment (after Carruthers and Smith, 1992). If the DC resistivity is the sole guide of the survey, there is nothing to chose between these two interpretations.

The parameters attributed to this zone are usually used to define suitable sites for hand-pumped rural water supply. It is to notice that due to high resistivity contrast between the regolith and the fresh bedrock, the fractured bedrock can not be resolved by the DC resistivity method. Carruthers and Smith (1992), pointed out that the distinction between regolith, fractured and fresh bedrock tends to reduce to one between a weathered zone and bedrock. Therefore, if the VES is the only guide in a field survey, there is nothing to choose between the two interpretations shown in figure 3.4-2. These two examples show clearly that, quantitative interpretation of DC resistivity soundings alone or combined with EM profiling, which is common practice in groundwater geophysics in Africa, can be misleading in many such geological environment. Therefore, a better combination of techniques which can yield a more precise estimates of the subsurface parameters would be desirable (say DC resistivity and IP). This could give a chance to make fast and better estimates of the hydrogeological characteristics of the aquifers, especially in terms of the clay and water content.

3.4.2. Sedimentary Basins

Locating Sandstone Aquifers in a Sedimentary Basin: Letlhakeng-Botlhapatlou Groundwater Project, Botswana.

The groundwater resources of many sedimentary basins in Africa or in areas located on their margins are relatively poorly understood, and droughts are frequent events in such regions. Therefore, it is important to determine the usefulness of geophysical techniques for mapping the hydrogeologically important stratigraphic units and any major structural controls on the aquifer distribution in the region. Two such surveys were carried out recently in two sites; (1) in Letlhakeng-Botlhapatlou area, Botswana (Bourgeois et al., 1994) and (2) in Senegal (Giroux et al., 1997). The first site is located in the Kalahari desert. A conceptual geological model which was constructed on the basis of boreholes for coal exploration is shown in figure 3.4-3. Its geology basically consists of a sequence of horst and graben structures, with the sandstone sequence constituting the aquifer of the basin. The basement is mainly made up of quartzites which according to the authors is uniformly dense ($d \approx 2.7 \times 10^3 \text{ kg/m}^3$) and resistive ($\rho \geq 2000 \Omega\text{m}$) and is non-magnetic. However, in places, quartzites are replaced by dolerite sills. Dolerite is a fairly magnetic rock material with an average density of $2.8 \times 10^3 \text{ kg/m}^3$ and a resistivity well above

3000 Ωm . The sediment cover consists of Karoo sediments whose density is approximately $2.4 \times 10^3 \text{ kg/m}^3$ and the electrical resistivity ranges from 10 to 200 Ωm .

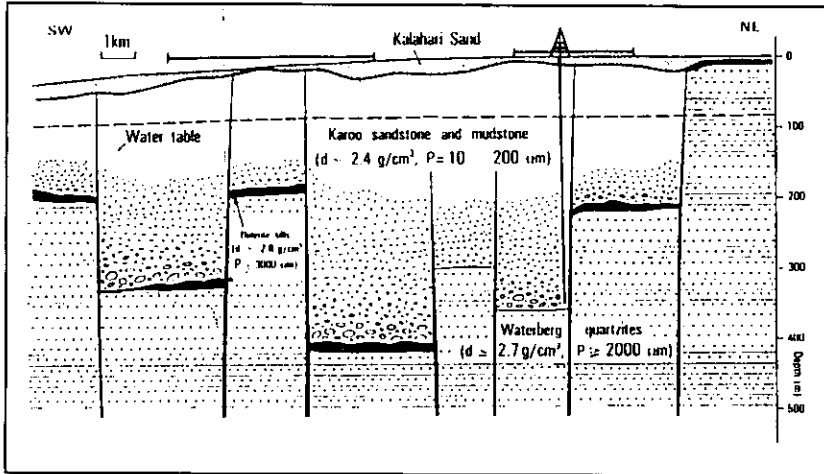


Figure 3.4-3. Conceptual geological and geophysical model of the the survey site in Botswana (after Bourgeois et al., 1994) showing the horst and graben structure. The Karoo sediments are light and relatively conductive if water saturated. The dolerite sills and the quartzites which are relatively dense and resistive form the base of the sequence. The hydrogeological target is the sandstone layer.

The whole sequence is overlain by the uniformly resistive Kalahari sands. The aim of the geophysical survey was, on regional scale to determine the horst and graben structure of the basin, in order to locate the main potential reservoirs. The thickness of the sediment cover as a whole ranges from 30 to more than 350 m. Bourgeois et al. (1994) compared AMT with gravimetric and magnetic techniques for the reconnaissance work which were supplemented by DC resistivity and HLEM for detailed mapping. For the processing and interpretation of AMT data the authors used a procedure which is based on the readings of a single frequency (10 Hz). The calculated apparent resistivity is then used to estimate the depth of the basement. With this procedure, they found a correlation between apparent resistivity and depth to basement which was used as the basis for the interpretation of AMT results. The authors point out that due to the electrical uniformity of sedimentary units in the region, there are no static shifts which makes the AMT method a cost-effective tool for

mapping the subsurface geology. The results of all other methods were processed using conventional interpretation procedures. The sample result of one of the profiles surveyed (figure 3.4-4) is self-explanatory. By using this procedure the authors could locate 20 holes in the area with more than 50% of them having a yield greater than 30 m³/h.

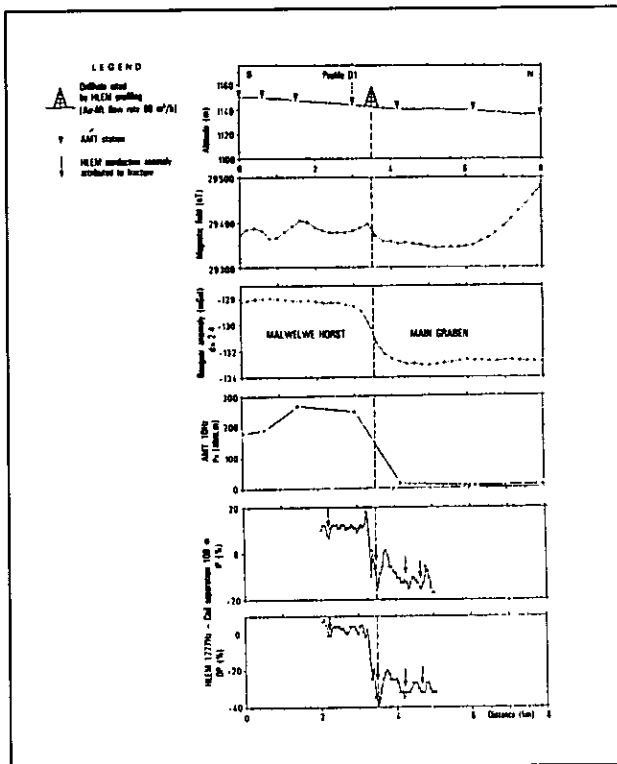


Figure 3.4-4. Sample result of the survey in Botswana (after Bourgeois et al., 1994). Notice the strong correlation between the AMT and the gravimetry. The information from the magnetic is not consistent with local geology. According to the authors this might be due to the inconsistency of the dolerite sills in terms of their thickness and magnetisation. The results from the HLEM suggest that the horst is overlain by conductive material (e.g. the Kalahari sands) and very conductive edge of the graben, which is attributed to the fractured zone related to the fault. The borehole drilled in the site indicated in the figure gave a yield of 66 m³/h.

Locating Sandstone Aquifers in a Sedimentary Basin: Senegal

In the second example Giroux et al. (1997) used the MT method to infer a model of the hydrogeological conditions in the Senegalese basin. The survey area experiences a semi-arid climate and is covered by a very thick sediment layer whose thickness can reach up to 8 km in the western part of the basin decreasing eastwards (figure 3.4-5), with the sandstone layer constituting the actual groundwater target.

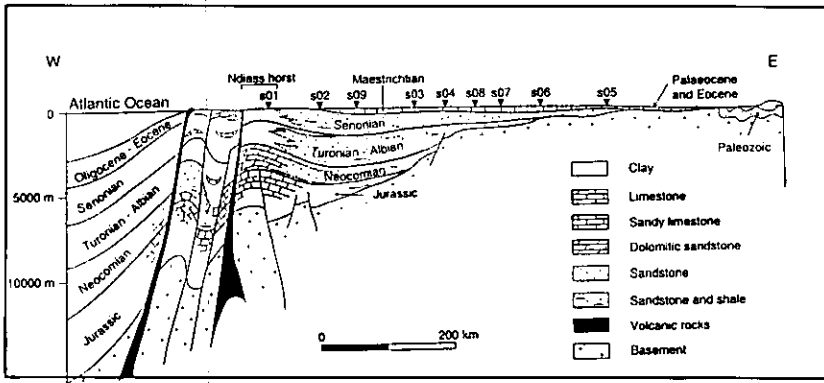


Figure 3.4-5. Schematic geological cross section of the survey area in Senegal (after Giroux et al., 1997).

Over the same area several geophysical surveys (MT, gravimetry, and DC resistivity) have been carried out prior to the study by Giroux et al. (1997), but they were concerned with deeper portions of the basin and no detailed information on the upper part of the basin (e.g. upper 1000 m) is available. The authors point out that previous MT studies were carried out prior to the development of the procedures for distortion analysis (e.g. Zhang et al., 1987; Groom and Bailey, 1991) and the high frequency energy content was poor in order to allow a reliable resolution of the upper part of the basin. Therefore, they performed a distortion analysis of their data set and showed that the sedimentary layers in the basin can be considered 1D and that no galvanic distortion occurs within the frequency range covered. A sample inversion result for the point labeled s03 (figure 3.4-5) is shown in figure 3.4-6. Furthermore, they could estimate the effective porosity from the MT combined with borehole data. They point out that due to weak resistivity contrasts in the overlying sedimentary sequence, the upper limit of the aquifer in the area could not be resolved.

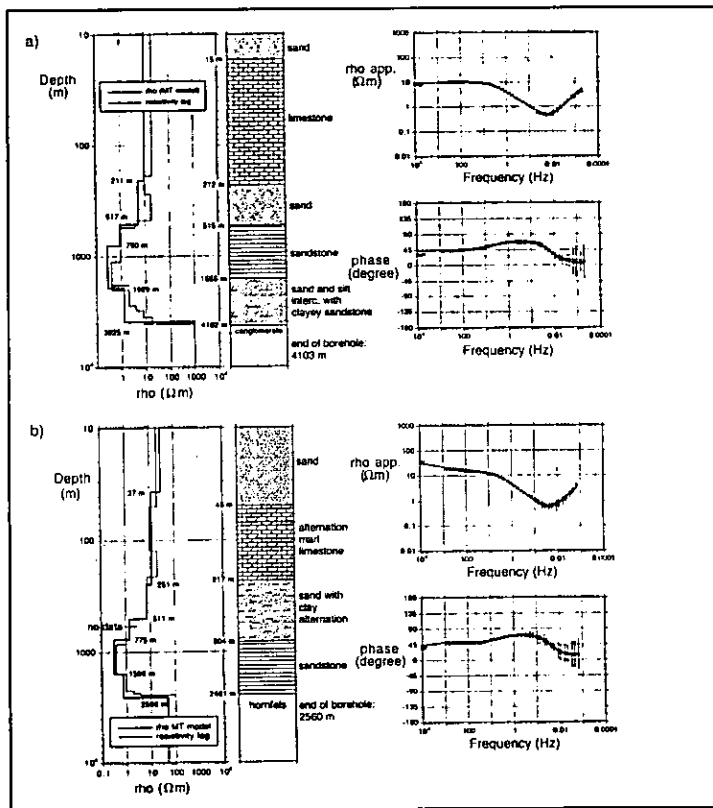


Figure 3.4-6. A sample MT sounding curve with the result of 1D interpretation (after Giroux et al., 1997). The 1D interpretation shows clearly the depth to the target layer (the sandstone) which is shown on the schematic representation of the lithology. On the right is shown the fitting between the measured apparent resistivity and phases (crosses) and the model response (solid line).

3.5. Summary

The main message to be retained in mind from this literature survey is that the application of geophysical techniques for groundwater prospecting in Africa is expanding and modern and more sophisticated techniques are widening up their applicability. Considering the type of groundwater targets common in Africa, future prospects of successful application are particularly bright for techniques such as AMT, CSAMT, TEM and ERT techniques. The application of GPR (to be reported in the next chapter) appears to be promising for prospecting

of groundwater in sandstones, where the clay content is usually not so high. However, the results of the surveys carried out so far suggest that there is still a need for more focussed studies in order to establish more accurately the applicability of many such techniques in such geological environments.

One of the factors that limit the efficiency of geophysics in groundwater prospecting in the CB areas is the degree of spatial variability of groundwater targets. The example given by Palacky et al. (1981) illustrates clearly the type of problems that affect the efficiency of geophysical techniques in such environments.

Another aspect that also affects the efficiency of geophysical surveys is that groundwater exploration programmes in Africa and elsewhere operate usually with small budgets and thus, the number of applied techniques is limited. In many cases reported in the literature, the DC resistivity technique is used alone or combined with EM profiling. However, in geological environments like the ones prevailing in the CB, this strategy might not be efficient especially for reducing the problems arising from equivalence.

Research results to date show that joint inversion of the geophysical data yields better model estimates with improvements in the resolution of several parameters related to the conductive target including resistivities and thicknesses. The usual strategy to reduce ambiguity is to combine and perform joint inversion of data sets of different geophysical techniques, e.g. DC resistivity with AMT, TEM or seismic refraction. Excellent examples showing the efficiency of this strategy have been reported by many authors e.g. van Overmeeren (1981); Raiche et al. (1985); Sandberg (1993); Meju et al. (1996); Sharma and Kaikkonen (1999) and many others.

On the other hand, better correlations are needed between geophysical and hydraulic parameters of the aquifers such as porosity, permeability, and clay content, which are very important for resource quantification, exploitation and monitoring.

Although several works have been carried out in this context (e.g. Mbonu et al., 1990; Yadav and Abolfazli, 1998; MacDonald et al., 1999), the impact in the practice of groundwater surveys is not yet significant.

4. Recent Developments in Geoelectric Methods for Shallow Studies

4.1. Introduction

Geoelectrical methods (i.e. DC resistivity and EM) play a central role in near surface studies particularly in groundwater and environmental studies for two reasons:

- due to similarity in the way that electric current and fluid flows depend on the interstitial pores of the rocks

and that

- more than any geophysical technique, the electrical and electromagnetic responses are directly affected by the presence of pore fluids and their electrical conductivity.

Moreover, heterogeneity and anisotropy of the electric properties may be related to similar effects in the hydraulic properties. On the other hand, geoelectrical methods are non-destructive methods in the sense that they can be used to investigate the subsurface without disturbing it and that they can give an areal coverage which may be impractical or impossible to achieve with other methods such as drilling. The large number of improvements in geoelectric instrumentation, field procedures and data interpretation over the last years (e.g. Ward, 1990; McNeill, 1990 and 1991; Dahlin, 1993; Nobes, 1996 and many others) are a testimony to the importance of these techniques in shallow studies.

4.2. Resistivity Methods

4.2.1. General

In the hydrogeological literature, most resistivity measuring systems use variants of the equally spaced Wenner and dipole-dipole configurations (e.g. Barker, 1981; Nobes, 1996). The offset Wenner technique devised by Barker (1981) proved to be particularly useful in areas with pronounced shallow lateral variations and was successfully applied in areas of CB in Zimbabwe (Barker et al., 1992).

In practice there is a plethora of resistivity configurations each one suitable for a particular type of survey. Ward (1990) summarises the

factors which must be considered in selecting a resistivity technique for a particular survey. Ward (1990) also point out to some modifications of the standard Schlumberger configuration such as the gradient profiling and the gradient array. However, the lack of practical examples of their applicability is a suggestion that they are not as widely used as the Wenner and dipole-dipole configurations.

Another modification of the traditional resistivity configurations that has been proposed by Matias and Habberjam, 1986, is the square array. This technique is particularly useful in the identification of directional anomalies and of anisotropy in the electrical properties that may arise from thinly-bedded dipping layers. The technique has been used to a limited extent for prospecting of fractured aquifers in Africa (e.g. Darboux-Afouba and Louis, 1989).

In areas with strong underlying structural controls such as the CB or in areas where the hydrogeology is dominated by subsurface channels, many workers propose the use of the apparent resistivity tensor (e.g. Bibby, and Hohmann, 1993) or alternatively, to rotate the resistivity array in order to determine the azimuthal dependence of the resistivity. However, the latter procedure places a logistical constraint in that the measurements have to be made twice for the same electrode spacing.

4.2.2. Basic Principles of Electrical Resistivity Tomography (ERT)

As pointed out by many workers (e.g. McNeill, 1980 and 1991; Ward, 1990; Nobes, 1996 and many others), the conventional resistivity techniques are often too cumbersome, time consuming and require more man power compared to their EM counterparts. In this context, the introduction of a number of automated resistivity survey systems using computer controlled multi-electrode arrays is one of the most remarkable development in DC resistivity over the last years. The introduction of automated systems subsequently led to the implementation of multi-dimensional resistivity survey systems which are often referred to as electrical resistivity tomography (ERT). The principles of multi-dimensional resistivity surveying or ERT are well established and extensive description of the different arrays and modes of deployment can be found in the literature (e.g. van Overmeeren and Ritsema, 1988; Griffiths and Barker, 1993; Dahlin, 1993; Li and Oldenburg, 1994; Sorensen and Sorensen, 1995; Brunner et al., 1999). Although the modes of array deployment may differ from one field procedure to another, basically, 2D resistivity coverage is performed in one of the following ways:

- by combining a set of resistivity profiles along the same line but with varying electrode spacing, i.e. Continuous Vertical Electrical Sounding (CVES) (van Overmeeren and Ritsema, 1988), usually starting from long electrode spacings and going towards shorter (Dahlin, 1993),

or alternatively,

- by using the roll-along technique as described by Griffiths and Barker (1993).

3D coverage on the other hand, is often performed by using a set of electrodes arranged on a regular 2D grid or in boreholes (e.g. Bibby and Hohmann, 1993; Li and Oldenburg, 1994; Zhang et al., 1995; Brunner et al., 1999). Until recently, ERT was mostly applied to smaller objects with a depth of investigation typically up to a few tens of metres. However, recent works (e.g. Bibby and Hohmann, 1993; Brunner et al., 1999) show that with some modifications, the technique can be extended up to depths of several kilometers. The use of such automated systems in the practice of resistivity surveys not only eased out some of the problems pointed out above, but also made it possible for the resistivity technique to be applied in areas of complex geology where the conventional resistivity techniques are unsuitable (e.g. Griffiths and Barker, 1993; Dahlin, 1993; Olayinka and Weller, 1997; Ritz et al., 1999a and 1999b). These authors have shown that the use of such automated systems makes the field surveys more efficient and the noise level in the data sets can be kept in a low level and thus, improving the resolution. On the other hand, since the whole process is automatic, the man power requirement, the duration and hence, the costs of the survey can be reduced significantly. The reduction of costs is particularly important because groundwater exploration programmes operate with small budgets and thus, any improvement in technology which reduces the costs and improves the resolution would permit a more efficient use of the development funds (e.g. Palacky et al. 1981; Senti, 1988; van Dongen and Woodhouse, 1994). In the following sections, the basic principles as well as variants of the technique are outlined.

4.2.3. Induced Polarisation (IP) Method

The technique operates under the principle that whenever a current in the ground is interrupted the voltage across the potential electrodes

does not drop to zero instantaneously. Instead, it relaxes for several seconds (or minutes) starting from an initial value which is a small fraction of the voltage before its interruption. The IP method can in principle, be performed with any of the configurations used for conventional resistivity surveys. However, as will explained later, there are some assumptions associated with the technique which limit and in some cases prevent the use of some of the configurations (e.g. electromagnetic coupling). The IP method was initially applied in mineral exploration, particularly for prospecting of ore deposits containing disseminated electronically conducting minerals such as galena, sphalerite, pyrite, etc.

However, recent works (e.g. Ward, 1990; Draskovits and Fejes, 1990; Weller and Börner, 1996; Vanhala et al., 1992; Parasnis, 1997; Braga et al., 1999 and many others) show that the IP method can be very useful in hydrogeological studies particularly, in aquifer characterisation due to the fact that clay particles are found in many hydrogeological systems as aquitards. In many such cases IP information can be used to distinguish between a resistivity anomaly due to fresh water aquifer (i.e. low clay content and thus, low IP effects) and an anomaly due to an aquitard (i.e. high clay content and thus, high IP effects). Although this procedure is not to be applied strictly, in some cases it may provide useful information in the interpretation of resistivity data e.g. to aid in identification of suppression and equivalence problems (Parasnis, 1997).

Moreover, new developments in spectral IP measurements as well as the increase in resolution of small polarisation effects are widening the application of this phenomenon in geophysical studies (e.g. Weller et al., 1996; Reynolds, 1997). In many cases, the quality of information that can be extracted from the technique is much higher compared to the conventional DC resistivity techniques (Weller et al., 1996).

The IP and any other resistivity technique operate under the assumption that the coupling between the transmitting and receiving circuits is galvanic. However, since IP methods apply low frequency alternating currents, electromagnetic coupling problems may be faced in some cases, particularly with increasing conductivity, frequency and the distance between the transmitting and receiving circuits (Ward, 1990; Parasnis, 1997). In many cases the EM coupling effects can distort seriously the IP measurements and render the information from the technique useless (Parasnis, 1997). On the other hand, the requirements of IP compared to conventional resistivity methods are much higher: non-polarisable electrodes are needed, the data recording is time consuming, the injection current must be higher, and the equipment is more expensive.

4.3. Electromagnetic (EM) Methods

4.3.1. Frequency Sounding EM Methods

As was described in section 3.3.1.2., major advances in the frequency domain EM methods applied to groundwater studies involve mainly adaptations of the horizontal loop EM method operating in the low frequency range. These systems have been widely used for mapping purposes as is reported in many works such as (e.g. McNeill, 1980, 1990, 1991; Palacky et al., 1981; Hazell et al., 1988 and many others). In many such works, the technique was used mainly in combination with conventional VES.

However, recent developments point to an increasing interest and use of multi-frequency HLEM techniques for studies of the vertical resistivity distribution in the subsurface. It is also widely recognized that frequency electromagnetic sounding offers distinct advantages over VES method, which include:

- Depth values obtained from EM data are not distorted by pseudo-anisotropy, since all induced currents flow horizontally (McNeill, 1980).
- Lateral effects are much smaller than with conventional resistivity soundings of the same depth of investigation because a smaller distance between transmitter and receiver is needed.
- Owing to its small size, the current loop is considerably safer than the long cables used for conventional VES.

However, HLEM sounding has the following disadvantages :

- Lower penetration of well conducting layers.
- The measured parameters, the inphase and the out-of-phase components, are less diagnostic with respect to the resistivity distribution with the depth.
- The lack of sophisticated interpretation tools.

Some multi-frequency EM devices operating in the kHz range such as MaxMin II, III and GEM-2 (Won et al., 1996) are being used in routine field surveys. Also in the context of frequency sounding, over the last years, the development of systems operating in the intermediate frequency range (i.e. between 300 KHz and 50 MHz) has attracted the attention of many workers (see section 4.4).

Although the concept of multi-frequency appears to be very attractive, there are however some practical questions which still

remain unanswered. In a recent work, McNeill (1996) argues that a multi-frequency EM system in order to give good information about layering it must cover a wide range of frequencies, the highest of which must be chosen so that the skin depth (δ) in the ground is significantly less than the intercoil spacing. This can be formulated as follows (McNeill, 1996):

$$\delta = 500 / \sqrt{\sigma f} \quad (4.1),$$

where,

$$\delta \ll r$$

where δ is the skin depth in m, r is the intercoil spacing, σ is the electrical conductivity in mS/m and f is the frequency in kHz. Therefore, unless the conductivity and/or the frequency are extremely high, it will be not possible to uniquely define the layering. In such cases the equivalence will become a major problem.

Furthermore, according to McNeill (1996) the problem of accurately setting and maintaining the instrumental zero becomes increasingly difficult with the increasing number of frequencies. On the other hand, the quality of HLEM data is generally affected by the sensitivity of the measuring systems to the coils misalignments and small errors in the intercoil spacings. However, Nobes (1999) in a recent work demonstrate that for diffuse boundaries, such as for leachate plumes and fault shear zone, the orientation has little effect on the response. He defines a diffuse boundary as a change in the terrain conductivity that occurs over a distance which is greater than the the intercoil spacing for the particular HLEM system used.

4.3.2. Controlled Source Radio MT (RMT) Method

A new electromagnetic system operating in the radio frequency range (14 to 500 kHz) and magnetic dipole sources from 1 kHz and upwards was recently designed and tested (Pedersen et al., 1999). The lower frequency limit of RMT transmitters is at around 14 kHz and below this limit (i.e. from 1 to 14 kHz) the natural EM energy is too low to be used for geophysical prospecting purposes. Basically, the system combines controlled source and RMT measurements which

is an essential strategy for mapping the upper 50 to 100 m. This system measures three magnetic and two horizontal electric components. Test measurements carried out recently in the Netherlands prove the usefulness of the technique for fast geophysical surveys.

4.3.3. Time Domain EM Methods

Compared to the frequency domain, the prospects of application of time domain techniques in shallow studies look more brighter particularly with the introduction of very early-time transient equipment, VETEM, (e.g. McNeill, 1991; Christensen, 1997). Such systems operate in nano to microseconds time ranges after transmitter turn-off. Therefore, they cover equivalent frequency ranges of the order of hundreds of kHz, i.e. the depth ranges needed for shallow studies.

TEM surveys for groundwater are commonly performed with two configurations; namely (1) the slingram (HLEM) mode in which the small transmitter and receiver are moved together down the survey lines and (2) the central loop sounding mode, in which the transmitter consists of a square single-turn coil whose dimensions vary from 20 to 150 m and the receiver is a small coil placed in the middle of the whole array. Each one of these configurations has distinct advantages and disadvantages that make it preferable for a particular groundwater survey (McNeill, 1991). However, recent studies suggest that for TEM geoelectric sounding a central loop configuration is desirable since it is less sensitive to local inhomogeneities, as long as they are smaller compared to the dimensions of the transmitting coil, i.e. the configuration is less susceptible to the errors caused by averaging out of lateral variations, meaning that the subsurface can be mapped in greater detail.

Recent studies suggest that by using the central loop configuration, due care must be taken in order to avoid IP effects. In such cases it is recommended to place the receiving coil just outside of the transmitting coil (McNeill, 1991).

4.3.4. Ground Penetrating Radar (GPR)

4.3.4.1. Basic Principles

The theory of GPR is not new and excellent description of the foundation of the technique can be found in e.g. Davis and Annan

(1989) and Parasnis (1997). However, for the purpose of the present work, some few concepts related to GPR will be summarised. Most traditional EM prospecting techniques operate in the low frequency ranges (i.e. up to 300 kHz) and therefore, the displacement currents in the Maxwell's equations are neglected. In such circumstances the propagation of EM energy is governed by diffusion equation (Ward and Hohman, 1987).

However, in the high frequency range such as the GPR (more than 50 Mhz), the dielectric effects play a central role and hence the electric loss terms become also important. In such cases the propagation of EM energy is governed by wave equations whose velocity (v) can be generally expressed as follows (Nobles, 1996):

$$v = c / \left\{ \frac{1}{2} \epsilon' \left[1 + (1 + \tan^2 \delta)^{1/2} \right] \right\}^{1/2} \quad (4.2),$$

with

$$\tan \delta = \frac{\epsilon''}{\epsilon'}$$

where, ϵ' is the real part of the complex dielectric coefficient, ϵ'' is the imaginary part or electric loss term (equation 3.4) and c is the speed of light in vacuum. For most geologic Earth materials in the radar frequency range, the electric loss terms are small and thus, $\tan \delta$ (or also loss tangent) can be assumed to be much less than 1. Therefore, the equation (4.2) can be approximated as (Nobes, 1996):

$$v \approx c / \sqrt{\epsilon'} \quad (4.3)$$

Another measuring parameter common in GPR applications is the attenuation of the amplitude of the radar wave when propagating through the geologic medium which is given the following equation (Davis and Annan, 1989):

$$A(z) = S(z)e^{-\alpha z} \quad (4.4),$$

with

$$\alpha = \frac{1}{2} \sigma_{GPR} \sqrt{(\mu / \epsilon')}$$

Where σ_{GPR} is the electrical conductivity in the radar frequency range which is not the same as the low-frequency conductivity and μ is the magnetic permeability. The analysis of the attenuation of radar energy was used also by some workers in order to estimate the electrical conductivity in the GPR range which is assumed to be higher than the low frequency conductivity. The usual approach followed in current surveys procedures is to start with standard electrical or EM techniques in order to define the potential areas for a subsequent application of GPR.

Over the last years the Time Domain Reflectometry (TDR), which is a variant of GPR, has been under development (e.g. Heimovaara, 1994; Heimovaara et al., 1994). However, its application is mainly focussed on soil studies and therefore, it is not of primary importance for the purposes of the present work.

4.3.4.2. Examples of Application in Hydrogeology

In the field of hydrogeology, recent encouraging results have been reported by Dahlin and Owen (1998) in Zimbabwe and by van Overmeeren (1998) in Netherlands. The former author applied the GPR technique to investigate alluvial aquifers (sand rivers) in the CB Zimbabwe and the latter presents an interesting example of application of the technique to characterise the hydrogeological targets in the mainly sediment covered coastal areas of Netherlands. Both examples suggest that the technique is particularly useful within coarse grained stream channel and sediment cover respectively, and that the depth of penetration is blocked if clay or silt lenses are present in the layering.

4.4. Hybrid Methods

Over the last years the development of methods which are a combination of both conventional DC resistivity and EM (e.g. Tabbagh et al., 1993; Christensen, 1987) and methods that explore more deeply the intermediate frequency range, i.e. that frequency gap separating the frequency ranges of standard EM methods (e.g. up to 300 kHz) and the GPR (e.g. more than 50 MHz) has been topical. The high frequency sounding and VETEM systems developed over the last years (e.g. Sternberg and Poulton, 1994 and 1997; Stewart et al., 1994; Pellerin et al., 1994 and 1995) belong to this category. In such cases, the electric and dielectric effects are equally important and thus, the EM response will be a mixture of both. The frequencies at which this mixing occurs depends on the electrical and dielectric properties of the subsurface.

Although these methods are not yet in widespread use, the concepts involved in both appear to be attractive in the sense that the combination of the methods and the exploration of the intermediate frequency range can provide more than one response type (e.g. galvanic and inductive responses in Christensen, 1987) or more than one parameter (e.g. electrical resistivity and relative dielectric permittivity in Sternberg and Pulton, 1994 and 1997; Birken et al., 1999) and thus, more information is available to constrain the inverse problem.

4.5. Nuclear Magnetic Resonance (NMR) Method

4.5.1. Basic Principles

The basic principles of nuclear magnetic resonance (NMR) on which the NMR method is based, are briefly summarised in the work of Goldman et al. (1994). The NMR method is basically operating under the principle that many atomic nuclei, including protons in water, possess an unbalanced dipole magnetic moment. The classical model describing the presence of the moment is a spinning charged particle. If a spinning charged particle having a magnetic moment, m , is placed on a magnetic field of strength H_0 , the moment will tend to align parallel to the field. As a result, the magnetic will precess around the applied field with the so called Larmor precession frequency, f_0 .

Resonance (NMR) method and the appropriate parameter is the resonance frequency frequency of the protons (H^+) of the water (H_2O) in the presence of a static magnetic field such as Earth magnetic

field. The background of the method is due to the fact that nuclei of the same species in different chemical environments, e.g. hydrogen in water, benzene or other hydrocarbons, possess different resonance frequencies. In the case of the hydrogen in water, the resonance frequency is defined as follows (Goldman et al., 1994) :

$$f_0(\text{in Hz}) = 0.04258H_0(\text{in nT}) \quad (4.5)$$

Basically, the principle of NMR consists in exciting the hydrogen protons contained in the groundwater with an external magnetic field with the Larmor frequency. The strength of the external magnetic is varied as to change the depth range of the excitation. The amplitude of the relaxation or resonance signal (after the external excitation is terminated), is proportional to the water contained in the pores.

The use of this principle for geophysical sounding purposes was originally suggested in the late 1970s by a group of Russian physicists. Recent advances of its use for direct water detection are reported by workers such as Goldman et al (1994); Mohnke and Yaramanci (1999); Yaramanci et al. (1999). Goldman and coauthors used the technique in combination with TDEM and this combination proved to be advantageous since the the loops can be used simultaneously for both techniques. Their results suggest also that the NMR technique in some cases not only detect the presence of water but also provides important information for the a better hydrogeological characterisation of the aquifer system and its subaquifers. TDEM on the other hand is particularly useful in indicating the quality of the groundwater. However, they point out some hardware problems which still affect the instrumentation used since the technique involves the detection of very low useful signals.

4.6. Summary

In this condensed review, an attempt has been made to show that there is a plethora of new techniques that can be applied in shallow studies, some of them are still in a trial phase but others are already well established and are being used in routine geophysical surveys. A particularly promising new development is the introduction of VETEM systems which now make it possible to extend the technique to the very shallow depths common in many hydrogeological and environmental studies. This is particularly important because in general, the TEM sounding offers several operational advantages compared to other geoelectric sounding techniques. However, the high cost of

VETEM systems still limits its widespread application in such surveys. The design and test of a new system operating in the radio frequency, i.e. from 14 to 500 kHz (EnviroMT system) as well as the development of a local source which makes it possible to extend the frequency cover from 1 to 14 kHz is widening the application of the technique to shallow depths and to areas with low coverage of EM transmitters in this frequency ranges.

The NMR applied for direct detection of groundwater is another interesting technique; however hardware limitations still hamper the use of its full potential. The technique operates under a lower signal level than that used in conventional geoelectric methods and this places a serious limitation since the currently used systems (hydrosopes) have a very poor ambient noise protection (Goldman et al., 1994). Moreover, the depth of penetration is limited to only some tens of meters (e.g. ca. 70 m; Goldman et al., 1994). However, if the applied in combination with another technique such as TEM, the NMR may provide usefull imformation for aquifer characterisation.

The examples given by many workers, prove also that the ERT is an efficient technique for a detailed geological and hydrogeological characterisation in shallow studies where heterogeneities of different scales predominate. The technique is particularly usefull in that apart from the resistivity distribution it is possible to infer upon specific geoelectrical heterogeneity of the investigated area on the basis of the measured data and thus, upon the lithological variations.

The combined use of the DC resistivity with the IP method is being suggested by many authors because in some cases it makes the discrimination of the resistivity anomaly in terms of clayey and clay free rock material possible. In some other cases it may also help reduce ambiguities in the interpretation of DC resistivity data which are associated with equivalence (Parasnis, 1997).

Over the last years, the application of GPR and TDR in shallow studies, particularly in hydrogeological and environmental studies has been reported. The applicability of these techniques in general suffers from high attenuation of the signals in high conductivity areas particularly in the radar frequency range. However, recent studies show that in some cases the attenuation of radar signals by conductive pore fluids can be used to the advantage in the context of environmental studies.

Finally, the results of the field trials of techniques which cover the intermediate frequency range or result from the modification of the mode of operation of conventional techniques suggest that due to the multi-parameter character of such techniques, e.g. the use of electrical resistivity and relative dielectric permittivity and/or the

simultaneous use of galvanic and induction responses, a better resolution of the subsurface structures may be attained.

5. Developments in the Interpretation of Geophysical Data

According to many workers (e.g. Christensen, 1997; Brunner et al., 1999), imaging and inversion are some of the main topics of research and development in geophysics today. Imaging involves fast approximate ways of interpretation of data, i.e. to produce a picture or a conceptual model of the subsurface geology. In practice there are several levels of imaging each one performed in a particular stage of a geophysical survey. 1D interpretation of the data is one of the levels of imaging. In order to be effective, imaging techniques must necessarily be fast and robust so that they can be applied on-line during a field survey and thus, making it possible to assess the effectiveness of the measuring strategy in real time.

5.1. Introduction

The DC resistivity inverse problem was investigated for the first time in the early 1930s (e.g. Slichter, 1933). From that time until the late 1980s, the methodology of field survey and character of data from the measurements remained unchanged. From the late 1980's and early 1990's until today, there has been considerable improvement in data collection and interpretation.

In the field of data collection automatic measuring systems using computer controlled multi-electrode arrays are becoming increasingly popular (van Overmeeren and Ritsema, 1988, Sorensen and Sorensen, 1995). At the same time interpretation techniques have developed profoundly. An excellent review work on the developments in the interpretation techniques of DC resistivity sounding data is given by Christensen (1986).

The development of interpretation technique of DC resistivity soundings was marked by three events; namely (1) the linear filter theory (e.g. Christensen, 1979), (2) the widespread use of digital computers and (3) the application of general linear inverse theory. With the latter the concept of automatic inversion and analysis became popular, in which computer programmes based on this theory were able to find the best fitting model automatically, provided they were given a reasonably accurate initial model and/or a priori information (e.g. Johansen, 1977). In MT inversion for example, the most commonly used algorithms in the automatic layered inversion are those of Constable et al. (1987) using a smoothed layered model for constructing models with a small number of layers.

In some geological environments however, especially in sedimentary areas, the real Earth structure often is layered with rather well defined resistivities that can be well differentiated from resistivities of other layers, even though each formation may show variations on a variety of scales. There is evidence from borehole investigations to suggest that electrical resistivity often varies abruptly from one formation to the next, and a description of the real world in terms of smooth models is thus not quite appropriate. Smooth models will fit the data equally well as models with a few distinct layers.

Linearized iterative solutions of the 1D geoelectrical problem requires an estimate of the initial solution for starting the iterations. However, this might cause the solution to become somewhat dependent on the initial guess. Therefore, research and development is directed toward inversion algorithms which are capable of resolving the pertinent structures regardless of the initial input parameters or automatically. Automation of DC resistivity data interpretation is essential considering its increasing application in shallow studies in connection with environmental, hydrogeological and geotechnical investigations. The approach developed by Zohdy (1989) was one step forward in this regard. In Zohdy's inversion scheme a layered model is obtained directly from a digitized sounding curve without defining a preliminary guess of model parameters. Dahlin (1993) applied this approach to interpret resistivity data.

On the other hand, it is well known that inversion methods based on standard iterative least squares alone often produce model estimates which depart from the real structure. Therefore, the inversion procedure must be regularised by for example a truncated singular value decomposition. Many DC resistivity inversion schemes use a combination of iterative least squares procedures with truncated singular value decomposition (TSVD) to optimise the solution. The success of applying the TSVD technique in order to improve the iterative least squares estimator depends to a great extent on a proper choice of the truncation parameter. In many inversion schemes the truncation level is usually set arbitrarily or by a trial and error procedure (e.g. Scales, 1996; Muiuane and Pedersen, 1999a). However, many authors (e.g. Xu, 1998) have shown that the lack of a workable criterion to determine the cut off level of the small singular values in the SVD may lead to biased results. Attempts to develop truncation criteria for small singular values have been made in the past by many authors e.g. the use of F-statistic (Dempster et al., 1977) however, this line was not pursued further for the purpose of geophysical data inversion. Recently, Hansen (1991 and 1992) proposed the use of the so-called L-curve approach to find the truncation

parameter that simultaneously minimises a norm of the residuals and a (semi-) norm of the model estimates. However, it turned out later that in some cases the L-curve truncation criterion may lead to instability of the convergence particularly in the case of random data (Vogel 1996). Xu (1998) proposes a quality-based mean squared error (MSE) truncation criterion.

In the present work, two approaches of 1D DC resistivity data inversion based on modified versions of standard iterative least squares and two criteria of TSVD are presented.

5.2. Automatic 1D Interpretation of DC Resistivity Sounding Data

5.2.1. Outline of the Method

The resistivity inverse problem is non-linear and as such, is usually solved using iterative least squares procedures which perform the quantitative adjustment of the model parameters (i.e. the resistivities and thicknesses) and yield the optimum parameter set minimizing the weighted sum of squares of data residuals (Johansen, 1977). The present approach is motivated by one of the properties of the resistivity sounding curves which is based on the fact that the form of a sounding curve follows the form of the true resistivity-depth curve. As the true resistivities increase or decrease with greater depth, the apparent resistivities increase or decrease with greater electrode spacings. Therefore, by splitting the data set in parts, different depths of the subsurface can be resolved. Furthermore, the present approach offers a possibility of circumventing the requirement of explicitly defining an initial model for the start of iterations. For the illustration of the present scheme a synthetic Schlumberger data set consisting of the current electrode spacings (i.e. $AB/2s$), the apparent resistivities and the corresponding uncertainties was used. AB denotes the distance between the current electrodes. In the next sections each of the several steps followed in the approach are described in detail.

5.2.1.1. Stripping the Earth from Top to Bottom

The usual strategy in linearized iterative solutions of the 1D geoelectrical problem is to start with an estimated solution and to solve the forward problem to obtain the predicted data. A perturbation is sought which, when added to the estimated solution yields a model which better reproduces the observed data. As pointed out above, this

causes the solution to become somewhat dependent on the initial guess, and in some cases leads to instability in the iteration process. The present approach offers a possibility of circumventing this problem. The total data set is divided into subsets, starting with the smaller electrode spacings ($AB/2$'s), i.e. resolving the upper part of the model first. When a best fitting model is found the next data segment is added and the iteration process continues by using the previous best fitting model as a starting model. As will be demonstrated in section 5.2.2, the splitting approach gives stability to the inversion procedure.

5.2.1.2. Reparameterisation of Model Parameters

The unknown model parameters are reparameterised in logarithmic space. Logarithmic parameters are advantageous in the sense that changes can easily be constrained to be less than a specified threshold and thus, preventing them to become too large or small. Another benefit of using logarithmic parameters is that only positive values of resistivities and thicknesses will be allowed. Current approaches may introduce layers that during the iteration process become extremely thin with extreme resistivities. The logarithmic parameterization will force all resistivities and thicknesses to stay within predefined limits:

$$x_m = \log \frac{\rho_m - \rho_{\min}}{\rho_{\max} - \rho_m} \quad (5.1a)$$

and

$$x_m^* = \log \frac{d_m - d_{\min}}{d_{\max} - d_m} \quad (5.1b)$$

where ρ_m and d_m are the resistivities and depths respectively, and x_m , x_m^* are the corresponding parameters in the logarithmic space. With this parameterisation it is ensured that all model parameters will fall within their bounds, i.e. $\rho_{\min} < \rho_m < \rho_{\max}$ and $d_{\min} < d_m < d_{\max}$. The bounds should not be chosen too close the true range of parameters. In this case, it may happen that convergence is impeded and a bad data fit may result.

5.2.1.3. Strategy for Finding Initial Models

The initial model for the start of inversion is found directly from the data, i.e. from the first data part corresponding to small electrode spacings. It is taken as a uniform halfspace whose resistivity is defined as follows:

$$\rho_1 = \frac{1}{n} \sum_{i=1}^n y_i^{meas} \quad (5.2),$$

where

$$y_i^{meas} = \rho_{ap}^{meas}.$$

The best fitting uniform halfspace is then used to define a new initial model with two layers. In the initial phase, the resistivities of the upper layer and of the underlying homogeneous halfspace are set at the same value. The layer boundary is chosen to be midway between the maximum and minimum values of $AB/4s$ in a logarithmic sense:

$$\log d_1 = (z_{\max} + z_{\min}) / 2 \quad (5.3)$$

in which

$$z_{\min} = \log(AB/4)_{\min}$$

and

$$z_{\max} = \log(AB/4)_{\max}.$$

$AB/4$ is the estimated depth of investigation (Barker, 1989). The best fitting two-layer model is subsequently used as the initial model with three-layers. The thickness of the extra layer (layer number two) is taken to be one third of the total logarithmic thickness. This process can be repeated as many times as needed for calculating a best fitting m -layered model.

For the general case of a m -layered Earth, the definition of new initial models is done by using the previous best fitting model and increasing the number of layers by one. The depth to the top of the extra layer (i.e. layer number m) is defined as:

$$\log d_{m-1} = z_{\max} - \frac{1}{m}(z_{\max} - z_{\min}) \quad (5.4)$$

The inversion scheme works in such a way that data fit with an extra layer is always better than or equal to the previous best fitting model without the extra layer since the previous best fitting m -layered model has exactly the same resistivity-depth distribution as the new initial $(m+1)$ -layered model. For a given number of layers, convergence of the iteration process to improve the fit is reinforced by initially choosing the number of degrees of freedom (i.e. the number of singular values in the singular value decomposition of the Jacobian matrix) to be equal to that of the previous m -layered model, i.e. $2m-1$ and incrementing that number in steps of one to the maximum number of degrees of freedom of the present model, i.e. $2m+1$.

5.2.1.4. The Final Model

The solution of the resistivity inverse problem by standard least squares procedures with SVD allows us to distinguish between well and poorly resolved linear combinations of model parameters. For a given inversion step, the construction of models that give a better data fit can be done with truncation of eigenvectors belonging to the least resolved combinations, and as the iteration process advances those singular values can be activated one by one. The most important aspect of the inversion scheme is to find models that are continuously giving improved fits without being trapped in local minima, and that such initial models for a given number of layers and data already fit the data well. The output of the iterative least squares procedure consists of the optimum parameter set (ρ_i^o, d_i^o) minimizing the weighted sum of squares of residuals, with the weights as estimated errors.

$$Q = \frac{1}{n-m} \sum_{i=1}^n \frac{|y_i^{meas} - y_i^{pred}|^2}{s_i^2} \quad (5.5)$$

where

$$y^{meas} = \log \rho_{ap}^{meas}, \quad y^{pred} = \log \rho_{ap}^{pred},$$

n and m are the number of data and model parameters respectively, n minus m is the number of degrees of freedom and s_i is the standard error on measurement number i . Another important aspect of this approach is that the addition of an extra layer in the final stage of the construction process described above may, in some cases, lead to estimates of model standard deviations that are exceedingly high. The final model is found if either of the following conditions is met:

- The addition of an extra layer does not improve the data fit defined by equation (5.5). In this case the previous best fitting model without the extra layer will be taken as the final model
- Or the addition of an extra layer leads to one singular value being below a given threshold, thus leading to model standard deviations that are too large to be of practical use, while at the same time the data fit is improved significantly. In this case the model with one very small singular value will be taken as the final model.

5.2.2. Illustration of the Inversion Scheme

5.2.2.1. General

In order to illustrate the principles and merits of the inversion scheme, two models with some ideal resistivity distributions of geological relevance were chosen. These models also represent some special cases of interest in the application of the DC resistivity technique.

Model A: Increasing resistivity with depth

$$\begin{array}{ll} \rho_1 = 30 \text{ } \Omega\text{m} & d_1 = 4 \text{ m} \\ \rho_2 = 100 \text{ } \Omega\text{m} & d_2 = 8 \text{ m} \\ \rho_3 = 500 \text{ } \Omega\text{m} & \end{array}$$

Model B: Resistor embedded between two conductors

$$\begin{array}{ll} \rho_1 = 30 \text{ } \Omega\text{m} & d_1 = 4 \text{ m} \\ \rho_2 = 500 \text{ } \Omega\text{m} & d_2 = 8 \text{ m} \\ \rho_3 = 100 \text{ } \Omega\text{m} & \end{array}$$

Model C: 5 layer model (resistivity increasing with depth with a resistive upper layer)

$$\rho_1 = 100 \text{ } \Omega\text{m} \quad d_1 = 4 \text{ m}$$

$\rho_2 = 50 \text{ } \Omega\text{m}$	$d_2 = 8 \text{ m}$
$\rho_3 = 100 \text{ } \Omega\text{m}$	$d_3 = 16 \text{ m}$
$\rho_4 = 250 \text{ } \Omega\text{m}$	$d_3 = 32 \text{ m}$
$\rho_5 = 500 \text{ } \Omega\text{m}$	

Model D: 5 layer model (resistivity decreasing with depth)

$\rho_1 = 500 \text{ } \Omega\text{m}$	$d_1 = 4 \text{ m}$
$\rho_2 = 250 \text{ } \Omega\text{m}$	$d_2 = 8 \text{ m}$
$\rho_3 = 100 \text{ } \Omega\text{m}$	$d_3 = 16 \text{ m}$
$\rho_4 = 50 \text{ } \Omega\text{m}$	$d_3 = 32 \text{ m}$
$\rho_5 = 30 \text{ } \Omega\text{m}$	

In general, models of type A are not difficult to resolve, whereas the resolution of those of type B and D is more difficult and the convergence is slow. In all cases, the layer thicknesses are distributed logarithmically with a density of 1 per octave. In hydrogeological terms, the the low resistive layers in models A and C could represent an aquifer. In both cases the aquifer is underlain by a sequence of layers whose resistivities gradually increase with depth (e.g. a fractured bedrock). The model responses were calculated using SELMA (Simultaneous Electromagnetic Modeling and Analysis) by Christensen and Jacobsen (1997). The data set consists of 30 data points distributed logarithmically with a density of 10 per decade. Gaussian distributed noise was added to the calculated responses in order to test the sensitivity of the inversion under field conditions. The noise levels investigated were 2% and 5%. According to Dahlin (1993), the 2% noise level is reasonable for areas with small resistivity contrasts and relatively low resistivities at the surface, whereas, the 5% noise level is typical for sites with high resistivity contrasts and higher electrode contact resistances. Throughout this study the bounds of the model parameters were set at the following values:

$\rho_{\min} = 1 \text{ } \Omega\text{m}$	$d_{\min} = 1 \text{ m}$
$\rho_{\max} = 1000 \text{ } \Omega\text{m}$	$d_{\max} = 50 \text{ m}$

5.2.2.2. Modelling results

Model A: Models with increasing resistivity with depth are quickly resolved with DC resistivity technique. In order to investigate the performance of this approach for the simplest case a model of this type is included. A 2% Gaussian noise is added to the synthetic data.

In the initial stage the whole data set was inverted in one step, i.e. without data splitting. Figure 5.2-1 shows the result of inversion. The data fit is quite good ($\log Q = -0.1$).

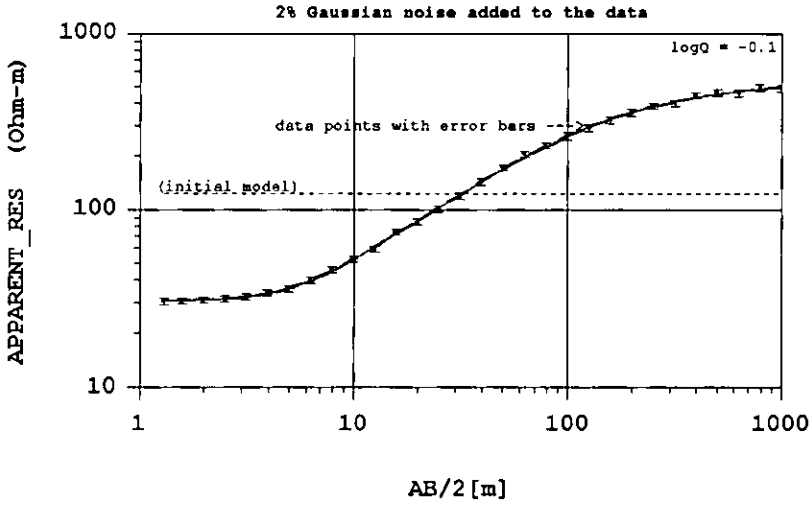


Figure 5.2-1(a)

Figure 5.2-1. Model A, 2% Gaussian noise added to the data, No data splitting. a) Apparent resistivity curve versus electrode spacing and b) Resistivity depth section.

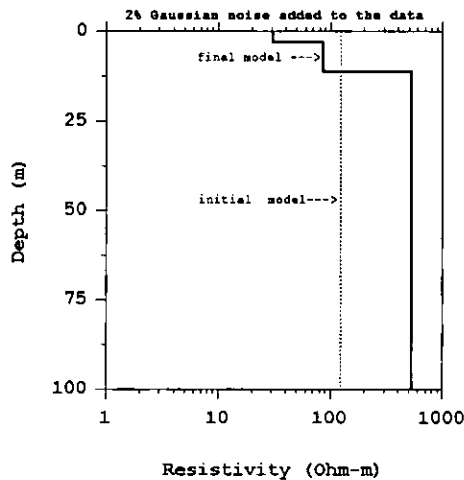


Figure 5.2-1(b)

The derived model parameters are close to their true values (i.e. Model A) except the resistivity of the intermediate layer which is slightly smaller than its true value. For this particular case of resistivity-depth distribution, the data splitting (not shown) apparently does not produce any significant improvement in the inversion results. Therefore, it was not investigated any further.

Model B: The inversion starts with a 2% Gaussian noise data set with a splitting interval of 1 decade per data segment, i.e. 10 data points per data segment. The results of inversion are shown in figures 5.2-2a, b and c. Figure 5.2-2a shows the curve of apparent resistivity versus $AB/2$.

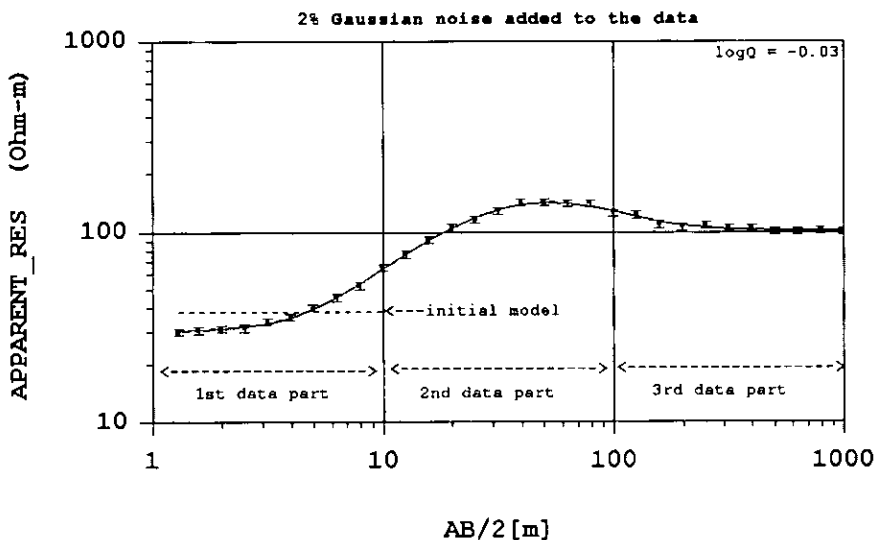


Figure 5.2-2(a)

Figure 5.2-2. Model B: Resistor embedded between two conductors; 2% Gaussian noise added to the data. a) Apparent resistivity curve for the best three-layer model determined by the inversion, data split into 3 parts, b) Resistivity-depth section; final model, data split into 3 parts and c) Resistivity-depth section; data split into 6 parts.

The inversion starts with a homogeneous halfspace (dashed horizontal line) with a resistivity of ca 40 Ω m and the first data part is fitted. When the best fitting model is found the second data part is added and the inversion continues by adjusting the model parameters and

/or adding more layers. This process is repeated until the whole data set is inverted. The data fit is quite good. In figure 5.2-2b the resistivity-depth distribution is shown. Shown are also the initial model, the intermediate initial models with two layers and the final three layer model. Notice that the resolved model parameters are quite close to the true ones. In the next step, the splitting interval is decreased to half a decade per data segment, i.e. 5 data points per decade. The resulting resistivity-depth curve is shown in figure 5.2-2c. It can be seen that there are no major differences between this and the previous result (figure 5.2-2b). The only difference is that the resistivity of the initial model (homogeneous half space) in this case is slightly smaller than in the previous example with three data parts.

These results suggest that the data splitting approach is a fast and stable procedure. This might be due to the fact that in this approach the data segments are smaller and, therefore, the model construction strategy as described above produces initial models which are not too far from the true ones for the corresponding data part. On the other hand, by inverting the whole data set in one step the starting model is too poor so that divergence occurs.

It can be concluded that by splitting the data set into parts, the iteration process will be stable and, therefore, the convergence to a global minimum will be safer. It should be noticed that that a splitting interval of 1 decade or less can be taken as a reasonable rule of thumb, since the produced inversion results (figures 5.2-2b and c) are comparable.

In the following, the effect of adding 5% Gaussian noise to the data will be demonstrated. The result of the inversion is shown in figure 5.2-3. The data set is split into 3 parts. As in the previous example the inversion starts with a homogeneous half space with a resistivity of ca 40 Ωm and the first data part is inverted by improving this model and/or adding more layers. After the best fitting model is found, the next data part is added and the inversion continues as explained previously until the whole data set is inverted. The data fit ($\text{Log}Q = 0.06$) is slightly above the threshold (i.e. $\text{log}Q \leq 0$.) but still acceptable. However, the parameter resolution is poor. Although the resistivities of the upper and lower homogeneous half spaces can be resolved perfectly, the thickness and the resistivity of the intermediate resistive layer deviates considerably from that of true model. This well known high resistivity equivalence is an intrinsic problem of this model. By inverting the data set with a splitting interval of half a decade, no further significant improvements are noticed in the inversion results (not shown).

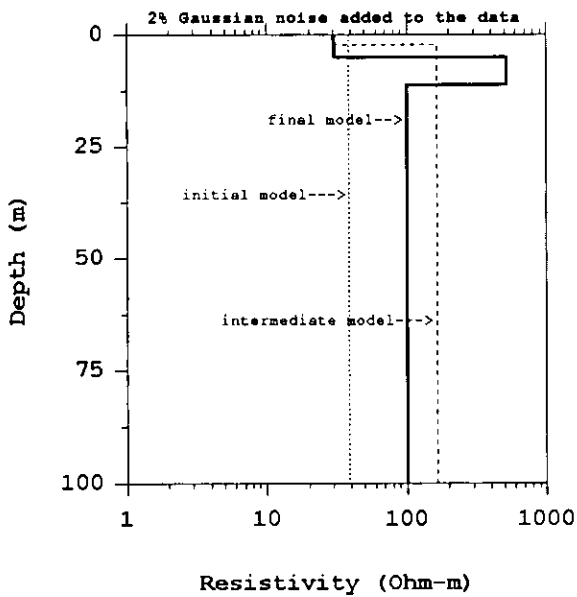


Figure 5.2-2 (b)

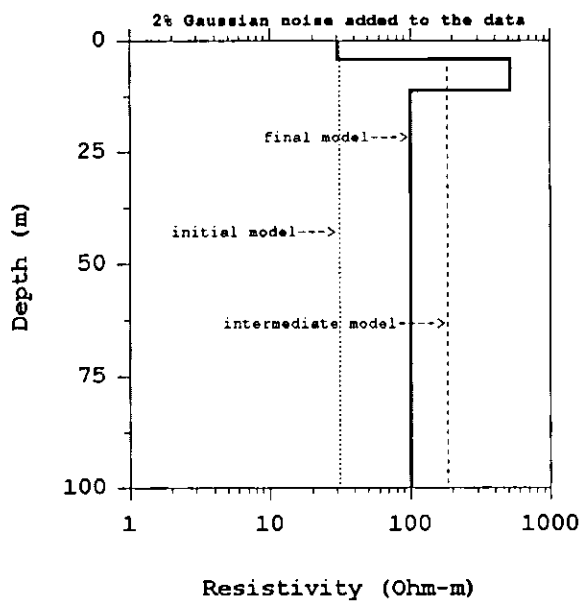


Figure 5.2-2 (c)

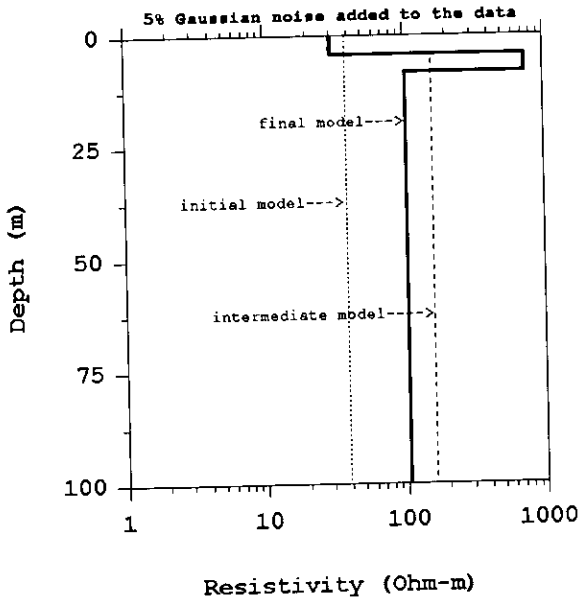


Figure 5.2-3. Model B: Resistor embedded between two conductors, 5% Gaussian noise added to the data, data split into 3 parts. Resistivity-depth section. Notice that the thickness of the second is underestimated and its resistivity is higher than the true one.

Model C: For this case only the results of the inversion when the data set (2% Gaussian noise) is split into 6 parts will be shown, i.e. 5 data points per data segment. For larger splitting intervals, e.g. 1 decade per data segment, the inversion scheme is not able to resolve the 5 layer model. Figure 5.2-4a shows the curve of apparent resistivity data versus $AB/2$. The data fit is quite good. The derived resistivity-depth curve is shown in figure 5.2-4b. The parameters of the first two layers are almost perfectly resolved. However, the remaining ones deviate considerably from those of the true model except the resistivities of the fourth layer and the underlying half space which are close to being optimal.

Model D: The results of inversion when the data set (2% Gaussian noise) is split into 3 parts (one decade per data segment) are shown in figures 5.2-5a and b. The data fit is perfect but the five-layer structure is not recovered. However, some model parameters are perfectly resolved, e.g. the resistivity of the upper layer and the

lower halfspace. Inversion results with shorter splitting intervals, e.g. half a decade (not shown), don't show any significant improvement.

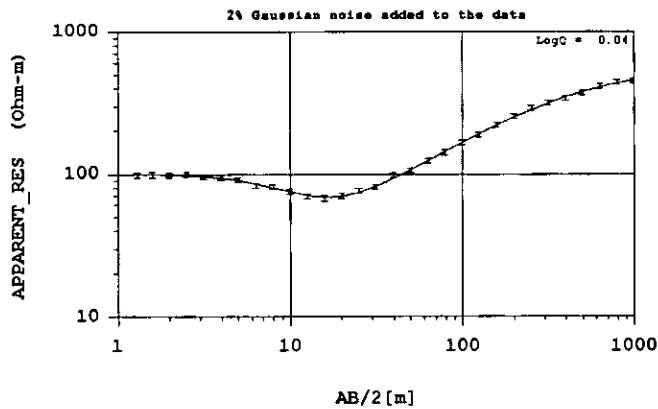


Figure 5.2-4 (a)

Figure 5.2-4. Model C: 5 layer model (resistivity increasing with depth with a resistive overburden), data is split into 6 parts. a) Apparent resistivity curve for the best five-layer model determined by the inversion and b) Resistivity depth section.

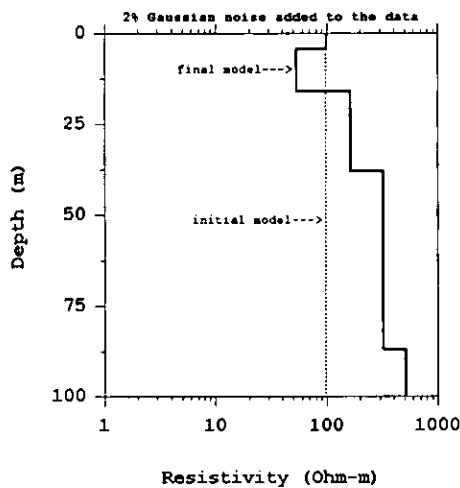


Figure 5.2-4 (b)

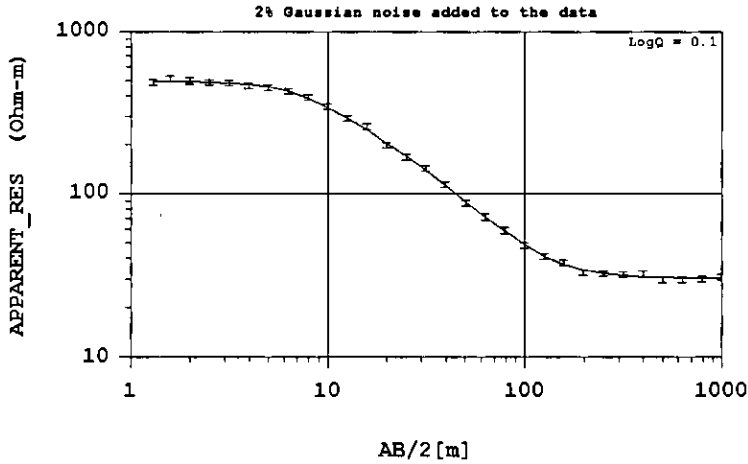


Figure 5.2-5 (a)

Figure 5.2-5. Model D: 5 layer model (resistivity decreasing with depth), data split into 3 parts. a) Apparent resistivity curve for the best five-layer model determined by the inversion and b) Resistivity-depth section. The data fit is quite good but the five layer structure of the subsurface is not resolved. However, the resistivities of the upper layer and the homogeneous halfspace are well resolved.

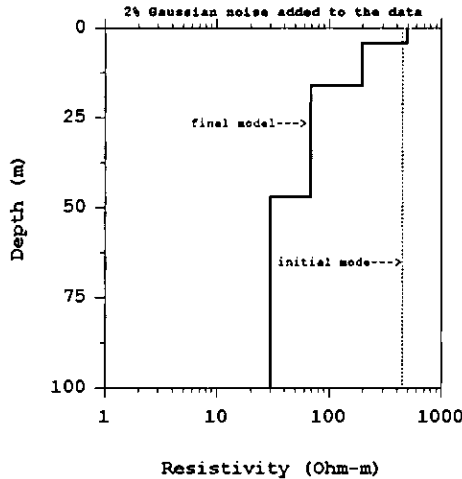


Figure 5.2-5 (b)

5.2.3. Discussion and Conclusions

A simple approach to 1D automatic inversion of DC resistivity sounding data has been presented. In the present inversion scheme the standard least squares procedures with Singular Value Decomposition is used. In order to reinforce convergence other measures of robustness such as splitting up of the data set and logarithmic parameters with bounds are applied. The bounds to be set in the inversion process should be chosen not too close nor too far from the expected values otherwise, geologically unrealistic results may result.

The initial model is found directly from the data. The inversion starts with a uniform half space whose resistivity is the logarithmic average of the apparent resistivity for the initial part. A general rule was found that in order the present algorithm to be successful, the data splitting interval should be 1 decade or less. The optimum splitting interval seems to depend on the type of resistivity-depth curve pertinent to each case as is apparent from the results of the models C and D. The no splitting case in many cases fails to yield reasonable results because the construction of the initial models involves the whole data set, and therefore, poor initial models may result. Poor initial models generally, lead to instabilities in the inversion process.

The model construction strategy is closely related to the use of the Singular Value Decomposition algorithm, whereby the maximum number of layers can be clearly identified by the occurrence of very small singular values. When this happens no more layers are introduced until eventually, during the stage of adding more and more data to be inverted, the smallest singular value goes above a given threshold.

This approach works well for data of good to moderate quality. For noisy data, e.g. 5%, there is a degradation of parameter resolution. Provided that the input parameters, such as the lower and upper limits of the model parameters are chosen properly, the present inversion scheme can yield a layer sequence agreeing with the measured data as well as with the geological concept. Notice that in this approach global bounds are used. In some cases, it might be possible to have estimates of the true parameters. This would, possibly, give a chance of setting local bounds on each layer. This possibility was not explored in the present work. The comparison of inversion results with different models suggests that the performance of the present algorithm is model dependent.

The present 1D inversion scheme is very fast and easy to implement. Therefore, it can be used for fast surveys in areas where

lateral variation is slow or as a first interpretation tool where the density of data is insufficient for a 2D or 3D interpretation. Finally it can be used as a tool to estimate how well the data should be fitted using 2D or 3D models.

5.3. Automatic 1D Inversion of DC Resistivity Data Using a Quality Based Truncated SVD

The present approach is based on the work of Xu (1998) in which a quality based truncation criterion of the smallest eigenvalues is established. Rather than defining explicitly the truncation level as in the previous procedure, this approach optimises the total Mean Squared Error i.e. the sum of the standard model variances and the bias variances.

5.3.1. Definition of the Initial Model

5.3.1.1. Vertical Resolution

The initial model is here defined as multi-layer homogeneous halfspace whose thicknesses are distributed logarithmically with depth as to take into account the decrease of the resolution of the technique with depth. The idea is based on the work of Pedersen and Rasmussen (1989) which show that for a homogeneous halfspace and for the MT method the sensitivity of a given layer is roughly proportional to the relative thickness of that layer. This can be formulated in terms of a geometric progression in layer thicknesses as follows:

$$\{d_1, d_2, \dots, d_n, \dots, d_{M-1}\} \quad (5.6)$$

$$\text{with } d_n = d_1 q^{n-1},$$

where M is the total number of layers including the substratum and q is the factor of the progression. The relative resolution as function of depth will then be constant. The depth to the top of the n^{th} layer can be defined as:

$$h_n = \sum_{i=1}^{n-1} d_i = d_1 \sum_{i=1}^{n-1} q^{i-1} = d_1 \frac{1-q^n}{1-q} \quad (5.7).$$

The minimum relative vertical resolution (r_v) is then given by the following equation:

$$r_v = \frac{1}{2}(d_{n-1} + d_n) / h_n = \frac{1}{2}(q^{n-2} + q^{n-1}) / (1 - q^n) \quad (5.8),$$

For q close to unity this sequence approaches the limit $(q-1)$ for large n . Choices of the factor q are in principle, based on the average resistivities to be expected in the area of survey. Throughout the present work q is set equal to $2^{1/8}$. However, in areas with large resistivity contrasts this factor should be chosen smaller in order to make use of the full resolving power of the data themselves and larger otherwise.

5.3.1.2. Resistivity of the Initial Model

The strategy adopted here for the definition of the the initial model for the start of iteration seems to work very well in cases where the ranges of the resistivity variations are not too high. However, as it will be demonstrated later in areas where the resistivities vary over a wide range the choice of a too low resistivity of the initial may result in a poor convergence of the inversion scheme. This is probably due to fact that the inversion scheme is able to excite significant non linearity which results in a poor exploration of the model space.

5.3.1.3. Reparameterisation of Model Parameters

In the present inversion scheme, the variable model parameter, the electrical resistivity is parameterised in terms of its natural logarithm. The logarithmic representation is robust in that changes in the parameters can easily be constrained to be less than a small threshold and thus, prevent them to be excessively large, in which case problems in the convergence of the inversion scheme may arise. In this approach the threshold for the the total change is set equal to natural logarithmus of 10. In some cases this may lead to an increase of the number of iterations but computation time is no longer a major problem today. Furthermore, the sharp cut-off of eigenvalues gives rise to some oscillations in the model estimates which if not

immediately recognised may lead to erroneous interpretations. The reparameterisation of the model parameters as formulated in equation (5.9) can partly remove these effects.

$$x_m = \log \frac{\rho_m - \rho_{\min}}{\rho_{\max} - \rho_m} \quad (5.9)$$

In this way, it is ensured that all layer resistivities in the course of inversion will fall within the bounds defined by the minimal and maximal resistivities, i.e. $\rho_{\min} < \rho_m < \rho_{\max}$. However, the bounds should not be too close to the true resistivities.

5.3.1.4. The Final Model

The output of the TSVD iterative least squares procedure consists of the optimum parameter set (ρ_i^o, d_i^o) minimizing the weighted sum of squares of residuals, with the weights as estimated errors.

$$Q = \frac{1}{n} \sum_{i=1}^n \frac{|y_i^{meas} - y_i^{pred}|^2}{s_i^2} \quad (5.10)$$

where

$$y^{meas} = \log \rho_{ap}^{meas}, \quad y^{pred} = \log \rho_{ap}^{pred},$$

n is the number of data points and s_i is the standard error on the i^{th} measurement. However, as it will become apparent in section 5.3.3., in this inversion scheme the minimisation of Q is done automatically in the sense that no bounds are defined in contrast to the previous inversion scheme where lower and upper limits are set by the user.

5.3.2. Some Considerations on Theoretical and Practical Aspects of Truncated SVD

5.3.2.1. Principles of Truncated SVD Inversion

Consider a m -layered model and a data set consisting of n data points. The errors in the data set are assumed to be statistically independent having the same unit variance. It is assumed that no a

priori information on the model is provided. The inverse problem can then be formulated in terms of optimising the prediction error energy E as follows:

$$E = \|d - Gm\|^2 \quad (5.11).$$

The singular value decomposition yields the following solution (e.g. Menke, 1989):

$$m^{est} = \hat{m}_p = V_p \Lambda_p^{-1} U_p^T d \quad (5.12),$$

Strictly speaking, this equation is valid only for the p largest singular values Λ_p and the associated eigenvectors. If the singular values are non-zero but very small the model variance will be very large. On the other hand, if all non-zero singular values are considered in the inversion, there will be no components in the null space of G . However, in most practical cases, it is not easy to define a null space due to numerical difficulties when attempting to calculate the smallest singular values. However, this is not a problem because the truncation level p is normally chosen to be smaller than the rank of the matrix G . Therefore, a proper choice of p is crucial and must be a compromise between the stability and quality of the solution. In fact, the lack of workable guidance criteria for discarding small singular values has been the major weakness of the TSVD.

Recently, Xu (1998) established a quality-based criterion to find the best TSVD estimators thereby providing a solid theoretical foundation for discarding the smallest singular values. The truncation procedures of Xu, basically consists in optimising the total solution variance which is made up of the sum of the standard model variance and bias variance. In the following the most important aspects of this approach will be summarised. Considering the equation (5.12) as the starting point its solution can be rewritten as:

$$\hat{m}_p = \sum_{i=1}^p \frac{u_i d}{\lambda_i} v_i = \sum_{i=1}^p \hat{\alpha}_i v_i = V_p \hat{\alpha}_p \quad (5.13),$$

where

$$\hat{\alpha}_i = \frac{u_i^p d}{\lambda_i}$$

denote the projections of the data vector on the eigenvector u_i backprojected into model space by λ_i^{-1} . The covariance matrix of α_p is given by:

$$\text{cov}[\hat{\alpha}_p] = \text{diag}\{\lambda_i^{-2}\} \quad (5.14a)$$

and

$$\text{cov}[\hat{m}_p] = V_p \Lambda_p V_p^T \quad (5.14b)$$

Defining the bias of the estimator as:

$$\text{bias}(\hat{m}_p) \equiv E[\hat{m}_p] - m \quad (5.15),$$

where $E[m_p]$ are the expected values of the random variable vector m_p . After some algebra, the bias term can be given as follows:

$$\text{bias}[\hat{m}_p] = -V_0 V_0^T m \quad (5.16).$$

Finally, the total model variance, henceforth denoted as MSE standing for mean squared error, can be given as:

$$\begin{aligned} \text{MSE}[\hat{m}_p] &= \text{Tr}\{\text{cov}[\hat{m}_p]\} + \{\text{bias}[\hat{m}_p]\}^T \text{bias}[\hat{m}_p] \\ &= \text{Tr}\{V_p \Lambda_p^{-2} V_p^T\} + m^T V_0^T V_0 m = \sum_{i=1}^p \lambda_i^{-2} + \sum_{i=p+1}^M b_i^2 \end{aligned} \quad (5.17),$$

In other words, the MSE depends on the accuracy of the statistically significant principal components associated with the p largest singular values and from the normalised eigenvectors corresponding to the $M-p$ smallest singular values. With decreasing p , the first term decreases and the second term increases. Therefore, the optimal MSE is a balance between the two terms. According to Xu (1998), the estimation of the bias term can be done by using ridge regression (damped least squares).

5.3.2.2. Implementation of the Minimum Mean Squared Error (MSE) in a Non-Linear Problem

Xu (1998) demonstrates how this approach work on a linear inverse problem. In the case of a linear inverse problem, the solution can be constructed easily for different choices of the truncation levels. The best choice of the truncation parameter p can be made based upon the data alone and assuming that the bias term can be reasonably well estimated. However, for non-linear inverse problems, the solution strategy is as always to linearise the problem and apply the same tools as for the linear case provided that the departure from the neighbourhood of a given estimate is not large. Thus, by expanding the non-linear functional to first order it is possible to apply linear theory in the neighbourhood of an estimate. However, for large departures from the estimate the approximation becomes rapidly inaccurate. Although other choices of the potential number of degrees of freedom (p) can be made, in the present approach, it is initially set equal to one and the best fitting solution is sought. Due to non-linearity of the problem, it is possible that many iterations may be required to reach the minimum prediction error.

The fact that the eigenvector v_1 changes direction from one iteration to the next means that the number of excited eigenvectors will be dependent on the number of iteration steps. Subsequently, p is increased by one whereby the solution is allowed to vary in the direction v_2 and again due to non-linearity the solution will also vary in the direction v_1 .

In the step p equal q , the main change occurs along the direction v_q with smaller perturbations along other active directions. In the final stage when p is sufficiently large, the release of new directions only gives minor perturbations because the corresponding data projections have already been adequately modelled in the previous iteration. The model corrections can then be calculated using a slight modification of the equation (5.13):

$$\begin{aligned} \hat{m}_q(k+1) &= \hat{m}_q(k) + \sum_{i=1}^q \frac{u_i^T(k)(d - g(\hat{m}_q(k)))}{\lambda_i(k)} v_i(k) \\ &= \sum_{i=1}^q \hat{\alpha}_i(k) v_i(k) \end{aligned} \quad (5.18),$$

where k is the iteration number and

$$\hat{\alpha}_i(k) = \frac{u_i^T(k)(d - g(\hat{m}_q(k)))}{\lambda_i(k)}$$

are the projections of the residual data vector on the eigenvector u_i backprojected into model space along the eigenvector v_i and $g(m)$ is the non-linear forward model functional. The present approach works in such a way that when q eigenvectors are included the solution already contains substantial projections along the eigenvectors numbered $q+1$ and larger. Then the new solution may be regarded as being closer to the true model and therefore, can be used to estimate the bias term in equation (5.17).

5.3.3. Results of Numerical Studies

The inversion scheme has been tested on synthetic and real data sets. The purpose of the tests are, 1) to illustrate the performance of the inversion scheme under controlled condition, i.e. resistivity-depth curve and noise contaminated data and 2) to assess its resolution capabilities against that of other inversion schemes of DC resistivity (e.g. Dahlin, 1993) and MT. It should be noted however that in the case of comparison between the DC resistivity and MT cases, although both data sets are genetically related (i.e. associated with the same physical model), the involved physics and subsurface volumes are quite different and therefore, the comparison is far from being perfect. It is only meant to show some general patterns in terms of resolution capabilities of both techniques for the models studied.

5.3.3.1. Illustration of the Inversion Scheme with Synthetic Data

For the illustration of the inversion scheme a 4 layer model consisting of a sequence of resistor-conductor-resistor-conductor is chosen. In the first part of the study the performance of the inversion scheme is demonstrated on one single model of this type. In the second part a sequence of 1D models with the same resistivity distribution but different layer thicknesses is investigated with respect to resolution capabilities of both techniques. For MT an inversion scheme based on the same principle is used (Pedersen 1999). Synthetic data sets for MT and DC resistivity (Schlumberger configuration) are generated with a density of 8 and 10 data points per decade

respectively. The frequency range for MT varies from 14 kHz to 250 kHz and the half electrode spacings (i.e. the $AB/2s$) vary from 4 to 100 m for DC resistivity. In the case of DC resistivity, these electrode spacings correspond to a theoretical penetration depth of ca 50 m (Parasnis, 1997; Barker, 1989). In order to simulate field conditions, a 1% and 2% Gaussian noise is added to the impedances and the apparent resistivities of the MT and DC resistivity data sets respectively.

Theoretical Model: Sequence of Resistor-Conductor-Resistor-Conductor

$$\begin{aligned}\rho_1 &= 100 \text{ } \Omega\text{m} & d_1 &= 4 \text{ m} \\ \rho_2 &= 10 \text{ } \Omega\text{m} & d_2 &= 20 \text{ m} \\ \rho_3 &= 100 \text{ } \Omega\text{m} & d_3 &= 20 \text{ m} \\ \rho_4 &= 10 \text{ } \Omega\text{m}\end{aligned}$$

The inversion starts with the a multi-layered homogeneous halfspace with a resistivity of 100 Ωm . The thicknesses of the layers of the initial model increase logarithmically with depth with a density of 8 per octave, whereby the minimum thickness is set equal to 1 m. Other choices of the minimum depth can be made depending on the problem and depths of interest. The inversion results of the tests with the single model given above are shown in figure 5.3-1 for both DC resistivity and MT. The data fit (i.e. Q in equation 5.10) is quite good and the inversion scheme is capable of detecting the main features of the layering. The main idea behind the automatic starting/stopping criterion used here is that: As long as the number of the degrees of freedom in the current iteration stage is less than or equal to the number of estimated degrees of freedom, the iterations will proceed until eventually this condition is violated in which case the iterations automatically stop. However, as we will see in the second part of this study, in some cases it may happen that the the iterations stop earlier, i.e. with Q higher than 1. In the case of DC resistivity there are some oscillations in the estimated parameters which are more pronounced in the upper layer. On the other hand one can also notice that from the MT inversion results the depth of penetration of the data set is clearly visible whereas DC resistivity only shows a gradual increase of the resistivity, i.e. the resistivity approaches the value of 100 Ωm which is the resistivity of the initial model used here.

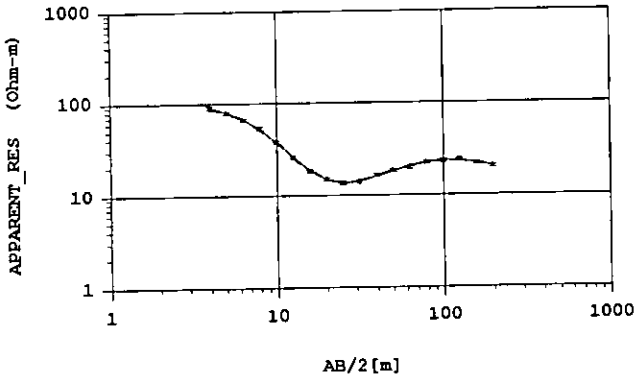


Figure 5.3-1 (a)

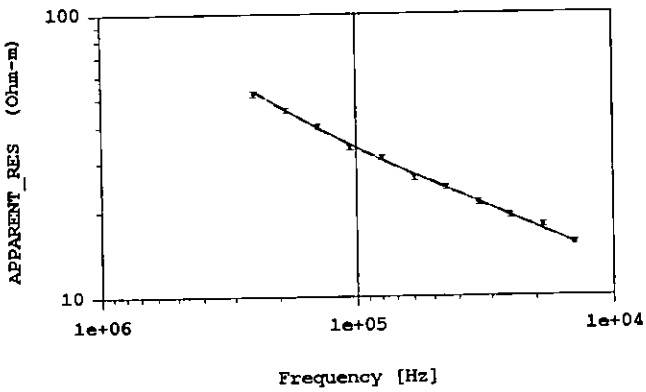


Figure 5.3-1 (b)

Figure 5.3-1. Inversion results for the single model. a) Apparent resistivity curve (DC resistivity), b) Apparent resistivity curve (MT), c) Resistivity-depth section (DC resistivity) and d) Resistivity-depth section (MT).

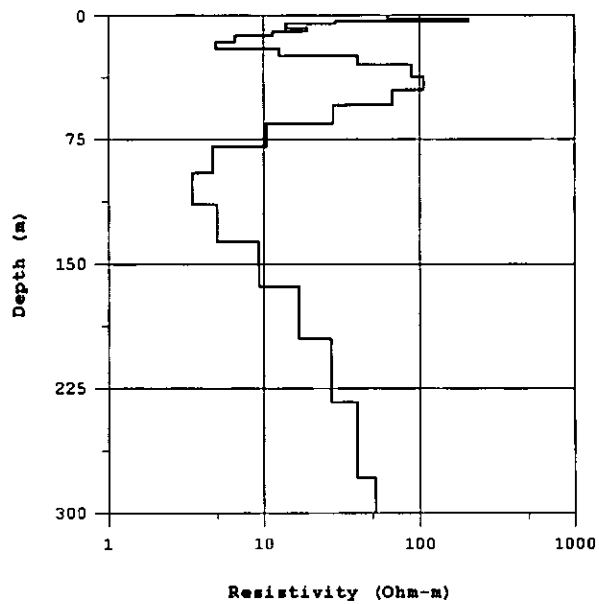


Figure 5.3-1 (c)

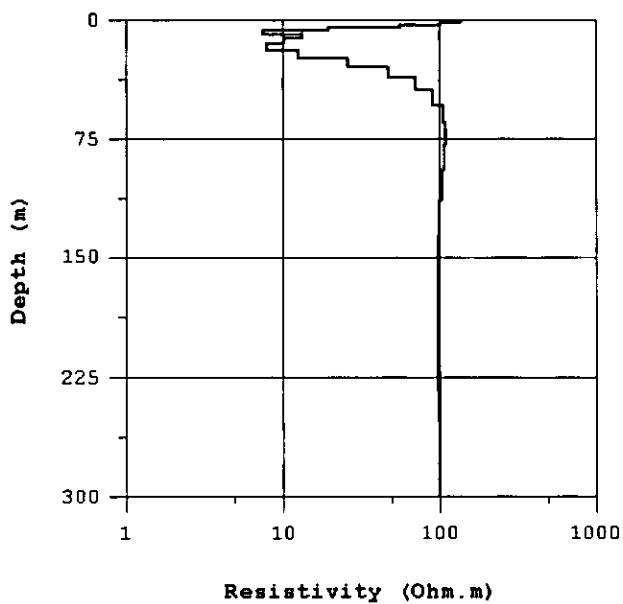


Figure 5.3-1 (d)

Figure 5.3-2 shows the behavior of several parameters in the course of inversion. Figures. 5.3-2a and b show the relation between the Mean Squared Error (MSE) and the number of estimated degrees of freedom. In the beginning of the inversion when p is set equal to 1 for DC resistivity (figure 5.3-2b), the inversion scheme estimates that 7 degrees of freedom will be needed to optimise the solution to the problem. Subsequent iteration steps, i.e. from p equal 2 through 7 give the same indication. For MT (figure 5.3-2a), the potential number of degrees of freedom is estimated at 11.

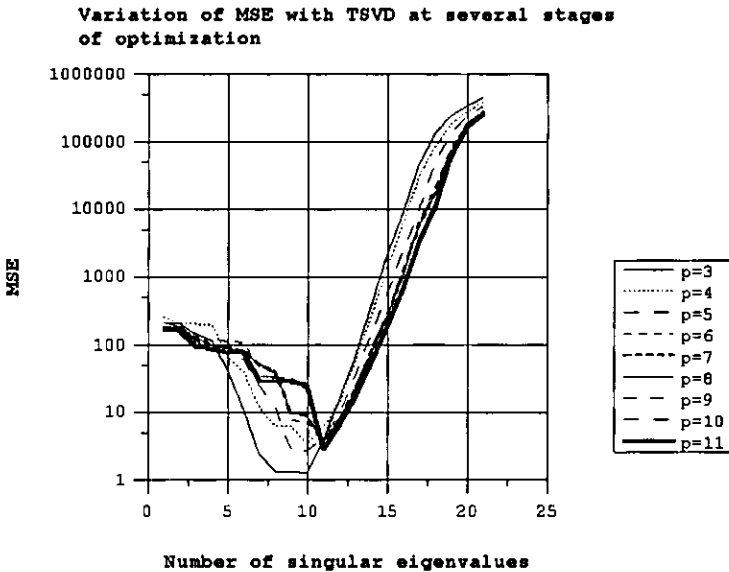


Figure 5.3-2 (a)

Figure 5.3-2. Inversion Results. a) Mean Squared Error (MSE) versus number of included singular values for MT, b) MSE versus number of included singular values for DC resistivity. Note that for both cases (i.e. MT and DC) in almost every steps the estimated optimal number of degrees of freedom is very close to the final one, c) Singular value versus singular value index, d) MSE versus iteration number. The figure illustrates the speed of convergence for both methods. The convergence of MT is generally faster than that of DC and e) Projection of final solution onto final eigenvectors versus eigenvector number. The figure illustrates the information content in both solution space (spanned by the p largest eigenvalues values) and the pseudo-null space (spanned by the $M-p$ smallest eigenvalues).

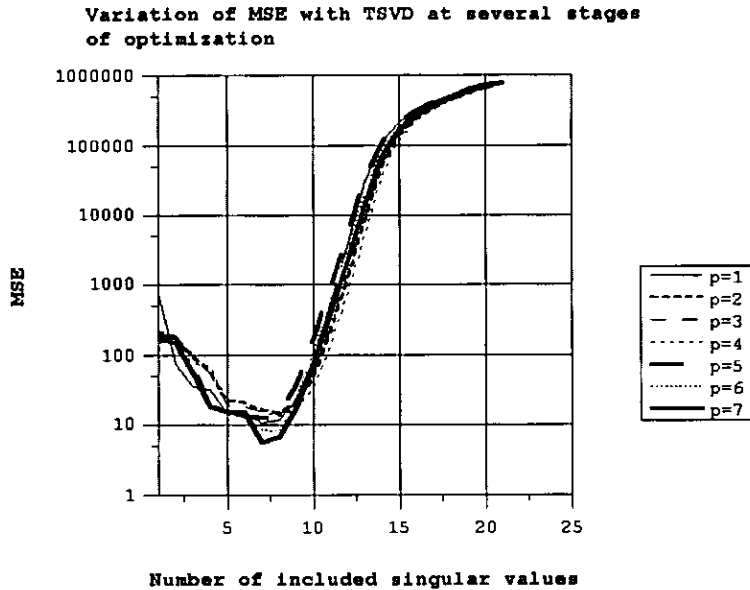


Figure 5.3-2 (b)

Figure 5.3-2c is a plot of the singular values against their index numbers. It is interesting to note that the slope of the line for MT is less steep than that of DC resistivity, suggesting that the dimension of the eigenvector matrices included in the inversion is higher in the former and therefore, its estimates are closer to the true solution. Figure 5.3-2d illustrates the data fit in several iteration steps. From this figure we can see that the speed of convergence is much faster for MT. Finally, in figure 5.3-2e the projections of the final model onto the final eigenvectors are shown. It is to notice that the projections associated with the smallest singular values are quite small.

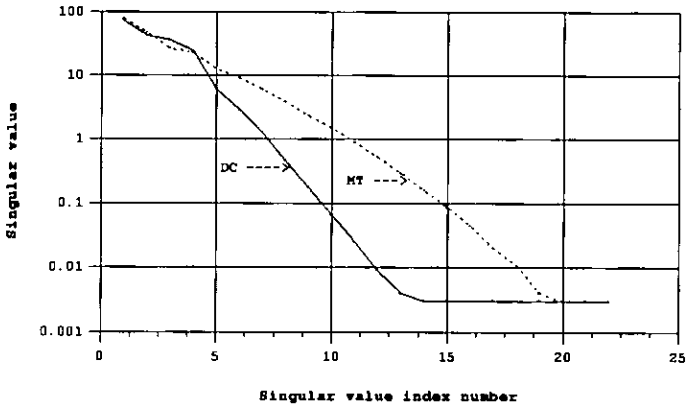


Figure 5.3-2. (c)

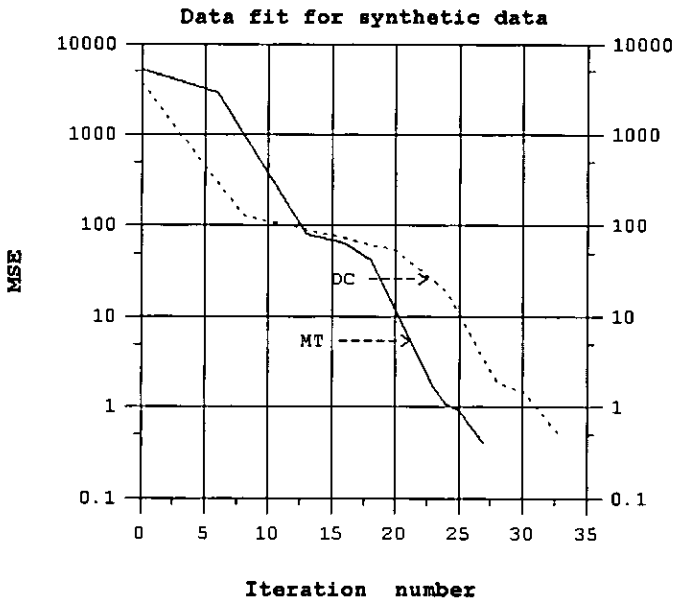


Figure 5.3-2. (d)

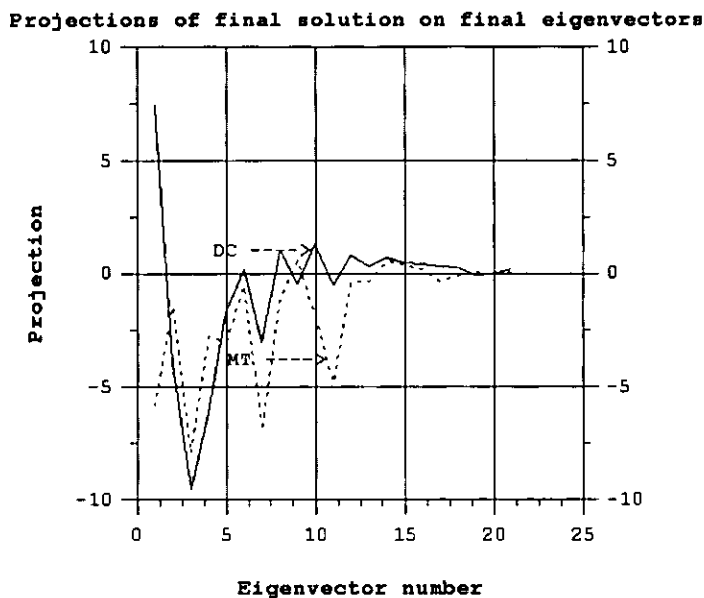


Figure 5.3-2. (e)

For the illustration of inversion scheme on a set of closely spaced VESs data sets are generated by keeping the resistivity of the layers constant as before while changing the thicknesses of the layers, one layer each time, logarithmically from 4 to 32 m with a density of 8 per octave. The noise level as well as other inversion parameters are set equal to the same values as before (i.e. 1% in the impedances and 2% in the apparent resistivities). The resulting model cross section is shown in figure 5.3-3a. For both cases the inversion was done with an initial model with a resistivity of 100 Ω m. Figures 5.3-3b and c show the cross sections constructed from concatenated single 1D inversions for MT and DC resistivity, respectively. Comparing both images one can see that MT inversion yields more stable estimates in the sense that there are few oscillations in contrast to DC inversion results which show strong oscillations especially in the upper part of the profile. Moreover, the occurrence of the low resistive layer is better reproduced in the MT inversion results, whereas the DC resistivity subsurface image below the upper resistor tends to be smeared out. On the other hand, one can notice that the depth of penetration of the data set used is clearly shown in the MT (i.e. the depth below which the resistivity of the initial model is not changed much). As mentioned before from DC resistivity such indication is not

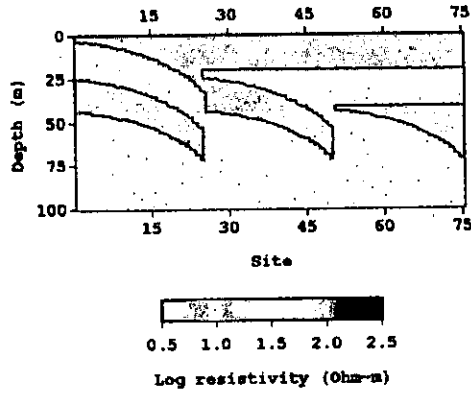


Figure 5.3-3 (a)

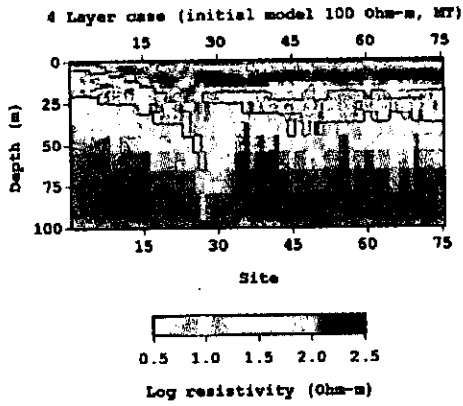


Figure 5.3-3 (b)

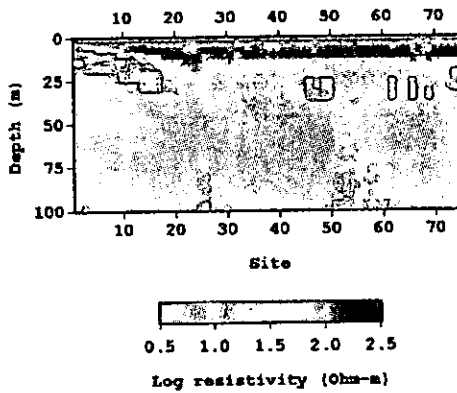


Figure 5.3-3 (c)

Figure 5.3-3. a) Theoretical resistivity-depth cross section: Sequence of closely spaced 1D Models. The models consist of 4 layers of constant resistivity (100,10,100,10 Ωm) but varying thicknesses from 4 to 32 m, b) Resistivity-depth cross section (MT), c) Resistivity cross section (DC resistivity) and d) Data fit (MT) and e) Data fit (DC resistivity). Notice that the fit for MT is better than that for DC resistivity.

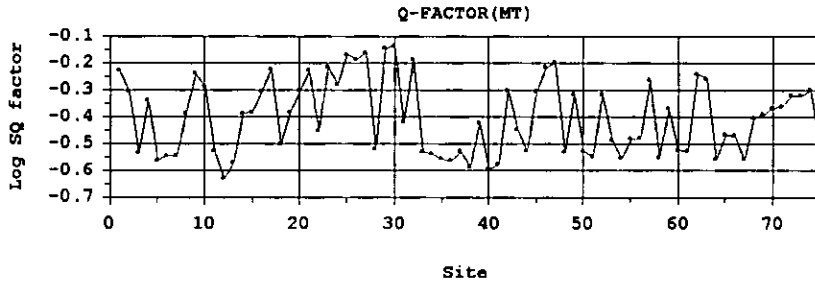


Figure 5.3-3 (d)

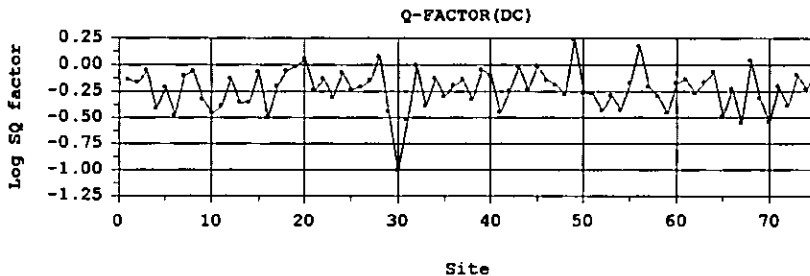


Figure 5.3-3 (e)

clear since the apparent resistivity relaxes over a wide depth range (e.g. figure 5.3-1c). Figures 5.3-3d and e show the data fit for every station (i.e. MT stations and VESs). While the fit is excellent for MT, DC resistivity shows some oscillations, e.g. stations 49 and 56 in figure 5.3-3e are not fitted properly. As mentioned before, such cases happen because the estimated number of degrees of freedom is less than the number actually required and thus, the iterations stop prematurely.

5.3.3.2. Illustration of the Inversion Scheme with Field Data

Field Data from the CB: Zimbabwe, Marondera.

In the following a few examples of the application of the inversion scheme in field resistivity sounding data will be presented. The data set was collected on a CB environment in Zimbabwe in the framework of a groundwater exploration programme and has been previously interpreted by Dahlin (1993). For the present work only a portion of the Marondera main profile, i.e. from 500 to 1000 m will be considered. The data consists of a set of 2D Wenner resistivity values at electrode spacings varying from 2 to 40 m. In order to make some comparative analysis of the performance of the present inversion scheme, 1D inversion of two VESs extracted at the positions 250 and 800 m, the same as those shown in Dahlin (1993), will be studied in detail. In addition, a quasi 2D interpretation of the profile section from 500 to 1000 m by concatenating the set of closely spaced VESs will be discussed. The VESs were extracted at every 5 m distance which makes 100 VESs along the profile. All extracted VESs have nine data points except the last 3 stations, i.e. at positions 985 and 990 with 7 and 995 with 5. It is to note that the use of the results of Dahlin (1993) is only meant for comparison by showing and analysing some of the aspects of the present inversion scheme. Therefore, this is not to be understood as an evaluation of either of the inversion procedures against the other.

The surface geology of the site is characterised by the occurrence of dambos which are seasonally waterlogged bottomlands. The stratigraphy of the dambos is invariably characterised by an upper clay lense overlying a sequence of weathering products. As was described in chapter two, the dambos and particularly the clay lenses play a very important hydrogeological role in areas with limited rainfall like the one studied here.

The results of 1D inversion of the VESs extracted at positions 250 and 800 m are shown in figures 5.3-4a, b, d and e. The datafit in both cases (equation 5.10) is quite good.

The high uncertainties in the data set seem to limit significantly the performance of the inversion scheme. However, the main trends of the layering are similar to those obtained by Dahlin (1993) i.e. a resistive upper layer underlain by a sequence of conductor and resistor (figure 5.3-4c). The inversion of the VES at position 250 m shows a gradual decrease of resistivity with depth underlying this sequence. Again, this is related with the inversion strategy used here as described in the previous section, i.e. below a certain depth the

resistivity of the inverted model relaxes towards the resistivity of the initial model (100 Ωm here).

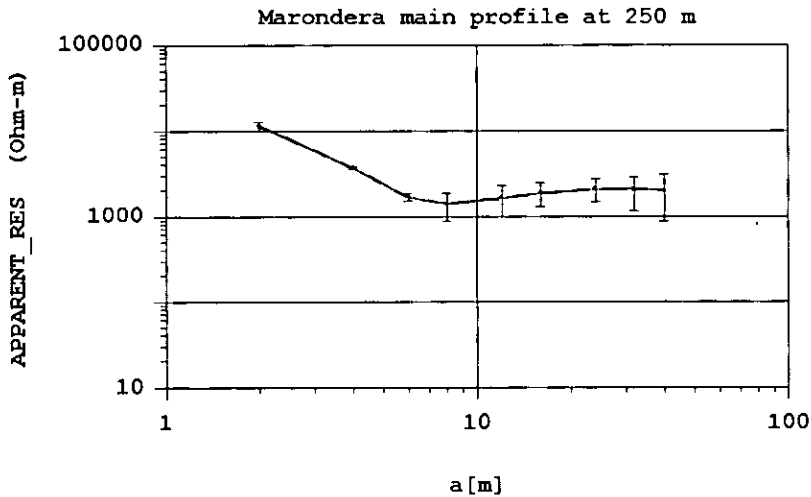


Figure 5.3-4 (a)

Figure 5.3-4. 1D inversion results; Marondera main profile at 250 m a) The fitting between the measured apparent resistivity (with error bars) and the model response (the solid line), b) The inverted resistivity-depth section and c) The inversion results at positions 250 and 800 m obtained by Dahlin (1993), d) and e) Inversion results for the VES at position 800 m.

Notice that the changes of resistivity with depth below the overburden are gradual. This might correspond to reality in many geological environments of the crystalline basement, which are mainly shaped by the effects of differential weathering, i.e. weathering that occurs at different rates due to differences in intensity of weathering between the upper and deeper parts of the subsurface. This tendency is shown in both VESs (i.e. 250 and 800 m). However, the high resistive cover is generally thin and in many cases can be clearly identified from the sounding curve. It results mainly from leaching processes, commonly where the topography is rough. The inversion results of the VES extracted at 800 m are shown in figures 3.5-4d and e. It is to notice that the tendency of gradual decrease or increase of resistivity does not show up here. This is probably due to

the fact that the overburden is less resistive, and thus the penetration depth is relatively higher compared to the VES at position 250 m.

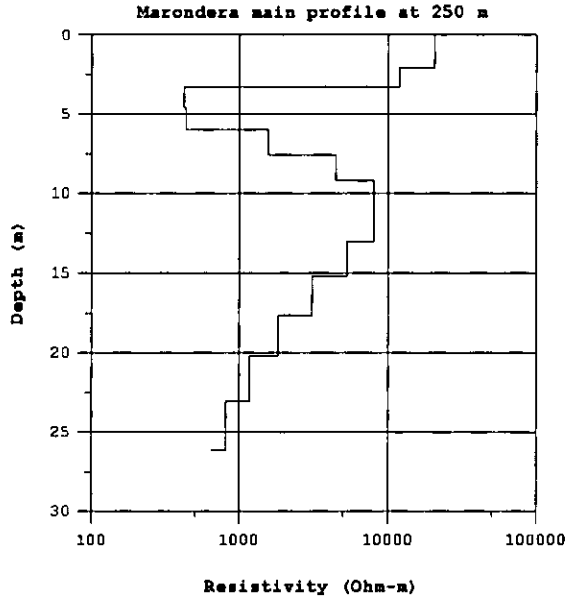


Figure 5.3-4 (b)

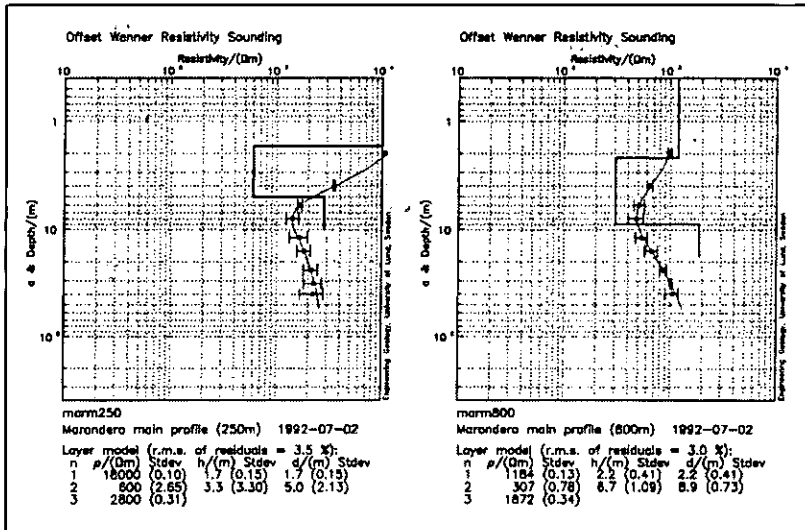


Figure 5.3-4 (c)

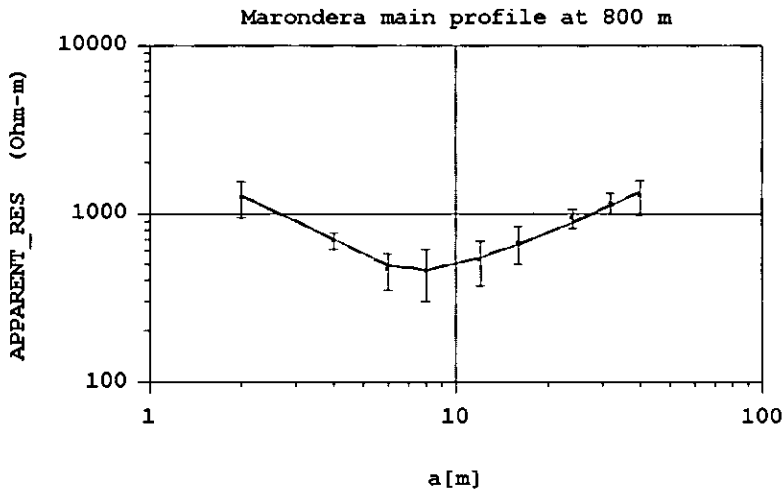


Figure 5.3-4 (d)

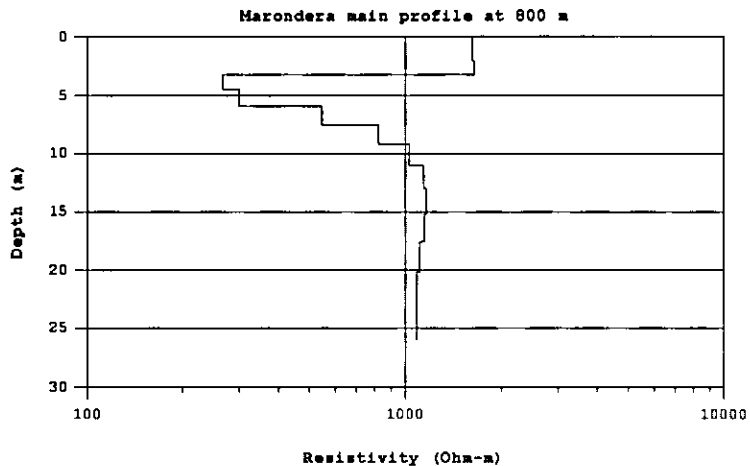


Figure 5.3-4 (e)

In the final example the inversion of closely spaced VESs along the profile from 500 to 1000 m is shown. The results of concatenated 1D inversions with different resistivities of the initial model, i.e. with 100 and 1000 Ωm are shown in figures 5.3-5a and b, respectively. In general, the cross sections show the same features as those interpreted by Dahlin (1993), figure 5.3-5c, i.e. a low conducting area between

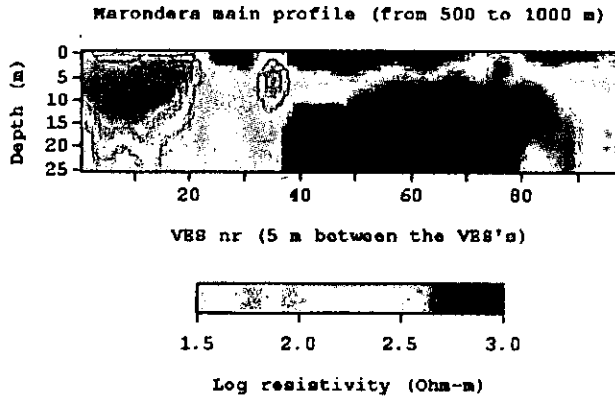


Figure 5.3-5 (a)

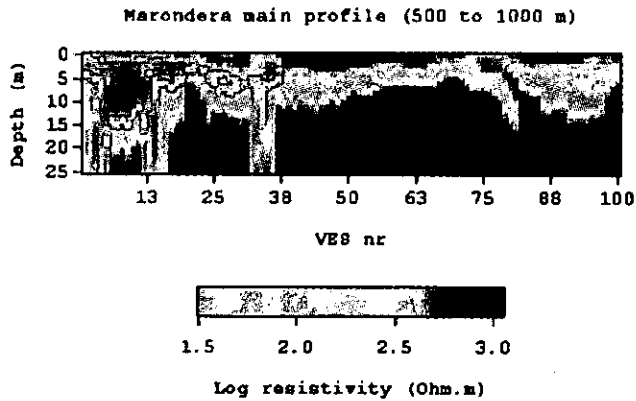


Figure 5.3-5 (b)

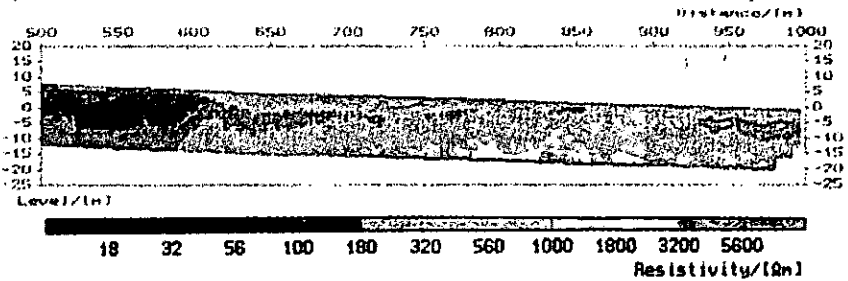


Figure 5.3-5 (c)

500 and 600 m (between VESs number 1 and 20 in figures 5.3-5a and b) and a resistive layer underlain by a sequence of conductor and resistor between 600 and 850 m (between VESs number 40 and 70 in figures 5.3-5a and b). However, the data fit is slightly better with an initial model with a resistivity of 1000 Ωm (figure 5.3-6c). However, there is always a risk of overfitting the data in which case unrealistic models may result. Another remark is that the inversion results show a low resistivity lens which is only appearing in the 2D inversion of Dahlin (1993).

The Initial Model

In order to make an assessment of the behaviour of the inversion scheme for a wide resistivity range, a test with a third resistivity (i.e. 10 Ωm) was also performed. The results are shown in figure 5.3-6. The data fit with an initial model with a resistivity of 1000 Ωm (figure 5.3-6c) is slightly better compared with that of an initial model with 100 Ωm , figure 5.3-6b. With a resistivity of 10 Ωm the data fit becomes worse.

Figure 5.3-5. 1D interpretation of closely spaced VESs Marondera main profile (500 to 1000 m) a) 1D interpretation cross section with an initial model with a resistivity of 100 Ωm (smoothed) and b) 1D interpretation cross section with an initial model with a resistivity of 1000 Ωm , c) 1D interpretation cross section after Dahlin (1993).

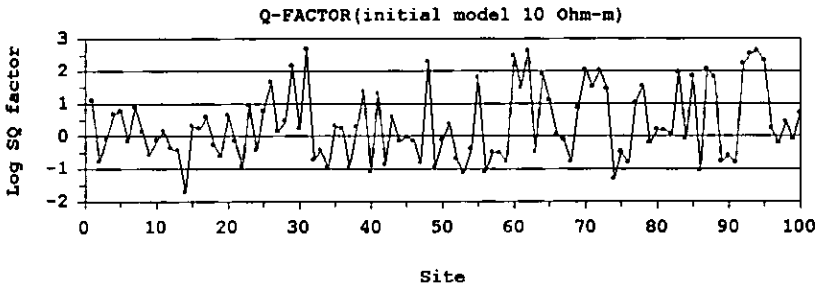


Figure 5.3-6 (a): Estimated RMS= 183.4%

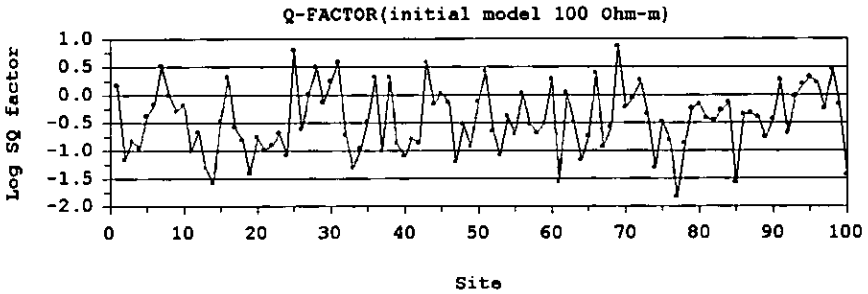


Figure 5.3-6 (b): Estimated RMS=27.65%

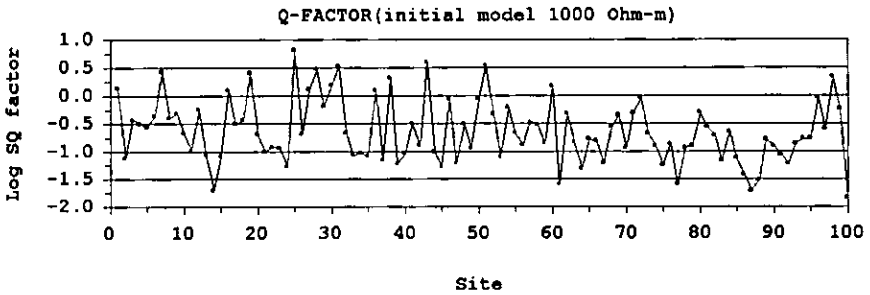


Figure 5.3-6 (c): Estimated RMS= 22.5%

Figure 5.3-6. The figure illustrates how the choice of the resistivity of the initial model can affect the inversion results. a), b) and c) Data fit for 1D interpretations of the VESs along the profile for different resistivities of the initial model and d) VES no. 69 (extracted at position 840 m). Singular value versus singular value index number for different resistivities of the initial model.

The result in figure 5.3-6 suggests that the resistivity should not be chosen too far from the average resistivities in area. The possible explanation for this is that with a low resistive homogeneous half space as initial model (e.g. 10 Ωm) and with average resistivities in area in the range of thousands Ωm , the inversion scheme is not able to excite significant non linearity. As mentioned before this results in a poor exploration of the parameter space which causes the iteration procedure to stop earlier in the present version of the scheme. In order to illustrate this effect, the VES extracted at position 840 m (i.e. VES no 69 here), which shows clearly this tendency was investigated closely in terms of the condition number of the involved matrices. The results are shown in figure 5.3-6d. Again, one can see that the slope of the curve of singular values versus their index number for different resistivities of the initial model is less steep with the higher resistivity. Therefore, the condition number of the eigenvectors matrices is much higher. This is probably the reason for the better data fit compared to the lower resistivity initial models.

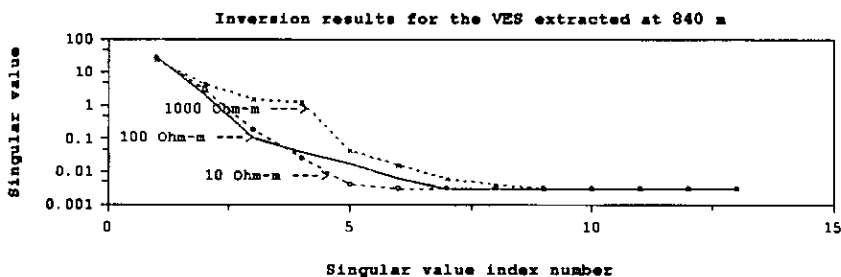


Figure 5.3-6(d)

5.3.4. Discussion and Conclusions

As stated above, the development of fast procedures for resistivity data interpretation is topical. The inversion scheme presented here proves to be very efficient for the evaluation of resistivity data soundings particularly in areas characterised by smooth changes of resistivity and thickness with depth such as in the crystalline basement. One of its merits is that the inversion is fully automatic in the sense that the inversion parameters such as the truncation level of the smallest singular values, the number of iterations, etc are set

intrinsically on the basis of the data. This is a great advantage over other inversion schemes such as the one described in the previous section or other schemes based on the principles of a smoothness constrained inversion (e.g. Occam inversion).

The tests with synthetic and field data show that the present inversion scheme is capable of resolving the essential features of the models. However, in order to be efficient, the bounds on the resistivity should not be chosen too close to the real ones because this would prevent the solution from reaching a global minimum. Another evidence drawn from the tests is that the resistivity of the initial model should be in the range of the expected values in the area in order to speed up the convergence. In contrast to the MT inversion results from which a qualitative indication of the depth of penetration can be obtained, from DC resistivity inversion results such tendency is not clearly shown since the resistivity relaxes over a very wide depth range and approaches the resistivity of the initial model with increasing electrode spacings (i.e. greater penetration depths of the current).

6. General Discussion and Conclusions

Over the last decades, hydrogeological investigations have evolved from simple resource detection into more sophisticated evaluations of increasingly complex problems involving aquifer delineation, quantification, monitoring and in some cases remediation. Over the same period, there has also been an increase in the number and diversification of the geophysical techniques applied in such surveys. However, the accelerated character and complexity level involved in many such investigations as well as the need for a real time decision making while carrying out the field surveys, are increasingly straining the capabilities of the existing exploration techniques to their limits. Therefore, current development efforts in geophysics are pushing towards fast and dense spatial sampling of high quality data, in-field processing and interpretation. In the present chapter parts of the present work are summarised.

6.1. General Discussion

6.1.1. Hydrogeology of Tropical Africa

Hardly anywhere on Earth is groundwater more difficult to detect and assess than in arid and semi-arid regions. In this context, the African continent is particularly distinctive compared to other regions because (1) it lies almost entirely between the tropics, (2) the surface geology is mainly characterised by hard rocks and (3) the continent's very dispersed rural population mostly living in small settlements. The fact that more than 50% of worldwide geophysical expenditure for groundwater is spent in Africa alone is a testimony to the degree of scarcity of this important resource.

Groundwater targets in Africa are highly heterogeneous and complex and thus, their exploration requires very sensitive techniques. Moreover, due to the fact that groundwater occurrence is also highly influenced by climatic factors which can lead to periodic depletion of the aquifers complicates the matters further. Therefore, the emphasis on hydrogeological studies in such environments is not only the resource detection but most importantly on its quantification. Resource quantification requires precise estimation of the hydraulic parameters such as permeability, porosity and thickness, etc.

Groundwater in Africa is mainly exploited from the crystalline basement aquifers i.e. within the weathered and/or fractured bedrock.

Viable aquifers wholly within either the weathered or fractured rock are of rare occurrence because of the low permeability and low storage capacity of the former and latter layers, respectively. Therefore, in order to be effective, development of the crystalline basement aquifers requires interaction with storage available in the overlying or adjacent saturated weathered layer (saprolite), or other suitable formations such as alluvium. Crystalline basement aquifers are essentially phreatic in character but may respond to localised abstraction in a semi-confined manner if the water table occurs in a low permeability horizon such as clayey regolith.

In general, crystalline basement aquifers are of local character due to the high spatial variability of the components of the weathered and fractured bedrock. This is one of the reasons of high failure rates of groundwater prospecting activities in Africa.

In the sedimentary and desert areas groundwater is mainly exploited from deep sandstone layers and/or fractured dolomite and limestone. Sandstone aquifers are generally confined and the groundwater occurring in them is of fossil character, i.e. they accumulated during ancient times when the climatic conditions were less severe. Although of sedimentary origin, the limestone and dolomite aquifers can in principle be considered as crystalline basement aquifers because they have very low porosity when solid. However, fracturing, solution and removal of rock components may increase their porosity and permeability.

6.1.2. Hydrogeophysics of Tropical Africa

The geophysical techniques which are extensively applied in groundwater exploration in Africa are the direct current (DC) technique in the sounding mode (mainly Schlumberger configuration) for the estimation of the thickness of the aquifers and the electromagnetic technique (e.g. HLEM, Slingram, conductivity meters) in the profiling mode mainly for fracture detection. Although this combination has proven to be very efficient in locating suitable borehole sites as is reported and recommended by many workers, its capability in providing some clues concerning equivalence and suppression effects is questionable. On the other hand, the EM profiling systems (conductivity meters) used in the practice of groundwater exploration operate mainly under the regime of low induction numbers (LIN) (e.g. McNeill, 1980) and measure directly some average conductivity of the subsurface. However, their applicability is generally limited to areas of low to moderate conductivities. In areas with high conductivities the LIN approximation

breaks down and the conductivity reading of the instrument is no longer proportional to the subsurface conductivity. CB environments are characterised by the occurrence of high conductivity clay lenses and thus, EM profiling data obtained with such instruments should be taken with caution. Another disadvantage of the EM systems is their sensitivity to errors in loop spacing and misorientation of the coils which are difficult to control when doing field surveys in rough terrains in Africa.

Therefore, for the layering typical in a weathering sequence with a conductive intermediate saprolite and moderately conductive saprock as targets, a more precise estimation of the parameters of these layers is crucial in order to determine the suitability of the site for a borehole. Therefore, the use of techniques which would enable a more precise quantification of the effects of equivalence and suppression is needed. The suggestions made by many workers of combining DC resistivity with either EM or IP techniques look promising in that the characteristics of the conductive intermediate layer (saprolite) can be better defined (e.g. Sandberg, 1993; Parasnis, 1997; Draskovits, 1990). The combination of DC resistivity and EM sounding techniques can yield better estimates of the resistivities and thicknesses of individual subsurface layers, since together the galvanic and inductive responses are used to reduce the problem of equivalence (e.g. Christensen, 1987; Sharma and Kaikkonen, 1999). The application of the TEM technique for shallow studies is becoming popular due to the development of Very Early TEM (VETEM) systems and due to several operational advantages compared to other geoelectrical sounding techniques. Recent advances in RMT particularly the development of a controlled source which is capable of generating frequencies from 1 kHz upwards is making the technique more interesting for shallow studies and for areas with poor coverage in transmitters in this frequency range (e.g. large parts of southern Africa).

One other aspect which characterises the surface geology of the CB environments is the occurrence of shallow lateral inhomogeneities, which can affect the resolution of conventional DC resistivity data. Although there are currently many procedures of reducing the effects caused by such features (e.g. Barker, 1981), the analysis of the results of many groundwater studies in Africa suggests that DC resistivity surveys are still mainly carried out with simple (one sounding at a time) field procedures and this may contribute to the poor quality of the data and thus to the low success rates. It is expected that the increased use of the recently developed computer controlled automated measuring systems (e.g. Dahlin, 1993) will ease out some of the difficulties with standard resistivity techniques because they allow for

combining vertical soundings and horizontal profiling into one 2D model.

In the case of the aquifers in sedimentary basins, the emphasis is on the exploration of sandstone aquifers and in some cases of the relatively shallower carbonate aquifers (dolomite and limestone). Dolomite and limestone aquifers can be explored by the usual techniques for fractured and weathered bedrock aquifers described before. However, the depths in which sandstone aquifers occur (up to or more than 1000 m) as well as the high resistivity of the cover, often preclude the use of the DC resistivity and EM profiling systems using small sources. Recent successful applications of MT and AMT techniques in groundwater studies in such environments suggest that these will continue to be the main tools of exploration. This is particularly true for some sedimentary areas with homogeneous sedimentary cover like the Kalahari beds (e.g. Bourgeois et al., 1994). Where near surface effects are predominant, these techniques can be replaced or complemented by the TEM technique (e.g. Schaumann, 1997).

6.1.3. Resistivity Data Interpretation

Resistivity surveys are designed to discriminate between anomalies reflecting subsurface electrical resistivity contrasts associated with lithologic and/or hydrogeologic boundaries. As was pointed out in chapter three, the vertical electrical sounding (VES) is the geophysical technique mainly applied in groundwater exploration in Africa as is reported by Senti (1988); van Dongen and Woodhouse (1994) and many others. The interpretation of VES data is usually made under an assumption of an Earth model whose resistivities and thicknesses vary with depth only, without lateral variations. Good to excellent approximations to this situation may be found in sedimentary areas, where the subsurface usually consists of gently dipping or flat-laying beds (Parasnis, 1997) or in the mainly planar upper parts of a weathering sequence. In many such areas, the vertical electrical sounding (VES) technique has been the most important tool for hydrogeological studies.

However, in several parts of the CB in Africa, significant spatial variations have been reported in the lithology of weathering profiles (Clark, 1985; Acworth, 1985; Tardy, 1993; Ritz et al., 1999a and 1999b). Therefore, under such circumstances, 1D interpretation of resistivity sounding data may not be appropriate. In areas of complex geology such as the CB overlain by thick weathered layers, a 2D resistivity imaging can be used for a more accurate characterisation of the

subsurface structures (e.g. Keller, 1993; Dahlin, 1993; Griffiths and Barker, 1993; Ritz et al, 1999a). Data sets resulting from such surveys are of 2D character and thus, 2D and recently even 3D inversion schemes are used instead (e.g. Loke and Barker 1995 and 1996; Brunner et al., 1999 and many others).

However, even though such 2D inversion schemes are able to indicate the structures of the subsurface, they do not provide a high resolution of the subsurface parameters (e.g. Ritz et al., 1999) because of lack of dense data sampling and rough model discretisation. Therefore, even in areas where the geology is complex, 1D inversion can still provide useful information to support and/or complement 2D models (e.g. Dahlin, 1993; Olayinka and Weller, 1997; Dahlin and Loke, 1998; Ritz et al., 1999a and 1999b; Sharma and Kaikkonen, 1999).

The accelerated character of the field requires automatic and robust techniques for 1D interpretation of resistivity data. The information obtained from such interpretations can be very useful for fast assessment of the subsurface geology of an area prior to the application of more sophisticated techniques. The conventional least squares solution (i.e. based solely on fitting the data as well as possible) of a non linear inverse problem often yields unrealistic models. Therefore, the procedure must be regularised in some way. The regularisation procedures applied in the two inversion schemes presented here prove to be robust in that simple models fitting the data are obtained. The models resulting from the data splitting strategy show a distinct layering which is particularly useful in sedimentary areas where the layering is well defined. However, in areas of the crystalline basement the interfaces separating different layers are more diffuse and thus, smooth models should be more realistic. Therefore, the second inversion scheme seems to be appropriate for such environments. However, if the resistivity of the initial model is chosen too low convergence problems may arise. This is probably due to the fact that with a too low resistivity the inversion scheme is not able to excite significant non linearity, which results in a poor exploration of the model parameter space. This causes the iterations to stop earlier. Numerical studies have shown that the resistivity should be not too far from the average of resistivities to be expected in the survey area. However, more studies are still needed in order to establish more efficient procedures of circumventing this drawback.

Comparative analysis of DC resistivity with RMT (i.e. in the frequency range of 14 to 250 kHz) shows that the resolution of the latter technique is higher and that qualitative indication of the depth of penetration of the data set used can be obtained from the interpreted cross sections. From DC resistivity inversion results such an indication is not apparent because there is a very wide depth

range over which the resistivity gradually changes to values close to that of the initial model used (e.g. 100 Ωm in figure 5.3-1c).

6.2. Conclusions

6.2.1. Geophysical Data Collection

- The main problems affecting the applicability of geoelectrical techniques in groundwater prospecting in the CB of tropical Africa are the presence of clay layers in the aquifer material, which can mask not only the geoelectrical anomalies, but also make an interpretation in terms of hydrogeological potential of the site highly ambiguous, and the spatial variability of the groundwater targets. Therefore, the efficiency of geophysical surveys in many such studies can be improved significantly by a strategic integration of several techniques especially those techniques responding to a different characteristic of the same target unit, e.g. the resistivity and the polarisability for DC resistivity and IP techniques respectively.
- Combination of EM and DC resistivity sounding both genetically related (but based on different physical principles) can be very efficient in reducing the effects of equivalence and suppression for some geological situations because their behaviour is different for different types of equivalence. This information would enable a more precise hydrogeological characterisation of the site. However, more often than not, the number of geophysical techniques applied in a particular groundwater survey will continue to be constrained by economic and logistic factors.
- Where high yields are required and the weathered layer is thick a range of methods such as DC and EM combined with magnetics is probably justified to provide the complementary data which will increase confidence in geophysical overall interpretation.
- Where low yields can be accepted and the weathered layer is thin (i.e. less than 10 m) the emphasis should be mainly to detect sites where the fractured bedrock is thick by using EM profiling techniques.
- There is evidence to suggest that automated 2D resistivity measuring systems because are fast and enable a better control of

the error sources affecting conventional resistivity sounding techniques, are increasingly becoming valid alternatives to in groundwater prospecting in the African CB.

6.2.2. Resistivity Data Interpretation

- 2D interpretation of DC resistivity data yields considerable detail about the subsurface and gives better pictures of the lateral extent of the features. However, for quantitative determination of the parameters of the subsurface it should be combined with 1D interpretation in selected points of the survey area or as a set of closely spaced VES in order to see if the measured data are fitted properly.
- The inversion schemes presented here, because they are automatic and require only few input parameters to start the iteration scheme, are suited for fast and/or in-field evaluation of resistivity data even in areas where the geological knowledge is poor.
- The first inversion scheme based on data splitting is robust and yields simple models with distinct layers. However, the tests have shown that if large data errors occur in the initial data part they may affect the whole inversion procedure.
- The second inversion scheme is more robust since the whole data set is inverted in one step and thus errors are averaged out. The resulting models are smooth (i.e. with gradual changes) which is close to reality in areas affected by differential weathering such as the crystalline basement.
- The resistivity of the initial model (homogeneous halfspace) should not be chosen too low compared with the average resistivities to be expected in the area. In such cases the inversion scheme will not be able to excite significant non linearity which results in a poor exploration of the model space and hence a poor description of pseudo-null-space meaning that the iterations stop earlier.
- The comparison of both inversion schemes with the MT inversion based on the same principles (Pedersen, 1999) shows that resolution is higher for the latter and the layers of low resistivity are better resolved. Furthermore, qualitative information concerning

the depth of penetration of the data set used can be extracted from the MT inversion. However, from DC resistivity inversion such indication is not very clear.

- The condition number of the matrices involved in the inverse is much higher for MT, which explains its better resolution compared to DC resistivity, at least for the same models tested here.

6.3. The Way Ahead

- The developments in the techniques, which operate in the intermediate frequency range (e.g. between 300 kHz and 50 MHz) although still mainly on a research level, are promising in that more than one parameter (e.g. electrical resistivity and dielectric constant) can be obtained and thus a more detailed description of the subsurface can be done. From conventional DC and EM techniques the apparent resistivity is the only parameter obtainable from the measurements.
- Better correlation between geophysical and hydraulic parameters are needed. The knowledge of the relationships between electric properties (e.g. apparent resistivity and dielectric properties) and the hydraulic parameters of the aquifers (e.g. porosity and permeability) is of great importance for a fast assessment of the suitability of a site for a borehole. Therefore, more focussed studies are still needed in order to establish more precisely the limitations and capabilities of the techniques in this regard.
- Comparative analysis of the inversion results of DC resistivity with MT in the frequency range 14 to 250 kHz (i.e. RMT) as well as the recent successful test measurements of the new EnviroMT system in the Netherlands (Pedersen et al., 1999) motivates field trials of the technique in selected areas of the crystalline basement in Africa.
- Recent developments in application of NMR technique to direct detection of water are encouraging. However, the few examples reported in the literature, suggest that there is still a lot of work to be done in order to make these systems feasible for routine groundwater surveys. Hardware limitations such as low noise

protection and the costs of the currently available systems are still hampering the application of this technique.

References

- Acworth, R.I., 1987, The development of crystalline basement aquifers in a tropical environment. *Quarterly Journal of Engineering Geology*, Vol. 20, 265-272.
- Balek, J., 1983, *Hydrology and water resources in tropical Africa*. Elsevier, 271 pp.
- Barker, R.D., 1981, The offset system of electrical resistivity sounding and its use with a multicore cable. *Geophysical Prospecting*, Vol. 29, 128-143.
- Barker, R.D., 1989, Depth of investigation of collinear symmetrical four-electrode arrays. *Geophysics*, Vol. 54, No. 8, 1031-1037.
- Barker, R.D., Houston, J.F.T., and White, C.C., 1992, Borehole siting in an accelerated drought relief project. In: Wright, E.P. and Burgess, W.G. (Editors), *The Hydrogeology of Crystalline Basement Aquifers in Africa*. Geological Society Special Publication, No. 66, 183-201.
- Bates, R.L. and Jackson, J.A., 1987, *Glossary of geology* (3rd Edition).
- Bibby, H.M., and Hohmann, G.W., 1993, Three dimensional interpretation of multi-source bipole-dipole resistivity data using the apparent resistivity tensor. *Geophysical Prospecting*, Vol. 41, 697-723.
- Birken, R.A., Poulton, M.M. and Lee, K.H., 1999, Neural network interpretation of high frequency electromagnetic ellipticity data Part I: Understanding the half-space and layered Earth response. *JEEG*, Vol. 4, No. 2, 93-103.
- Botha, W.J., Wiegmans, F.E., Van der Walt, J.J., and Fourie, C.J.S., 1992, Evaluation of electromagnetic exploration techniques in groundwater exploration in South Africa. Report to the water research commission, Geology Department, University of Pretoria.
- Bourgeois, B., Mathieu, F., Vachette, C., and Vaubourg, P., 1994, AMT measurements compared with gravimetry and magnetometry for structural study of a sedimentary basin: Letlhakeng- Botlhapatlou groundwater project, Botswana. *Journal of Applied Geophysics*, Vol. 31, 7-25.

Bowen, R., 1986, Groundwater. Elsevier Applied Science Publishers LTD (2nd Edition), 427 pp.

Braga, A.C., Malagutti F., W., Dourado, J.C. and Chang, K., 1999, Correlation of electrical and induced polarisation data with geotechnical survey standard penetration test measurements. JEEG, Vol. 4, No. 2, 123-130.

Brunner, I., Friedel, S., Jacobs, F., Danckwardt, E., 1999, Investigation of a tertiary maar structure using three-dimensional resistivity imaging. Geophys. J. Int., Vol. 136, 771-780.

Carroll, D., 1970, Rock weathering. Plenum Press, 203 pp.

Carruthers, R.M., Greenbaum, D., Peart, R.J. and Herbert, R., 1991, Geophysical investigations of photolineaments in south-east Zimbabwe. Quarterly Journal of Engineering Geology, Vol. 24, 437-451.

Carruthers, R.M. and Smith, I.F., 1992, The use of ground electrical survey methods for siting water-supply boreholes in shallow crystalline basement terrains. In: Wright, E.P. and Burgess, W.G. (Editors), 1992, Hydrogeology of Crystalline Basement aquifers in Africa. Geological Society Special Publication, No 66, 203-220.

Chapellier, D., Fitterman, D., Parasnis, D.S., and Valla, P. (Editors), 1991, Application of Geophysics to water prospecting in arid and semi-arid areas. Geoexploration, Vol. 27, Special Issue.

Chapellier, D., Fitterman, D., de Stadelhofen, M., Parasnis, D.S., Steeples, D.W. and Valla, P. (Editors), 1994, Geophysics and Environment. Journal of Applied Geophysics, Vol. 31, Special Issue.

Christensen, N.B., 1979, Fast Hankel transforms. GeoSkifter, Vol. 12, 68 pp.

Christensen, N.B., 1986, Geoelectrical sounding method. A historical review of interpretation techniques and the interpreter's evaluation of the method. Twenty five years of geology in Aarhus. Geoskifter, No. 24, 91-102.

Christensen, N.B., 1987, The AC/ Geoelectrical sounding method: a combined electrical/electromagnetic prospecting tool. Boreas, No. 16, 387-392.

Christensen, N.B. and Sorensen, K.I., 1994, Integrated use of electromagnetic methods for hydrogeological investigations. In: Proceedings of the Symposium on the Application of Geophysics to Engineering and Environmental Problems (SAGEEP), Boston, March, 163-176, Environmental and Engineering Geophysical Society, P.O.Box 4475, Englewood, CO 80155, USA.

Christensen, N.B., 1997, Electromagnetic subsurface imaging. A case for an adaptive Born approximation. *Surveys in Geophysics*, Vol. 18, No. 5, 447-510.

Christensen, N.B. and Jacobsen, B.H., 1997, Simultaneous Electromagnetic Layered Modelling and Analysis (SELMA). Manual for the electromagnetic inversion program, University of Aarhus.

Clark, L., 1985, Groundwater abstraction from basement complex areas of Africa. *Quarterly Journal of Engineering Geology*, Vol. 18, 25-34.

Constable, S.C., Parker, R.L. and Constable, C.G., 1987, Occam's inversion: A practical algorithm for generating smooth models from electromagnetic sounding data. *Geophysics*, Vol. 52, No. 3, 289-300.

Dahlin, T., 1993, On the automation of 2D resistivity surveying for engineering and environmental applications. Ph.D. Thesis, ISRN: LUTVDG/VTG-1007-SE, Department of Engineering Geology, Lund Institute of Technology, Lund University, 179 pp.

Dahlin, T. and Owen, R., 1998, Geophysical investigations of alluvial aquifers in Zimbabwe. In: Proceedings of the 4th EEGS Meeting, Barcelona, 14-17, September 1998.

Dahlin, T. and Loke, M.H., 1998, Resolution of 2D Wenner resistivity imaging as assessed by numerical modelling. *Journal of Applied Geophysics*, Vol. 38, 237-249.

Darboux-Afouba, R. and Louis, P., 1989, Contribution des mesures de anisotropie electrique a la recherche des aquifers de fracture en milieu cristallin au Benin. *Geophysical Prospecting*, Vol. 37, 91-106.

Davis, J.L. and Annan, A.P., 1989, Ground Penetrating Radar for high resolution mapping of soil and rock stratigraphy. *Geophysical Prospecting*, Vol. 37, 531-551.

Dempster, A., Schatzoff, M. and Wermuth, N., 1977, A simulation study of alternatives to ordinary least squares. *J. Am. Stat. Assoc.*, Vol. 72, 77-106.

Dobecki, T.L. and Romig, P.R., 1985, Geotechnical and groundwater geophysics. *Geophysics*, Vol. 50, No. 12, 2621-2636.

Draskovits, P. and Fejes, I., 1990, Near-surface groundwater research and protection from surface pollution. In: Ward, S.H. (Editor), *Geotechnical and environmental geophysics. Vol. II, Environment and groundwater*, Society of Exploration Geophysicists, 333-337.

Effereso, F. and Sorensen, K.I., 1996, A new approach to in situ determination of the hydraulic conductivity. In: *Proceedings of the symposium on the application of geophysics to engineering and environmental problems (SAGEEP)*, Keystone, Colorado, 1107-1113.

Faillace, C., 1973, Location of groundwater and the determination of the optimum depth of wells in metamorphic rocks of Karamoja, Uganda. 2nd Conv. Int. Sulle Acque Sotteranee, Palermo.

Farquharson, F.A.K., and Bullock, A., 1992, The Hydrogeology of Basement Complex Regions of Africa with Particular Reference to Southern Africa. In: Wright, E.P. and Burgess, W.G. (Editors), *The Hydrogeology of Crystalline Basement Aquifers in Africa*. Geological Society Special Publication, No. 66, 59-76.

Fetter, C.W., 1988, *Applied hydrogeology*. Macmillan Publishing Company, 1988.

Fitterman, D.V. and Stewart, M.T., 1986, Transient electromagnetic sounding for groundwater. *Geophysics*, Vol. 51, 995-1006.

Freeze, R. A., and Cherry, J. A.. 1979, *Groundwater*. Prentice-Hall. Englewood Cliffs N.J., 604 pp.

Frischknecht, F.C., Labson, V.F., Spies, B.R., and Anderson, W.L., 1991, Profiling methods using small sources. In: Nabighian, M. (Editor), *Electromagnetic methods in applied geophysics. Vol. 2, Application, Part A*, Society of Exploration Geophysicists, 105-270.

Gieske, A., 1993, Statistical analysis of long-term groundwater level fluctuations in dolomite aquifers of eastern Botswana. In: *Africa Needs*

Groundwater. Proceedings of the International Groundwater Convention, Johannesburg, South Africa 6-8 Sept. 1993.

Giroux, B., Chouteau, M., Descloitres, M., and Ritz, M., 1997, Use of the magnetotelluric method in the study of the deep Maestrichtian aquifer in Senegal. *Journal of Applied Geophysics*, Vol. 38, 77-96.

Goldman, M., Rabinovich, B., Rabinovich, M. Gilad, D., Gev, I., Schirov, M., 1994, Application of integrated NMR- TDEM method in groundwater exploration in Israel. *Journal of Applied Geophysics*, Vol. 31, 27-52.

Greef, G.J., 1993, Geohydrological results of geomagnetic prospecting over sand-covered Malmesbury shale bedrock. In: Proceedings of the International Groundwater Convention, Africa Needs Groundwater, Johannesburg, South Africa 6-8 Sept. 1993.

Greenbaum, D., 1992, Structural influences on the occurrence of groundwater in SE Zimbabwe. In: Wright, E.P. and Burgess, W.G. (Editors), 1992, *Hydrogeology of Crystalline Basement aquifers in Africa*. Geological Society Special Publication, No 66, 77-85.

Griffiths, D.H. and Barker, R.D., 1993, Two-dimensional resistivity imaging and modelling in areas of complex geology. *Journal of Applied Geophysics*, Vol. 29, 211-226.

Groom, R.W. and Bailey, R., 1989, Decomposition of magnetotelluric impedance tensors in the presence of local three-dimensional galvanic distortion. *Journal of Geophysical Research*, Vol. 94, No. B2, 1913-1925.

Gwavava, O., Swain, C.J. and Podmore, F., 1996, Mechanisms of isostatic compensation of the Zimbabwe and Kaapvaal cratons, the Limpopo Belt and the Mozambique basin. *Geophys. J. Int.*, Vol. 127, 635-650.

Hansen, P.C., 1990, Truncated singular value decomposition solutions to discrete ill-posed problems with ill-determined numerical rank. *SIAM J. Sci. Comput.*, Vol. 11, 503-518.

Hansen, P.C., 1992, Analysis of discrete ill-posed problems by means of the L-curve. *SIAM Review*, Vol. 34, 561-580.

Hazell, J.R.T., Cratchley, C.R. and Preston, A.M., 1988, The location of aquifers in crystalline rocks and alluvium in Northern Nigeria using

combined electromagnetic and resistivity techniques. *Quarterly Journal of Engineering Geology*, Vol. 21, No. 2.

Heimovaara, T.J., 1994, Frequency-Domain analysis of time domain reflectometry waveforms, 1. Measurement of the complex dielectric permittivity of soils. *Water Resources Research*, Vol. 30, 189-199.

Heimovaara, T.J., Bouten, W., and Verstraten, J.M., 1994, Frequency domain analysis of time domain waveforms, 2. A four component complex dielectric mixing model for soils. *Water Resources Research*, Vol. 30, 201-209.

Herbert, R., Barker, J.A. and Kitching, R., 1992, New approaches to pumping test interpretation for dug wells constructed on hard rock aquifers. In: Wright, E.P. and Burgess, W.G. (Editors), 1992, *Hydrogeology of Crystalline Basement aquifers in Africa*. Geological Society Special Publication, No. 66, 221-242.

Hinze, W.J., 1990, The role of gravity and magnetic methods in engineering and environmental studies. In: Ward, S.H. (Editor), *Geotechnical and environmental geophysics*. Vol. 1, Review and Tutorial, Society of Exploration Geophysics, 75-126.

Houston, J.F.T., and Morrey, M.J., 1982, The hydrogeological basis for a water supply to Kabwe, Zambia. *Journal of The Institution of Water Engineers and Scientists*, Vol. 36, 27-42.

Houston, J.F.T., 1988, Rainfall-Runoff- Recharge relationships in the basement rocks of Zimbabwe. I. Simmers (Editor), *Estimation of natural groundwater recharge*, 349-365.

Houston, J.F.T., and Lewis, R.T., 1988, The Victoria province drought relief project, II. Borehole yield Relationships. *Groundwater*, Vol. 26, No. 4, 309-316.

Johansen, H.K., 1977, A man/ computer interpretation system for resistivity soundings over horizontally stratified Earth. *Geophysical Prospecting*, Vol. 25, 667-691.

Jones, M.J., 1985, The weathered zone aquifers of the basement complex areas of Africa. *Quarterly Journal of Engineering Geology*, Vol. 18, 35-46.

Keller, G.V., Frischknecht, F.C., 1966, *Electrical Methods in Geophysical Prospecting*. Pergamon Press, 1966.

Keller, G.V., 1987, Rock and mineral properties. In: Nabighian, M.N. (Editor), *Electromagnetic methods in applied geophysics*. Vol. 1, Theory, Society of Exploration Geophysics, 13-51.

Keller, G.V., 1993, Electrical and electromagnetic methods in areas of complex geology. *Journal of Applied Geophysics*, Vol. 29, 181-192.

Key, R.M., 1992, An introduction to the crystalline basement of Africa. In: Wright, E.P. and Burgess, W.G. (Editors), *The Hydrogeology of Crystalline Basement Aquifers in Africa*. Geological Society Special Publication, No. 66, 29-57.

King, L.C., 1962, *The Morphology of the Earth*. Oliver and Boyd, Edinburgh, UK.

Lankston, R.W., 1990, High-resolution refraction seismic data acquisition and interpretation. In: Ward, S.H. (Editor), *Geotechnical and environmental geophysics*. Vol. 1, Review and Tutorial, Society of Exploration Geophysics, 45-73.

Li, Y. and Oldenburg, W., 1994, Inversion of 3D DC resistivity data using an approximate inverse mapping. *Geophys. J. Int.*, Vol. 116, 527-537.

Loke, M.H. and Barker, R.D., 1995, Least-squares deconvolution of apparent resistivity pseudosections. *Geophysics*, Vol. 60, No. 6, 1682-1690.

Loke, M.H. and Barker, R.D., 1996, Rapid least-squares inversion of apparent resistivity pseudosections by quasi-Newton method. *Geophysical Prospecting*, Vol. 44, 131-152.

MacDonald, A.M., Burleigh, J. and Burgess, G., 1999, Estimating transmissivity from surface resistivity soundings. An example from the Thames Gravels. *Quarterly Journal of Engineering Geology*, Vol. 32, 199-205.

Matias, M.J.S. and Habberjam, G.M., 1986, The effect of structure and anisotropy on resistivity measurements. *Geophysics*, Vol. 51, 964-971.

Mbonu, P.D.C., Ebeniro, J.O., Ofoegbu, C.O., Ekine, A.S., 1990, Geoelectric sounding for the determination of aquifer characteristics in parts of the Umahia area of Nigeria. *Geophysics*, Vol. 56, No. 2, 284-291.

McFarlane, M.J., 1992, Groundwater movement and water chemistry associated with weathering profiles of the African surface in parts of Malawi. In: Wright, E.P. and Burgess, W.G.(Editors), *The Hydrogeology of Crystalline Basement Aquifers in Africa*. Geological Society Special Publication, No. 66, 101-129.

McFarlane, M.J., Chilton, P.J., and Lewis, A., 1992, Geomorphological controls on borehole yields: A statistical study in an area of basement rocks in central Malawi. In: Wright, E.P. and Burgess, W.G.(Editors), *The Hydrogeology of Crystalline Basement Aquifers in Africa*. Geological Society Special Publication, No. 66, 131-154.

McNeill, J.D., 1980, Electromagnetic terrains conductivity measurement at low induction numbers. Technical note, TN-6, Geonics Limited.

McNeill, J.D., 1990, Use of electromagnetic methods for groundwater studies. In: Ward, S.H. (Editor), *Geotechnical and environmental geophysics. Investigations in Geophysics*. Vol. 1, Review and Tutorial, Society of Exploration Geophysics, 191-218.

McNeill, J.D., 1991, Advances in electromagnetic methods for groundwater studies. *Geoexploration*, Vol. 27, 65-80.

McNeill, J.D. and Labson, V.F., 1991, Geological mapping using VLF radio fields. In: Nabighian, M. (Editor), *Electromagnetic methods in applied geophysics*. Vol. 2, Application, Part B, Society of Exploration Geophysicists, 521-712.

McNeill, J.D., 1996, Why doesn't Geonics Limited build a multi-frequency EM31 or EM38?. Technical note, TN-30.

Meju, M.A, Fontes, S.L., Oliveira, M.F.B., Lima, J.P.R., Ulugergerli, E.U., and Carrraquilla, A.A., 1999, Regional aquifer mapping using combined VES-TEM-AMT/EMAP methods in the semiarid eastern margin of Parnaiba, Brazil. *Geophysics*, Vol. 64, No. 2, 337-356.

Mohnke, O. and Yaramanci, U., 1999, A new inversion scheme for surface NMR amplitudes using simulated annealing. In: *Proceedings*,

EAGE 61st Conference and Technical Exhibition-Helsinki, Finland, 7-11 June 1999.

Muiuane, E.A. and Pedersen, L.B., 1999a, Automatic 1D interpretation of DC resistivity sounding data. *Journal of Applied Geophysics*, Vol. 42, No. 1, 35-45.

Muiuane, E.A. and Pedersen, L.B., 1999b, Automatic 1D Inversion of DC Resistivity Data Using a Quality Based Truncated SVD. (to be submitted for publication in the *Journal of Applied Geophysics*).

Nabighian, M.N., 1987 (Editor), *Electromagnetic methods in applied geophysics*. Vol. 1, Theory, Society of Exploration Geophysicists, 513 pp.

Nabighian, M.N., 1991 (Editor), *Electromagnetic methods in applied geophysics*. Vol. 2, Application, Parts A and B, Society of Exploration Geophysicists, 972 pp.

Nobes, D.C., 1996, Environmental applications of electrical and electromagnetic methods. *Surveys in Geophysics*, Vol. 17, No. 4, 393-454.

Nobes, D.C., 1999, How important is the orientation of the horizontal loop EM system? Examples from a leachate plume and fault zone. *JEEG*, Vol. 4, No. 2, 81-85.

Olayinka, A.I. and Weller, A., 1997, The inversion of geoelectrical data for hydrogeological applications in crystalline basement areas of Nigeria. *Journal of Applied Geophysics*, Vol. 37, 103-115.

Palacky, G.J., Ritsema, I.L., and De Jong, S.J., 1981, Electromagnetic prospecting for groundwater in precambrian terrains in the Republic of Upper Volta. *Geophysical Prospecting*, Vol. 29, 932-955.

Palacky, G.J., and Kadokaru, K., 1979, Effect of tropical weathering on electrical and electromagnetic measurements. *Geophysics*, Vol. 44, 69-88.

Palacky, G.J., 1987, Resistivity characteristics of geological targets. In: Nabighian, M.N. (Editor), *Electromagnetic methods in applied geophysics*. Vol. 1., Theory, Society of Exploration Geophysics, 131-311.

Parasnis, D.S., 1997, Principles of applied Geophysics. Chapman and Hall, 430 pp.

Pedersen, L.B. and Rasmussen, T.M., 1989, Inversion of magnetotelluric data: a non-linear least-squares approach. Geophysical Prospecting, Vol. 37, 669-695.

Pedersen, L.B., 1999, Least singular values inversion of magnetotelluric data. (to be submitted for publication).

Pedersen, L.B., Dynesius, L., Bastani, M. and Matzander, U., 1999, EnviroMT-A new radio/controlled source system. In: Proceedings, EAGE 61st Conference and technical Exhibition-Helsinki, Finland, 7-11 June 1999.

Pellerin, L., Labson, V.F., Pfeifer, M.C., and others, 1994, VETEM- a very early time electromagnetic system. In: Proceedings of the Symposium on the Application of Geophysics to Engineering and Environmental Problems (SAGEEP), Boston, Massachusetts, 795-802, Environmental and Engineering Geophysical Society, P.O. Box 4475, Englewood, CO 80155, USA.

Pellerin, L., Labson, V.F., Pfeifer, M.C., and others, 1995, VETEM- a very early time electromagnetic system- the first year. In: Proceedings of the Symposium on the Application of Geophysics to Engineering and Environmental Problems (SAGEEP), Orlando, Florida, 725-731, Environmental and Engineering Geophysical Society, P.O. Box 4475, Englewood, CO 80155, USA.

Qui, X., Priestley, K., and McKenzie, D., 1996, Average lithospheric structure of southern Africa. Geophys. J. Int., Vol. 127, 563-587.

Raiche, A.P., Jupp, D.L.B., Rutter, H. and Vozoff, K., 1985, The joint use of coincident loop transient electromagnetic and Schlumberger sounding to resolve layered structures. Geophysics, Vol. 50, No. 10, 1618-1627.

Raunet, M., 1985, Les bas-fonds en Afrique et a Madagascar. Z. Geomorph. N.F. 52, 25-62.

Reynolds, J.M., 1997, An Introduction to Applied and Environmental Geophysics. John Wiley & Sons, 806 pp.

- Ritz, M., Parisot, J.C., Diouf, S., Beauvais, A., Dione, F. and Niang, M., 1999a, Electrical imaging of lateritic weathering mantles over granitic and metamorphic basement of eastern Senegal, West Africa. *Journal of Applied geophysics*, Vol. 41, 335-344.
- Ritz, M., Robain, H., Pervago, E., Albouy, Y., Camerlynck, C., Descloitres, M. and Mariko, A., 1999b, Improvement to resistivity pseudosection modelling by removal of near-surface inhomogeneity effects: application to a soil system in south Cameroon. *Geophysical Prospecting*, Vol. 47, 85-101.
- Robain, H., Descloitres, M., Ritz, M. and Atangana, Q.Y., 1996, A multi-scale electrical survey of lateric soil system in the rain forest of Cameroon. *Journal of Applied Geophysics*, Vol. 34, No. 4, 237-253.
- Romig, P.R., 1986, Engineering and groundwater geophysics. *Geophysics*, Vol. 51, Special Issue.
- Ruffet, C., Darot, M. and Gueguen, Y., 1995, Surface conductivity in rocks. A review. *Surveys in Geophysics*, Vol. 16, No. 1, 83-105.
- Saarenko, T., 1998, Electrical properties of water in clay and silty soils. *Journal of Applied Geophysics*, Vol. 40, 73-88.
- Sandberg, S., 1993, Examples of resolution improvement in geoelectrical soundings applied to groundwater investigations. *Geophysical Prospecting*, Vol. 41, 207-227.
- Scales, J.A., 1996, Uncertainties in seismic inverse calculations. In: Jacobsen, B., Mosegaard, K. and Sibani, P. (Editors). *Inverse Methods*, 79-97. Springer Verlag, Berlin.
- Schön, J.H., 1996, Physical properties of rocks: Fundamentals and principles of petrophysics. Pergamon press, 583 pp.
- Schaumann, G., 1997, Anwendung der transienten Elektromagnetik zur Grundwassersuche in Namibia. *Z. Angew. Geol.*, Vol. 43, No. 2, 70-74.
- Senti, R.J., 1988, Special Report; Geophysical Activity in 1987. *Geophysics*. The Leading Edge of Exploration, SEG.
- Sharma, S.P. and Kaikkonen, P., 1999, Appraisal of equivalence and suppression problems in 1D EM and DC measurements using global

optimisation and joint inversion. *Geophysical Prospecting*, Vol. 47, 219-249.

Shaw, E., 1994, *Hydrology in practice* (3rd edition). Stanley Thornes Pub. Ltd, 569 pp.

Slichter, R.E., 1993, The interpretation of the resistivity prospecting method for horizontal structures. *Physics*, Vol. 4, 307-322.

Sorensen, K.I. and Sorensen, K.M., 1995, Pulled array continuous vertical electrical sounding (PACVES). In: *Proceedings of the SAGEEP'95*, Orlando, Florida, 893-897.

Steeple, D.W. and Miller, R.D., 1990, Seismic reflection methods applied to engineering, environmental, and groundwater problems. In: Ward, S.H. (Editor), *Geotechnical and environmental geophysics*. Vol. 1, Review and Tutorial, Society of Exploration Geophysics, 1-30.

Sternberg, B.K., Washburne, J.C., Pellerin, L., 1988, Correction for the static shift in magnetotellurics using transient electromagnetic soundings. *Geophysics*, Vol. 53, 1459-1468.

Sternberg, B.K. and Poulton, M.M., 1994, High resolution subsurface imaging and neural network recognition. In: *Proceedings of the symposium of the application of geophysics to engineering and environmental problems (SAGEEP 1994)*, San Diego, CA, 847-855.

Sternberg, B.K. and Poulton, M.M., 1997, High resolution subsurface imaging and neural network recognition: Non-intrusive buried substance location Final Report, DOE Contract #DE-AC21-92MC29101 A001.

Stewart, D.C., Anderson, W.L., Grover, T.P. and Labson, V.F., 1994, Shallow subsurface mapping by electromagnetic sounding in the 300 kHz to 30 MHz range: Model studies and prototype system assessment. *Geophysics*, Vol. 59, 1462-1471.

Stoner, R.F. and Bakiewicz, W., 1987, Groundwater abstraction-construction, operation and maintenance: an international overview.

Tabbakh, A., Hesse, A., and Grard, R., 1993, Determination of electrical properties of the ground at shallow depth with an electrostatic quadrupole: Field trials on archaeological sites. *Geophysical Prospecting*, Vol. 41, 579-597.

- Tankard, A.J., Jacson, M.P.A., Eriksson, K.A., Hobday, D.K., Hunter, D.R. and Minter, W.E.L., 1982, *Crustal evolution of southern Africa*. Springer, New York.
- Tardy, Y., 1993, *Pedologie des laterites et des sols tropicaux*. Masson, Paris.
- Telford, W.M., Geldart, L.P., and Sherif, R.E., 1990, *Applied Geophysics*. Cambridge University Press, 1990.
- Van Der Leeden, F. , Troise, F.L. and Todd, D.K. , 1990, *The water encyclopaedia (2nd edition)*. Lewis Publishers, Inc.
- Van Dongen, P. and Woodhouse, M., 1994, *Finding groundwater. A project manager's guide to techniques and how to use them*. UNDP-World Bank Water and sanitation programme. Technical Report.
- Vanhala, H, Soinen, H., and Kukkonen, I., 1992, Detecting organic chemical contaminants by spectral-induced polarisation method in glacial till environment. *Geophysics*, Vol. 49, 1014-1017.
- Van Overmeeren, R.A., 1981, A combination of electrical resistivity, seismic refraction, and gravity measurements for groundwater exploration in Sudan. *Geophysics*, Vol. 46, No. 9, 1304-1313.
- Van Overmeeren, R.A. and Ritsema, I.L., 1988, Continuous vertical electrical sounding. *First Break*, Vol. 6, 313-324.
- Van Overmeeren, R.A., 1998, Radar facies of unconsolidated sediments in The Netherlands. A radar stratigraphy interpretation method for hydrogeology. *Journal of Applied Geophysics*, Vol. 40, 1-18.
- Vogel, C.R., 1996, Non-convergence of the L-curve regularisation parameter selection method. *Inverse Problem*, Vol. 12, 535-547.
- Vozoff, K., 1991, The magnetotelluric method. In: Nabighian, M. (Editor), *Electromagnetic methods in applied geophysics*. Vol. 2, Application, Part B, Society of Exploration Geophysicists, 641-711.
- Ward, S.H., and Hohmann, G.W., 1987, Electromagnetic theory for geophysical applications. In: Nabighian, M.N. (Editor), *Electromagnetic methods in applied geophysics*. Vol. 1, Theory. Society of Exploration Geophysicists, 131-311.

Ward, S.H., 1990, Resistivity and Induced Polarisation Methods. In: Ward, S.H. (Editor), Geotechnical and environmental geophysics. Investigations in Geophysics. Vol. I, Review and Tutorial, Society of Exploration Geophysics, 147-189.

Weller, A. and Börner, F.D., 1996, Measurements of spectral induced polarisation for environmental purposes. *Environmental Geology*, Vol. 27, 329-334.

Weller, A., Seichter, M. and Kampke, A., 1996, Induced polarisation modelling using complex electrical conductivities. *Geophys. J. Int.*, Vol. 127, 387-398.

White, C.C., Houston, J.F.T., and Barker, R.D., 1988, The Victoria province drought relief project, I. Geophysical siting of boreholes. *Groundwater*, Vol. 26, No. 3, 309-316.

Won, I.J., Keiswetter, D.A., Fields, G.R.A. and Sutton, L.C., 1996, GEM-2: A new multi-frequency electromagnetic sensor. *JEEG*, Vol. 1, No. 2, 129-137.

World Development Report (WDR), 1994, Infrastructure for Development. Published for the World Bank by Oxford University Press, 264 pp.

World Health Organisation (WHO), 1997a, Guidelines for drinking-water, quality (Internal Report).

World Health Organisation (WHO), 1997b, Health and Sanitation in Sustainable Development (Internal Report).

Wright, E.P., 1992, The Hydrogeology of Crystalline Basement Aquifers in Africa. In: Wright, E.P. and Burgess, W.G. (Editors), The Hydrogeology of Crystalline Basement Aquifers in Africa. Geological Society Special Publication, No. 66, 1-27.

Wright, E.P. and Burgess, W.G. (Editors), 1992, The hydrogeology of crystalline basement aquifers in Africa. Geological Society Special Publication, No. 66.

Xu, P., 1998, Truncated SVD methods for discrete linear ill-posed problems. *Geophys. J. Int.* Vol. 135, 505-514.

Yadav, G.S. and Abolfazli, H., 1998, Geoelectrical sounding and their relationship to hydraulic parameters in semiarid regions of Jalore, north-western India. *Journal of Applied Geophysics*, Vol. 39, 35-51.

Yaramanci, U., Lange, G. and Hertrich, M., 1999, Surface NMR combined with geoelectrics and radar for aquifer studies in Nauen, Berlin. In: *Proceedings, EAGE 61st Conference and technical Exhibition-Helsinki, Finland, 7-11 June 1999.*

Yongxin, X, Fengshi, M. and Partridge, T.C., 1993, Time series analysis of rainfall, piezometric fluctuations and spring flow in the dolomite aquifer system of Wondergat-Dinokana area, north-east of Mafikeng. In: *Proceedings of the International Groundwater Convention, Africa Needs Groundwater, Johannesburg, South Africa 6-8 Sept. 1993.*

Zeil, P., Volk, P., and Saradeth, S., 1991, Geophysical methods for lineament studies in groundwater exploration. A case history from SE Botswana. *Geoexploration*, Vol. 27, 165-177.

Zhang, P., Roberts, R.G., and Pedersen, L.B., 1987, Magnetotelluric strike rules. *Geophysics*, Vol. 52, 267-278.

Zhang, J., Mackie, R.L., and Madden, T.R., 1995, 3D resistivity forward modelling and inversion using conjugate gradients. *Geophysics*, Vol. 60, No. 5, 1313-1325.

Zohdy, A.A.R., Eaton, G.P., Mabey, D.R., 1974, Application of surface geophysics to groundwater investigations. *Techniques of Water-Resources Investigations of the United States Geological Survey. Book 2, Chapter D1.*

Zohdy, A.A.R., 1989, A new method for the automatic interpretation of Schlumberger and Wenner sounding curves. *Geophysics*, Vol. 54, No. 2, 245-256.

Zonge, K.L. and Hughes, L.J., 1991, Controlled source audio-frequency magnetotellurics. In: Nabighian, M. (Editor), *Electromagnetic methods in applied geophysics. Vol. 2, Application, Part B, Society of Exploration Geophysicists*, 713-809.